2825 7/1/89 DTIC FILE COPY

U

SECURITY CLASSIFICATION OF THIS PAGE

JMENTATION PAGE

Form Approved OMB No. 0704-0188

AD-A213 230

1b. RESTRICTIVE MARKINGS: NA

3. DISTRIBUTION / AVAILABILITY OF REPORT: Distribution unlimited

2b. DECLASSIFICATION / DOWNGRADING: NA

4. PERFORMING ORGANIZATION REPORT NUMBER(S): Project No. 4414817-01/14 Apr 1988/1141SB

5. MONITORING ORGANIZATION REPORT NUMBER(S): NA

6a. NAME OF PERFORMING ORGANIZATION: Univ. of Maryland at Baltimore School of Medicine Dept. of Pathology

6b. OFFICE SYMBOL (If applicable): NA

7a. NAME OF MONITORING ORGANIZATION: Office of Naval Research

6c. ADDRESS (City, State, and ZIP Code): 10 South Pine Street Baltimore, MD 21201

7b. ADDRESS (City, State, and ZIP Code): 800 N. Quincy Street Arlington, VA 22217-5000

8a. NAME OF FUNDING / SPONSORING ORGANIZATION: Office of Naval Research

8b. OFFICE SYMBOL (If applicable): ONR

9. PROCUREMENT INSTRUMENT IDENTIFICATION NUMBER: N00014-88-K-0427

8c. ADDRESS (City, State, and ZIP Code): 800 N. Quincy Street Arlington, VA 22217-5000

10. SOURCE OF FUNDING NUMBERS

PROGRAM ELEMENT NO.	PROJECT NO.	TASK NO.	WORK UNIT ACCESSION NO.
61153N	RR04108		

11. TITLE (Include Security Classification): Altered signal transduction in renal cell injury following hemorrhagic shock or anoxia

12. PERSONAL AUTHOR(S): Trump, Benjamin F., Berezesky, Irene K., Smith, Mary W., Anthony, Ronald.

13a. TYPE OF REPORT	13b. TIME COVERED	14. DATE OF REPORT (Year, Month, Day)	15. PAGE COUNT
Annual	FROM 07/88 TO 07/89	89/07/01	

16. SUPPLEMENTARY NOTATION

17. COSATI CODES		
FIELD	GROUP	SUB-GROUP
06		

18. SUBJECT TERMS (Continue on reverse if necessary and identify by block number): ion deregulation; calcium; pH; cell injury; signal transduction; DNA synthesis; gene expression; proximal tubule epithelium; anoxia; hemorrhagic shock;

19. ABSTRACT (Continue on reverse if necessary and identify by block number)

This project is aimed at the delineation of the relationship between ion deregulation e.g., $[Ca^{2+}]_i$, $[H^+]_i$, $[Na^+]_i$, $[K^+]_i$, and $[Mg^{2+}]_i$, cell injury, signal transduction, altered DNA synthesis, and gene expression as they relate to cell death, regeneration, inflammation, and repair in the rat and human proximal tubule epithelium (PTE). Techniques utilized include electron microscopy; phase and Nomarski light microscopy; digital imaging fluorescence microscopy (DIFM) and video microscopy, image analysis, and photon counting; fluorescent probes, e.g., BCECF, rhodamine 123, and propidium iodide; assays of the PI pathway including IP_3 and DAG; assays of protein kinase C; and measurements of mRNA modulation of c-**fos**,. c-**myc**, and c-**jun**. The injuries are studied *in vivo* using a model of hemorrhagic shock and *in vitro* using models of

20. DISTRIBUTION / AVAILABILITY OF ABSTRACT: ☒ UNCLASSIFIED/UNLIMITED ☐ SAME AS RPT ☐ DTIC USERS

21. ABSTRACT SECURITY CLASSIFICATION: U

22a. NAME OF RESPONSIBLE INDIVIDUAL: Dr. J. A. Majde

22b. TELEPHONE (Include Area Code): (202) 696-4055

22c. OFFICE SYMBOL: ONR

DD Form 1473, JUN 86 — Previous editions are obsolete. — SECURITY CLASSIFICATION OF THIS PAGE

S/N 0102-LF-014-6603

ischemia and of oxidative stress. The emphasis is on mechanisms and modulationof responses using assays and inhibitors of Ca^{2+}-activated proteases, phospholipases, and nucleases; and of Ca^{2+}-calmodulin-mediated events. Interactions between cell membrane, cytoskeleton, and nuclear function are stressed.

During the first year of the project, we have established the in vitro models with rat and human PTE in vitro, and have studied $[Ca^{2+}]_i$ regulation using CN+IAA, the xanthine - xanthine oxidase system, and Ca ionophores. These studies have led us to a new model of the relationship between $[Ca^{2+}]_i$ and cell injury and have clarified the relationship between $[Ca^{2+}]_i$, cell injury including bleb formation and cell death. Preliminary data suggest significant roles of Ca^{2+}-activated proteases. The application of imaging technology to the study of $[Ca^{2+}]_i$ has led to unexpected but exciting heterogeneities of $[Ca^{2+}]$ in the cell and set the stage for studies in the second year on modulation of gene expression.

12. Personal Author(s) - Continued

Elliget, M.S., Maki, A.

18. Subject Terms - Continued

digital imaging fluorescence microscopy, video microscopy, photon counting

Accession For
NTIS GRA&I
DTIC TAB
Unannounced
Justification
By
Distribution/
Availability Codes
Dist
A-1

COPY INSPECTED

R & T Code: 441q802

DATE: July 1, 1989

ANNUAL REPORT ON CONTRACT N00014-88-K-427

PRINCIPAL INVESTIGATOR: Benjamin F. Trump, M.D.

CONTRACTOR: University of Maryland at Baltimore
Department of Pathology

CONTRACT TITLE: Altered Signal Transduction in Renal Cell Injury Following Hemorrhagic Shock or Anoxia

START DATE: July 1, 1987

I. INTRODUCTION

Our objective in this project is to delineate the relationship between transmembrane signalling; ion deregulation, e.g., $[Ca^{2+}]_i$, $[H^+]_i$, and $[Mg^{2+}]_i$; cell injury; inflammation; and repair. Our laboratory has been engaged in this type of work for some years and have recently reviewed the subject (Trump et al., 1984; Trump and Berezesky, 1985). The achievement of this objective will have important implications for the prevention, diagnosis, and treatment of shock, trauma, related cell injury, and cell death.

Ion regulation is fundamental to the maintenance of cellular homeostasis, including cell volume control and signal transduction and, it appears, gene regulation. All of the above are now susceptible to critical analysis using current cellular and molecular biology technology. We can, therefore, ask questions, previously not possible, concerning the possible interactions between these variables and the outcomes of cell death, cell proliferation, and cell differentiation (Trump and Berezesky, 1987a,b). The experiments described in the accompanying Progress Report and published abstracts and papers document that changes in $[Ca^{2+}]_i$ precede a variety of intracellular phenomena which can be linked to the progression of cell injury and cell death. This is illustrated in our working hypothesis (see Figure) (Trump and Berezesky, 1983), each branch point of which will be tested during the next few years. We have, therefore, defined the following objectives to enable our laboratory to approach these questions.

I. RESEARCH OBJECTIVES

A. To study changes of $[Ca^{2+}]_i$ in rat, rabbit, and human proximal tubular epithelium (PTE) in vivo and in vitro following anoxia, shock, or models thereof. The models to be used in vitro include inhibition of energy metabolism with KCN or iodoacetate (IAA) and the use of xanthine/xanthine oxidase to generate active oxygen species simulating reflow injury (Nitta et al., 1989).

B. To characterize the relationship between changes in $[Ca^{2+}]_i$ and $[H^+]_i$ in cell injury.

C. To investigate the relationship between changes in $[Ca^{2+}]_i$ and gene expression.

D. To characterize the relationship between altered ion regulation, the activation of the PI pathway, and altered gene expression.

E. To study the relationship between objectives (A) through (D) and deregulation of protein kinase C and the Na^+/H^+ antiport as they relate to cell injury, including shock, trauma and ischemia, and gene expression.

F. Although our Pathobiology Imaging Workstation does not represent a goal or objective of this particular project, its development is essential to enable the proposed work to be accomplished. We, therefore, wish to explain its planned development, and the changes that have occurred since the original proposal was submitted. We have further developed our integrated microcopy resource to include a sophisticated digital imaging fluorescence microscopy system (DIFM); a photon counting system; video intensified microscopy; phase, dark field, fluorescence and Nomarski optics; image analysis including stereology, 3-D reconstruction and all necessary statistical and other data processing; and laser scanning confocal microscopy. The entire system is based on a 32-bit 68020 microprocessor and will possess AT-based remote workstations. This portion of the project has been funded by Departmental and Institutional Funds not derived from this contract. These monies were based on overall research productivity of the Department of Pathology at the University of Maryland and, as such, represent a substantial contribution to this project.

II. MATERIALS AND METHODS

A. Cell isolation

Human, rat, and rabbit proximal tubule epithelia were isolated as previously described (Trifillis et al., 1986; Smith et al., 1987; Elliget and Trump, 1989) and will be only briefly described here. Human and rabbit proximal tubules were isolated by a kidney perfusion technique with collagenase, followed by centrifugation and filtration for purification of proximal tubule fragments. In the case of the rat, small pieces of the cortex were collagenase-digested in a Tekmar Stomacher Lab Blender followed by centrifugation and filtration steps for specific purification of proximal tubules. In all cases, the cultured cells were 100% PTE, as evidenced by histochemical staining with gamma glutamyl transpeptidase. Cultured PTE cells were negative for Factor VIII, positive for keratin, negative for vimentin, exhibited Na^+-glucose co-transport, and stained with a specific lectin for rat PTE. Typically, the PTE monolayers were used for experimentation between day 2-4 of culture.

B. Studies using PTE in suspension

For studies using fluorescent probes in suspended PTE, cell monolayers in culture flasks were loaded with the appropriate probes (e.g., Fura 2 or BCECF)(Smith et al., 1987; Trump et al., 1989a,b,c). Subsequent to loading, the monolayers were then rinsed with Ca^{2+}-free HBSS and the cells collected through mild digestion with trypsin-EDTA. When the cells started to detach, Ca^{2+}-containing HBSS with 10 U/ml DNAse was added. The cells were gently removed with a rubber-policeman, pooled, diluted, and centrifuged. Cell pellets were

then washed to remove trypsin and extracellular dye. PTE cell suspensions were diluted to a concentration of 2-4 x 10^6 cells/ml.

C. Preparation of cells for digital imaging fluorescence microscopy (DIFM) studies

PTE cells were grown to approximately 50% confluence in culture chambers constructed of a standard 60 mm tissue culture dish (e.g., Falcon) in which a 14 mm hole was drilled and covered by a 22 mm glass cover-slip (Tucker et al., 1989). The acid-washed coverslip was attached to the plastic using a silicone sealant and sterilized by UV irradiation. Cells in these specialized dishes were then mounted on a temperature controlled stage on the inverted microscope, which constitutes part of the Pathobiology Imaging Workstation. The microscope is equipped for brightfield, phase, and Nomarski optics to facilitate dual analysis with phase and fluorescence microscopy. Microscopic images can be photographed or recorded in real-time or time-lapse modes on video tape to correlate morphologic changes with the kinetics of changes, for instance, in $[Ca^{2+}]_i$ or other ions.

D. Digital Imaging Fluorescence Microscopy and Video Microscopy

Our digital imaging fluorescence microscopy (DIFM) and video microscopy laboratory contains a FluoroPlex III (Tracor Northern, Middleton, Wisconsin) dual excitation and advanced image analysis system (TN 8502) for fluorometric, microscopic single or multiple cell examination and analysis. The system is specifically designed for characterization of cells that have been labelled with fluorescent probes such as Fura 2 for $[Ca^{2+}]_i$, BCECF for pH_i, etc., which provide the capability of localization and quantitation of concentrations during studies of time-dependent kinetic events. Through the use of fiber optics, dual excitation wavelengths are transferred to the epi-illuminator of a Nikon Diaphot inverted microscope. Images of the alternating excitations are then digitized via an intensified (OPELCO, Washington, D.C.) Newvicon video camera (Dage-MTI, Inc.) for maximum detection sensitivity. The dual wavelength excitation system consists of a xenon light source, a chopper, two monochromators, and a bifurcated fiber optic output so that either a single sustained or a dual chopped excitation can be sent to the sample. A frame grabber is synchronized with the microprocessor-controlled chopper system so that two independent images can be collected and averaged simultaneously and the ratios computed to provide a quantitative image of the fluorescent probe distribution within the cell. Included in the TN system is the recent acquisition of a microscopic photon counting detection system. This system permits high detection sensitivity for fluorescent probes in single cells, thereby allowing fluorescence data to be acquired at the fastest chopping rate of the dual excitation source and thus measurement of millisecond cellular kinetic phenomena and rapid calibration (Morris et al., 1989).

In addition to the above, other features of the TN system include: a high speed M68020 32 bit microprocessor, 1.5 Mb CPU memory, 8 Mb image frame memory, 3 bit overlay planes, 16 binary overlay planes, and "real time" 30 frame per second image digitization. Integrated with the system are complete, advanced image analysis capabilities which include software programs for 3-D reconstruction, stereology, and advanced statistics and plotting.

The Fluoroplex III system is interfaced with a Nikon Diaphot inverted light microscope equipped for epi-fluorescence. In addition, a quartz collector lens and recently introduced CF fluor oil immersion objective lenses are present. Also present is a constant temperature device (Micro Devices, Inc.) which maintains the microscope stage at temperature ranges from +5°C to +55°C with an accuracy of ± 0.2°C. A laminar flow accessory can provide a flow of gas across the sample area which can be heated to 38-45°C to provide a sterile work space and also prevent moisture from condensing on the petri dish cover.

Attached to the light microscope will be a Narishige NT-8 ultrafine hydraulic micromanipulator which allows manipulation of a pipette or electrode with ultrafine accuracy at high magnifications so that single cells can be injected with probes, proteins, genes, etc. A PICO-INJECTOR PLI-100 (Medical Systems Corp., NY) which delivers reproducible microliter volumes for injection or patch-clamping is present. Accessory equipment includes Conrac high resolution monochrome monitors, Sony high resolution color monitor and Panasonic video tape and time-lapse recorders, both with time-date generators.

This laboratory also contains a Zeiss upright photomicroscope III equipped with epifluorescence, phase contrast, and Nomarski DIC illumination with a tungsten as well as a mercury arc lamp. Several ports allow for 35 mm photography and video cameras as well as time-lapse cinemicrography.

E. Fura 2-loading

Cells were loaded with Fura 2 as previously described (Smith et al., 1987). Briefly, Fura was diluted to 5 mM in modified Hank's balanced salts prepared according to Gibco without sodium bicarbonate or phenol red, but containing 1.3 mM Ca^{2+}, 1 g/l glucose, and 10 mM Hepes (pH 7.2); after rinsing 2 times with HBSS, the working solution of Fura 2AM was added and allowed to load for 60 min at 25°C.

F. $[Ca^{2+}]_i$ determinations

1. Fura 2

Fura 2 is a dual excitation, single emission fluorescent probe that can be used to measure $[Ca^{2+}]_i$ concentrations in living cells (Grynkiewicz et al., 1985). This compound, developed by Tsien and his co-workers, binds calcium in a 1 to 1 ratio and undergoes an excitation maxima shift upon binding calcium with little or no change in emission maxima. In the cytoplasm of a living cell, calcium-free Fura 2 has an excitation maxima of 380 nm, upon binding with calcium that maxima shifts to 340 nm (Grynkiewicz et al., 1985). characteristic shift allows one to take the ratio of emission at 340 nm excitation to that of emission at 380 nm excitation and calculate $[Ca^{2+}]_i$ concentration using the following equation:

$$[Ca^{2+}]_i = K_D \left(\frac{R - R_{min}}{R_{max} - R}\right) \beta$$

where R = an experimental measurement of 340/380, R_{min} = that minimal 340/380 emission when fura is calcium-free, R_{max} = calcium saturated fura or maximal

fluorescence, β = emission at 380 excitation under calcium-free conditions over emission at 380 excitation under calcium saturating conditions (Grynkiewicz et al., 1985). The value of K_D can, in theory, be affected by viscosity, e.g., nucleus vs. cytosol or between different organelles. The possible errors, if any, that might result from this have not been resolved.

Fura 2 can be loaded in cells in its AM (acetoxymethylester) form which is lipid soluble and membrane permeant. Upon entry into the cytosol, the ester groups are cleaved by native cytosolic esterases leaving the hydrophobic molecule trapped in the cell (Grynkiewicz et al., 1985). The pentasodium salt can also be microinjected into cells (See Tank et al., 1988). While Fura 2 is the most popular of the fluorescent calcium indicators, there are potential problems with its use. When the AM form enters a cell, it is possible for several species of the indicator to exist in stages of partial deesterification producing calcium-insensitive fluorescent signals (Scanlan et al., 1987). There have been reports of Fura 2 compartmentalization within subcellular organelles or cell types that readily pump Fura 2 out of the cytosol (for review, see Tsien, 1989). In our experience, this needs to be carefully assessed prior to measurement, but does occur as a function of time.

2. Performance of assays

Assays were carried out by collecting image pairs at alternating 340 and 380 nm excitation. Image pairs (10 frames each) were collected at serial time intervals, stored to disk, and processed for obtaining the ratioed images (Trump et al., 1989). Backgrounds collected from cell-free areas were subtracted from the ratioed images. Calibration was performed by treating the cells with ionomycin for R_{max} or ionomycin + 5 mM EDTA for R_{min}. Simultaneous or alternate observation by phase microscopy permitted correlation of morphologic changes with the changes in $[Ca^{2+}]_i$; viability was assessed using trypan blue or the fluorescent dye, propidium iodide.

Imaging studies were correlated with studies of cells in suspension using a spectrofluorometer (Smith et al., 1987). In this case, cells were grown in flasks for 8-14 days, rinsed with HBSS, and loaded for 1 hr with Fura 2AM as described above. Cells were then collected through mild digestion with trypsin and EDTA, gently removed, washed, and concentrations adjusted to 2-4 x 10^6 cells/ml. Fura 2 fluorescence was measured using a Perkin Elmer MPF-66 spectrofluorotometer by following the 510 emission with continuous 340 nm excitation. When imaging studies are performed, care is taken to utilize cells with homogeneous Fura 2 cytosolic distribution.

G. Cell viability

General viability is measured either in suspension or on monolayers by monitoring fluorescence of propidium iodide complexed to DNA or by trypan blue staining. Propidium iodide can be used either in suspension or in monolayers. In suspensions, it was measured at 535/614 nm with a Perkin Elmer MPF 66 spectrofluorometer (Smith et al., 1987). 100% killing was obtained at the completion of each run by addition of 0.7% triton-x 100. In recent experiments on imaging of $[Ca^{2+}]_i$, trypan blue was maintained in the culture medium, as it does not interfere with fluorescence measurements and can allow direct assessment of the state of viability of a given cell.

H. Electron microscopy

1. Transmission and scanning electron microscopy

For routine transmission electron microscopy, cells grown in monolayers or suspension were fixed in 4% formaldehyde, 1% glutaraldehyde fixative (McDowell and Trump, 1986). For studies where Ca precipitates are to be analyzed in mitochondria, fixation was performed in 1% osmium tetroxide in phosphate buffer (Hagler et al., 1981).

For routine scanning electron microscopy, cells on coverslips were fixed in 4% formaldehyde, 1% glutaraldehyde, followed by post-fixation in OsO_4. They were then dehydrated in acetone, critical point dried, coated with gold and examined in the AMR 1000 SEM or the JEOL 100 CX TEMSCAN.

2. X-ray microanalysis

X-ray microanalysis was performed either on an AMR 1000 scanning electron microscope or a JEOL 100CX TEMSCAN. Both microscopes are fitted with a 30 mm^2 Kevex SiLi drifted detector (resolution 158 eV). The AMR 1000 is interfaced with a Tracor Northern NS880 multichannel analyzer and the JEOL 100CX TEMSCAN with a Tracor Northern (TN 5500) Advanced Microanalysis System. A Porter-Blum MT-2 ultramicrotome is present and is equipped with a Sorval cryokit for cutting frozen-dried ultrathin sections. Other special equipment for ion analysis includes a nitrogen gas-powered cryogun for instant freezing and retrieval of tissue in situ, a desiccation device for the storage of cryosections and a Virtis tissue-dryer. In addition to performing quantitative x-ray microanalysis using the TN 5500, processing of digital images can also be done with its advanced imaging capabilities. These include ratioing of x-ray and video images, x-ray intensities superimposed on grey scale video images, 64 grey level imaging, topographic/isometric contours, area fraction calculation, etc.

Coverslips on which monolayers have been grown were frozen by direct quenching in propane slush cooled by liquid nitrogen, freeze-dried overnight at -30°C in a Virtis Automatic Freeze-Fryer (Model No. 10-010) and allowed to warm slowly to room temperature. They will then be mounted on aluminum stubs, taking precaution against rehydration, and stored in a dessicator until examination.

X-ray measurements will be made on frozen-dried ultrathin sections or on frozen-dried, unsectioned cultures grown on coverslips in a JEOL 100 CX TEMSCAN equipped with a free lens control, a high resolution scanning attachment, fitted with a Kevex 30 mm^2 energy dispersive detector (resolution 158 eV), and interfaced with a Tracor Northern NS 880 multichannel analyzer. Analyses will be performed in a scanning transmission mode (STEM) at 80 kV, 50 microamps emission current, beam diameter of 40-80 nm, 30° specimen tilt and a specimen to detector distance of 12 mm. Spectra acquisition will be in the raster mode with a live counting time of 100 sec.

Peak to background ratios for both ultrathin sections and unsectioned monolayer samples will be computed using the Tracor Northern "Super ML" software program according to the expression $P-B_1/B_2$ where P is the peak of interest, B_1

is the background count under the peak and B_2 is the continuum count between 5.50-6.50 keV after the continuum from the support film has been subtracted. Reference spectra will be acquired from standards of known electrolyte concentrations using the same microscope parameters as for the sections or monolayer samples. Data analysis, following the multiple least squares fitting routine, will result in calculations giving the concentrations of each element of interest in mmol/kg dry weight. Measurements will be taken over nuclei, mitochondria, adjacent cytoplasm, extracellular space and support film.

III. RESULTS

A. Models of ischemia and anoxia

We have so far characterized the response of both human, rat, and rabbit PTE cells to KCN and IAA as a model of ischemia (Trump et al., 1989). Initially, the $[Ca^{2+}]_i$ levels approximate 100 nM in cells from all three species. Following the addition of KCN + IAA, there is a rapid rise within a few minutes of $[Ca^{2+}]_i$ from approximately 100 nM concentration, the steady state level, to levels approximating 400-500 nM (Phelps et al., 1989). Using DIFM, this increase is not diffuse in the cytoplasm, but begins in the perinuclear region, perhaps corresponding to portions of the endoplasmic reticulum (ER) and/or Golgi. The increase in $[Ca^{2+}]_i$ is independent of $[Ca^{2+}]_e$, strongly suggesting a redistribution from intracellular stores, such as the mitochondria, or the ER as contrasted to influx across the plasma membrane (Smith et al., 1987). This increase is initially reversible, as seen in anoxia experiments. If reoxygenation occurs within 30 min, the $[Ca^{2+}]_i$ levels return to baseline values. If the injury persists, however, the $[Ca^{2+}]_i$ levels stabilize and redistribute, apparently increasing as well over the nuclear region.

B. Calcium ionophores

In contrast to the modest increase produced by KCN + IAA, the addition of Ca ionophores such as A23187 or ionomycin produce sudden increases of $[Ca^{2+}]_i$ from the normal 100 nM to uM levels. This is followed by rapid and massive blebbing and soon by cell death. It is likely that similar effects occur in a chain-type reaction following other types of injury where Ca ionophore-like materials are liberated from breakdown products of membrane hydrolysis occasioned by Ca-activated phospholipases. These questions will be approached during the coming year.

C. Oxidative stress

To simulate the potential action of oxidative stress during reflow following shock or ischemia, we are characterizing the responses of the rat PTE to the superoxide anion generated via the xanthine/xanthine oxidase system. Initial studies using paraquat have been completed, abstracts published (Nitta et al., 1989a,b) and papers now being submitted. Briefly, xanthine/xanthine oxidase (2.5-25 mU/ml) treatment for 1, 2, and 3 hr gives a dose response curve and leads to an increase of $[Ca^{2+}]_i$. Initially the response is transient, dependent on $[Ca^{2+}]_e$ followed by a secondary increase apparently dependent on redistribution within the cell and independent of $[Ca^{2+}]_e$. We infer that the superoxide anion, interacting with the plasma membrane, results in the creation or enlargement of Ca channels, resulting in an increase of $[Ca2+]_i$ and then a

later redistribution of Ca^{2+} which precedes cell death. At the present time, we are completing additional studies, including electron microscopy, to examine the effects of superoxide anion on the course of reversible and irreversible cell injury.

IV. DISCUSSION

A. Alterations in $[Ca^{2+}]_i$

As described above, it is evident that models of anoxia or ischemia, uncouplers of phosphorylation, or anoxia itself, result in significant elevations of $[Ca^{2+}]_i$, which are regional in the cell as determined by Fura 2 imaging. We are currently studying the meaning of these regional distributions and are planning to correlate such with changes in total Ca in various sub-compartments using x-ray microanalysis (Trump and Berezesky, 1989) as well as further correlations with phase and Nomarski microscopy of intracellular organelles. It appears that the source of most of the initial increase of $[Ca^{2+}]_i$, which rises to approximately 400-500 nM, is redistribution from intracellular stores, principally the mitochondria (Smith et al., 1987). This theory is based on the observation that, following maximum release with CN + IAA or CCCP, addition of sulfhydryl agents such as $HgCl_2$, N-ethylmaleimide, or ionomycin in the absence of $[Ca^{2+}]_e$ + EGTA exhibit their usual large response with values of $[Ca^{2+}]_e$ approximating 1-2 mM (Phelps et al., 1989; Smith et al., 1987). We would infer from this that PTE has a large capacity within the ER, or subsections of that organelle, for the modulation, i.e., the uptake and release of $[Ca^{2+}]_i$. Renal epithelia also contain a significant Na^+-Ca^{2+} exchange mechanism; therefore, ouabain can significantly increase $[Ca^{2+}]_i$, but that response is dependent on influx from $[Ca^{2+}]_e$. Lowering of $[Ca^{2+}]_e$, however, does not seem to affect the typical response to mitochondrial inhibitors or uncouplers, even in the presence of IAA. Therefore, it is reasonable to suppose that even though ATP is deficient with mitochondrial inhibition, the primary cause of increased $[Ca^{2+}]_i$ could not be energy depletion for the Na^+-K^+ ATPase. Further studies, however, will be needed to examine the combined effects of anoxia models with inhibition of Na^+-K^+ ATPase with ouabain. Interestingly, recent studies in the rat PTE show that killing of cells with CN + IAA is retarded if $[Ca^{2+}]_e$ is reduced to less than 5 uM and if EGTA is added.

In these experiments, the apparent $[Ca^{2+}]$ increases within the nuclear compartment as time progresses. At the present time it is difficult to determine if this nuclear increase is meaningful. Several possibilities exist. One is the theoretical possibility that the K_D for Fura 2 differs in the nucleus because of viscosity differences. Although this problem has not been fully resolved, it is our feeling that it does not represent the explanation.
Another possibility is that the increased $[Ca^{2+}]_i$ has been released from perinuclear cisternae and, because of the thickness of the cell in the region of the nucleus, only appears to be extranuclear while, in fact, is superimposed since with conventional fluorescence microscopy, one cannot make "optical" sections. While we also think this possibility is unlikely, it can be tested critically when we obtain our confocal microscopy system. The third, and most likely possibility is that, following deregulation of $[Ca^{2+}]_i$, Ca^{2+} accumulates in the nucleus. Recently, Nicotera et al. (1989) observed active uptake of Ca^{2+} by isolated nuclei. If this could be established in intact cells, it might relate to regulation of DNA transcription by $[Ca^{2+}]_i$. The details of this

possibly complex interrelationship will be explored during the coming year.

B. Bleb formation

The formation of cytoplasmic blebs at the cell surface is a very common reaction to a variety of injuries, both in vivo and in vitro (Phelps et al., 1989). In vivo, with shock or clamping of the renal artery, blebs rapidly form during the reversible phase of cell injury, detach, and drift down the nephron, forming casts in the loop of Henle. Exactly similar detachment without loss of viability is seen in our experiments in cultured epithelia in vitro. Using DIFM, it is apparent that $[Ca^{2+}]_i$ is very high (approximately 2 uM) in the blebs as time progresses. In other recent studies, measuring total Ca using x-ray microanalysis over blebs formed by ionophores, we observed high total Ca concentrations (Trump and Berezesky, 1989). These blebbed areas are lucent by phase or Nomarski microscopy and, with extensive Brownian movement, they, therefore, appear very dilute. By TEM, they contain cytosol and principally ribosomes. Often there is a band of thin filaments at the base of the bleb and, in some experiments, we have observed staining with actin monoclonal antibodies of this band. One hypothesis to explain this phenomenon would be Ca-activated contraction of actin, Ca-activated protease, catalyzed detachment of cytoskeletal related proteins from the cell membrane followed by thin filament contracture, squeezing out of the bleb, and membrane sealing. We have observed and published (Phelps et al., 1989), that bleb formation begins at about a threshold of 400 nM $[Ca^{2+}]_i$ and is also associated with changes in the staining patterns of actin and possibly actin modification. Blebs can also be produced by modification of tubulin and, therefore, in the coming contract year we plan to characterize both actin and tubulin by a variety of techniques, including phalloidin staining, and Western blot electrophoresis.

C. Mechanism of cell death

In the Figure are illustrated several possible mechanisms involved with progression from the prelethal to the lethal phase, focusing on the role of $[Ca^{2+}]_i$. The principal mechanisms involve membrane, cytoskeletal, and nuclear damage through the Ca^{2+}-mediated effects on phospholipases, proteases, and nucleases, respectively. We have previously shown evidence of early modification of membrane phospholipids following renal ischemia (Smith et al., 1980), but are now in the process of refining this phenomenon using a series of inhibitors and additional chromatography techniques. The study of Ca-activated proteases is complex; however, there are a series of inhibitors with which one can begin to explore this possibility. Recently, Kathryn Elliget, our graduate student working on this program, has obtained interesting data showing significant delay or modification of cell death following models of anoxia and ischemia by the addition of Ca protease inhibitors (Elliget et al., 1989). In some types of injury, such as T-cell mediated killing, hydrolysis of nuclear chromosomal DNA seems to occur and can be simulated by Ca ionophores, such as A23187. We are, therefore, systematically investigating this phenomenon during the coming funding period. Ca-activated nuclease inhibitors are available commercially, which, in some systems, can modify cell killing; these will be used in this project. Certainly, modification of chromosomal DNA is of potential importance in the possible generation of mutagenesis and neoplasia, as well as conceivably affecting repair.

D. Relation to signalling and repair

In several systems, changes in $[Ca^{2+}]_i$ have been associated with activation of gene expression that is related to cell division and/or cell differentiation. Modification of this response could be of major importance in facilitating repair following various types of traumatic or shock-induced injury, for example, increases of $[Ca^{2+}]_i$ occasioned by redistribution from the ER with growth factors or by Ca ionophores that have been associated with activation of transcription of several cellular genes related to division, including c-**fos**, c-**myc**, c-**jun**. These reflect modification of regulatory nuclear proteins which putatively modify DNA transcription. During the coming year, we will be characterizing these genes in our laboratory and correlating them with changes in morphology, concentrations of $[Ca^{2+}]_i$, and rate of cell division (Trump et al., 1989a). Transmembrane signalling, often involving G proteins related to the **ras** oncogene, can, with Ca-dependent phospholipase C, result in activation of the PI pathway with release of IP_3 and possibly with other cyclic phosphoinositide derivatives. These may in turn release $[Ca^{2+}]_i$ from the ER. At the same time there is putative liberation of diacylglycerol, which activates, at least in some cells, protein kinase C (see Figure). We will, however, be measuring PI metabolites using HPLC, and the membrane translocation of protein kinase C to evaluate the significance of these in this program. Alkalinization of cells has been reported by Moolenaar et al. (1986) to act as a growth factor and alkalinization also occurs at fertilization in a variety of marine eggs. The Na^+-K^+, amiloride-sensitive antiport, therefore, must be investigated in relation to activation of PI metabolites and protein kinase C. This appears to be a very promising area for future characterization in relation to the prevention and treatment of shock-related cell injury.

V. SUMMARY

During the first year of this project, progress has been more rapid than we expected. Characterizations of $[Ca^{2+}]_i$, using both cell suspensions and spectrofluorometry and monolayers and DIFM, have led us to a new model of the relationship between $[Ca^{2+}]_i$ and cell injury and have clarified apparent conflicts in the literature. Thus, increased $[Ca^{2+}]_i$ can result from (a) influx from $[Ca^{2+}]_e$; (b) redistribution from the ER, mitochondria, or both; and (c) from both (a) and (b). Therefore, it is not surprising that reduction of $[Ca^{2+}]_e$ does not always ameliorate cell killing.

Also, surprisingly, bleb formation bears a strong relationship to $[Ca^{2+}]_i$. Our data suggest a role of Ca^{2+}-mediated cytoskeletal membrane abnormalities with a threshold of approximately 400 nM $[Ca^{2+}]_i$. Modulation of cell killing and bleb formation by Ca-protease inhibitors was also observed.

Finally, the unexpected rapid development of our Pathobiology Imaging Workstation has revealed fascinating intracellular heterogeneities in $[Ca^{2+}]_i$. These illustrate the power of this new technology, raise approachable questions about intranuclear Ca^{2+} regulation of gene expression, and provide a firm substrate for our studies during the coming year of Ca-mediated intracellular signalling.

VI. REFERENCES

Elliget, K.A. and Trump, B.F.: Culture and characterization of normal rat kidney proximal tubule epithelial cells in defined and undefined media. 1989. (Submitted)

Grynkiewicz, G., Poenie, M. and Tsien, R.: A new generation of Ca^{2+} indicators with greatly improved fluorescence properties. J Biol Chem 260: 3440-3450, 1985.

Hagler, H.K., Lopez, L.E., Murphy, M.E., Greico, C.A., and Buja, L.M.: Quantitative x-ray microanalysis of mitochondrial calcification in damaged myocardium. Lab Invest 45: 241, 1981.

McDowell, E.M., and Trump, B.F.: Histologic fixatives suitable for diagnostic light and electron microscopy. Arch Pathol Lab Med 100: 405-414, 1976.

Moolenaar, W.H.: Effects of growth factors on intracellular pH regulation. Ann Rev Physiol 48: 363-376, 1986.

Morris, A.C., Hagler, H.K., Willerson, J.T., and Buja, L.M.: Relationship between calcium loading and impaired energy metabolism during Na^+, K^+ pump inhibition and metabolic inhibition in cultured neonatal rat cardiac myocytes. J Clin Invest 83: 001-000, 1989.

Nicotera, P., McConkey, D.J., Jones, D.P., and Orrenius, S.: ATP stimulates Ca^{2+} uptake and increases the free Ca^{2+} concentration in isolated rat liver nuclei. Proc Natl Acad Sci USA 86: 453-457, 1989.

Nitta, N., Elliget, K.A., Smith, M.W., Phelps, P.C., Berezesky, I.K., and Trump, B.F.: Cell injury on cultured rat proximal tubule epithelium (PTE) by paraquat (PQ)-induced oxidative stress. FASEB J 3: A922, 1989b.

Phelps, P.C., Smith, M.W., Elliget, K.A., and Trump, B.F.: The effect of $HgCl_2$ on cytosolic calcium ($[Ca^{2+}]_i$) and blebbing of rat proximal tubule cells. FASEB J 3: A445, 1989.

Phelps, P.C., Smith, M.W. and Trump, B.F.: Cytosolic ionized calcium and bleb formation after acute cell injury of cultured rabbit renal tubule cells. Lab Invest 60: 630-642, 1989.

Scanlan, M., Williams, D.A., and Fay, F.S.: A Ca^{2+}-insensitive form of fura-2 associated with polymorphnuclear leukocytes: assessment and accurate Ca^{2+} measurement. J Biol Chem 262: 6308-6312, 1987.

Smith, M.W., Ambudkar, I.S., Phelps, P.C., Regec, A.L., and Trump, B.F.: $HgCl_2$-induced changes in cytosolic Ca^{2+} of cultured rabbit renal tubular cells. Biochem Biophys Acta 931: 130-142, 1987.

Smith, M.W., Collan, Y., Kahng, M.W., and Trump, B.F.: Changes in mitochondrial lipids of rat kidney during ischemia. Biochem Biophys Acta 618: 192-201, 1980.

Tank, D.W., Sugimori, M., Connor, J.A., and Llinas R.R.: Spatially resolved calcium dynamics of mammalian Purkinje cells in cerebellar slice. Science 242: 773-777, 1988.

Trifillis, A.L., Regec, A., Hall-Craggs, M., and Trump, B.F.: Effects of cyclosporine on cultured human renal tubular cells. Toxicol Pathol 14: 210-212, 1986.

Trump, B.F., and Berezesky, I.K.: The role of calcium deregulation in cell injury and cell death. Introduction. Surv Synth Pathol Res 2: 165-169, 1983.

Trump, B.F., and Berezesky, I.K.: Cellular ion regulation and disease. A hypothesis. In: Shamoo, A.E., editor. Regulation of Calcium Transport in Muscle. Vol. 25. New York: Academic Press, pp. 279-319, 1985.

Trump, B.F., and Berezesky, I.K.: Cell injury, ion regulation, and tumor promotion. In: Butterworth, B.E., and Slaga, T.J., editors. Nongenotoxic Mechanisms in Carcinogenesis. Banbury Report 25 pp. 69-79. New York: Cold Spring Harbor Laboratory, 1987a.

Trump, B.F., and Berezesky, I.K.: Ion regulation, cell injury and carcinogenesis. Carcinogenesis 8: 1027-1031, 1987b.

Trump, B.F. and Berezesky, I.K.: Cell injury and cell death. The role of ion deregulation. Comments Toxicology 3: 47-67, 1989.

Trump, B.F., Berezesky, I.K., Sato, T., Laiho, K.U., Phelps, P.C., and DeClaris, N.: Cell calcium, cell injury and cell death. Environ Health Perspect 57: 281-287, 1984.

Trump, B.F., Berezesky, I.K., Smith, M.W., Phelps, P.C., and Elliget, K.A.: The relationship between cellular ion deregulation and acute and chronic toxicity. Toxicol Appl Pharmacol 97: 6-22, 1989a.

Trump, B.F., Berezesky, I.K., Smith, M.W., Phelps, P.C., Elliget, K.E., Harris, C.C., Tillotson, T., Resau, J.R., and Jones, R.T.: Digital imaging fluorescence microscopy (DIFM): A new approach to characterize ionic changes following cell injury. Lab Invest 90:98A, 1989b.

Trump, B.F., Berezesky, I.K., Smith, M.W., Phelps, P.C., Elliget, K.A., and Tillotson, T.T.: The role of digital imaging fluorescence microscopy (DIFM) in the study of cell injury. Presented at the Intl Conf on Video Microscopy, Chapel Hill, NC, June 4-7, 1989c.

Tsien, R.Y.: Fluorescence microscopy of living cells in culture. Methods in Cell Biology 29: Part A, 127-153, 1989.

Tucker, R.W., Chang, D.T., and Meade-Cobun, K.: Effects of platelet-derived growth factor and fibroblast growth factor on free intracellular calcium and mitogenesis. J Cell Biochem 39: 139-151, 1989.

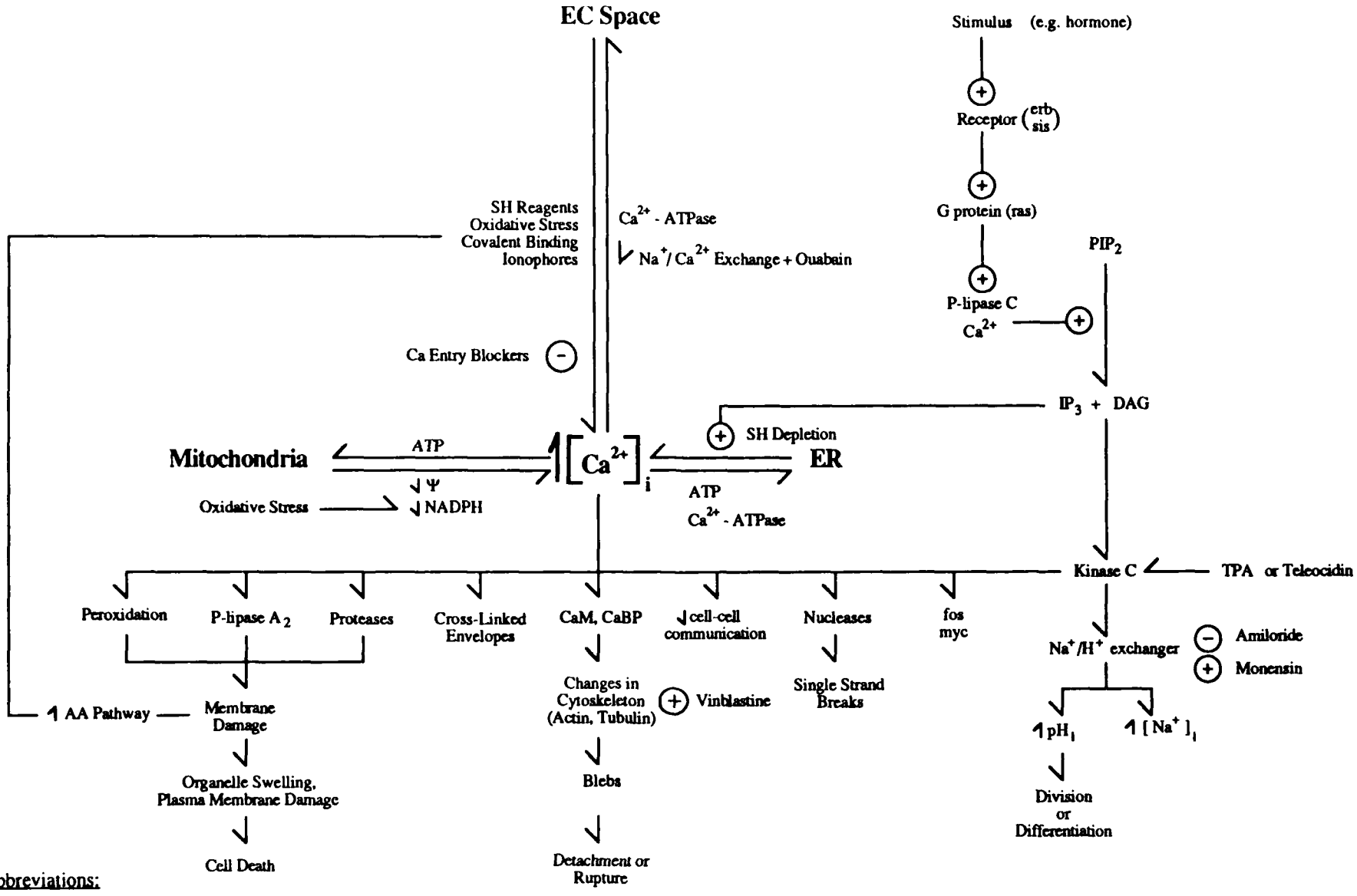

Abbreviations:

PIP = Phosphatidylinositol 4, 5 - diphosphate
Ψ = Mitochondrial membrane potential
CaM = Calmodulin
CaBP = Other calcium-binding proteins
TPA = 12 - O - Tetradecanoylphorbol - 13 - acetate

From Trump and Berezesky: Carcinogenesis 8:1027-1031, 1987.

UM# 2825

13

6/29/89

VII. APPENDIX

Enclosed papers, chapters, and abstracts emanating from this contract which are in preparation, in press, or submitted.

1. B F Trump and I K Berezesky. Is $[Ca^{2+}]_i$ important in cell injury? In: Christman C L, Albert E N, eds., Cochlear implants: A model for the emerging medical device technology. Kluwar Academic Publishers, 1989 (In Press).

2. K A Elliget and B F Trump. Culture and characterization of normal rat kidney proximal tubule epithelial cells in defined and undefined media. 1989 (In Preparation).

3. B F Trump, M W Smith, P C Phelps, K A Elliget, T W Jones, and I K Berezesky. How is intracellular ionized $[Ca^{2+}]_i$ in proximal tubule epithelium (PTE) related to nephrotoxicity digital imaging fluorescence microscopy (DIFM) studies? Fourth International Nephrotoxicity Symposium, July 23-28, 1989 (Submitted).

4. P C Phelps, M W Smith, K A Elliget, and B F Trump. The effect of $HgCl_2$ on cytosolic calcium ($[Ca^{2+}]_i$) and blebbing of rat proximal tubule cells. FASEB J, 1989.

5. B F Trump, I K Berezesky, K A Elliget, M A Smith, and P C Phelps. Nephrotoxicity in vitro: Role of ion deregulation in signal transduction following injury - Studies utilizing digital imaging fluorescence microscopy (DIFM). Second International Conference on Practical In Vitro Toxicology, July 23-27, 1989 (Submitted).

6. K A Elliget, M W Smith, P C Phelps, I K Berezesky, and B F Trump. In vitro toxic effects of mercuric chloride on primary rat proximal tubule epithelial cells. Toxicologic Pathology, 1989 (Submitted).

7. N Nitta, K A Elliget, M W Smith, P C Phelps, I K Berezesky, and B F Trump. Cell injury on cultured rat proximal tubule epithelium (PTE) by paraquat (PQ)-induced oxidative stress. FASEB J, 1989.

8. N Nitta, A Maki, M Smith, P Phelps, K Elliget, I Berezesky, and B Trump. The effects of oxidative stress on rat proximal tubular epithelium (PTE): A role for cytosolic calcium ($[Ca^{2+}]_i$). Circ Shock 27:333-334, 1989.

9. B F Trump, I K Berezesky, M W Smith, P C Phelps, and K A Elliget. $[Ca^{2+}]_i$ does relate to cell injury, cell death, cell differentiation, and cell division: Studies using digital imaging fluorescence microscopy (DIFM). The Fourth Aspen Cancer Conference, Carcinogenesis: From Molecular Mechanisms to Molecular Epidemiology, July 23-26, 1989 (Submitted).

10. B F Trump, I K Berezesky, M W Smith, P C Phelps, and K A Elliget. Calcium signalling in cell injury: The effects of anoxia and shock models on kidney proximal tubule epithelium (PTE) in vitro. Presented at "Biology of Cellular Transducing Signals," Ninth International Washington Spring

Symposium, Washington DC, May 8-12, 1989 (Submitted).

11. B F Trump, I K Berezesky, and A C Morris. New technique for the assessment of cellular injury: Digital imaging fluorescence microscopy (DIFM), A. In: Baker J and Bach P, eds. The Applications of Histochemistry to Toxicology. London: Chapman and Hall, 1989 (In Press).

12. B F Trump, I K Berezesky, M W Smith, P C Phelps, K E Elliget, C C Harris, T Tillotson, J R Resau, and R T Jones. Digital imaging fluorescence microscopy (DIFM): A new approach to characterize ionic changes following cell injury. Lab Invest 90:98A, 1989.

13. B F Trump, M W Smith, P C Phelps, K A Elliget, and I K Berezesky. The role of $[Ca^{2+}]_i$ deregulation in acute toxic cell injury of renal proximal tubular epithelium (PTE): Studies using digital imaging fluorescence microscopy (DIFM). Toxicologic Pathology, 1989 (In press).

14. B F Trump, I K Berezesky, M W Smith, P C Phelps, K A Elliget, and T T Tillotson. The role of digital imaging fluorescence microscopy (DIFM) in the study of cell injury. Presented at the International Conference on Video Microscopy, University of North Carolina, Chapel Hill, NC, June 4-7, 1989 (Submitted).

15. B F Trump, I K Berezesky, M W Smith, P C Phelps, N Nitta, and T T Tillotson. Deregulation of cytosolic ionized calcium $[Ca^{2+}]_i$ in toxic cell injury: Studies using digital imaging fluorescence microscopy (DIFM). Fifth International Congress of Toxicology, July 1989 (Submitted).

16. B F Trump, M W Smith, P C Phelps, R T Jones, M Miyashita, and C C Harris. Deregulation of $[Ca^{2+}]_i$ following injury to a human bronchial epithelial cell line: Effects of the putative tumor promoters H_2O_2, formaldehyde, acrolein, and acetaldehyde. Toxicologic Pathology, 1989 (Submitted).

17. I K Berezesky, M W Smith, P C Phelps, K A Elliget, and B F Trump. Digital imaging fluorescence microscopy (DIFM). Toxicologic Pathology, 1989 (Submitted).

IS $[Ca^{2+}]_i$ IMPORTANT IN CELL INJURY?

Benjamin F. Trump and Irene K. Berezesky

Department of Pathology, University of Maryland School of Medicine and the Maryland Institute for Emergency Medical Services Systems, Baltimore, MD 21201

I. Introduction

An understanding of the mechanisms of acute and chronic cell injury is fundamental to medical practice. Through the years, pathologists have sought to define both the criteria of cell injury and cell death and, at the same time, have tried to understand the reason or reasons why cell injury occurs, why it may be reversible, and why it may lead to the death of the cell. The answers to these questions are fundamental to the design of effective scenarios for the prevention, diagnosis, and treatment of virtually all animal and plant disease.

Some years ago, the subject of reactions of cells to injury was perplexing biomedical scientists. It was important, therefore, to undertake a series of systematic studies of such reactions, correlating as much as possible, organelle, membrane, and genetic changes with cell viability and cell function. At that time, we determined that the most suitable, currently available system for study was the isolated flounder kidney tubule in vitro as this system was well characterized, could be readily studied for structure by light microscopy (LM) and transmission electron microscopy (TEM) or scanning electron microscopy (SEM), studied for function by observing organic anion and cation transport, and was susceptible to studies of ion transport and content (Trump and Ginn, 1969).

Therefore, using a series of model injuries, we characterized the cellular responses to injury at the LM and EM levels and ultimately defined a sequence of reversible and irreversible stages (for recent review, see Trump and Berezesky, 1985a). Later these stages clearly applied to virtually all other animal (including human) species after injury by a variety of toxic insults.

Until the invention of phase, electron, and analytical microscopy, the pathologist was, however, precluded from the exploration of this problem. It was recognized that calcium deposits clearly occurred in areas of dead and dying cells originally called "dystrophic calcification." These deposits typically begin as amorphous $Ca_3(PO_4)_2$ and later transform to calcium hydroxyapatite, identical to that which forms bone. They most often occur in mitochondria, along the inner membrane, and thus require active transport of calcium and phosphate; as a result they typically occur at the edges of infarcts or focally in areas of chemical toxicity. Thus, total cellular calcium concentration often correlates with cell injury and cell death in vivo, as well as in vitro.

Then, some years later, we (Trump et al., 1971, 1974, 1979, 1980, 1981, 1988, 1989; Trump and Berezesky, 1985b, 1987a,b,c,d 1989) and others began to explore the possibility that calcium may be playing an active role in the mechanisms of acute, as well as chronic cell injury. Simultaneously, the possible role of calcium as a second messenger in a variety of physiological regulations was undergoing extensive exploration. More recently, with the development of fluorescent probes, such as Fura 2 for the measurement of intracellular calcium

($[Ca^{2+}]_i$) (Grynkiewicz et al., 1985), it has become possible not only to measure $[Ca^{2+}]_i$ in living cells with digital imaging fluorescence microscopy (DIFM) (DiGuiseppi et al., 1985), but also to correlate these measurements with ongoing changes in morphology and cell biology using time-lapse video recording and phase or Nomarski optics and then, at any desired point, to fix for TEM and/or SEM. Also, cells and tissues can be frozen, freeze-dried sections cut, and examined with analytical EM (energy-dispersive x-ray analysis) for measurements of total content of Na, K, Ca, Mg, and Cl. Moreover, other fluorescent probes for viability (propidium iodide), mitochondrial membrane potential (rhodamine 123), pH (BCECF), K^+ (PBFI), Na^+ (SBFI), and Mg^{2+} (Furapta) can also be included. Thus, it is not surprising that rapid improvements in our knowledge of these areas have occurred in the last two years.

As we will illustrate in this review, increases of $[Ca^{2+}]_i$ occur very early after a variety of acute injuries and some chronic injuries. Furthermore, we will develop our hypothesis that modulation of $[Ca^{2+}]_i$ may provide an important link between the results of acute lethal cell injury and chronic proliferative states, e.g., cancer and atherosclerosis - much of this through its involvement with certain G proteins, the PI pathway, protein kinase C, and the Na^+/H^+ antiport.

The strategy of the present chapter is to summarize data on several models of different types of cell injury, relate these to deregulation of $[Ca^{2+}]_i$, and then to develop our hypothesis concerning the mechanism(s). The models that we will discuss, all of which are highly relevant to injury in the CNS are: (A)

Inhibition of ATP synthesis, (B) Damage to membrane permeability with complement, (C) Calcium ionophores, and (D) SH reactive compounds, and (E) oxidative stress.

An understanding of these basic models of several of the key types of acute cell injury should lead to an understanding of the mechanisms of injury and also should foster the development of strategies for the prevention, diagnosis, and treatment of human disease.

II. Models of Cell Injury

The following cell injury models are representative of the effects of a variety of toxic and injurious agents that can potentially affect virtually all organ systems.

A. Inhibition of ATP Synthesis

Inhibition of ATP synthesis follows treatment with a variety of agents including metabolic inhibitors, which inhibit or uncouple oxidative phosphorylation, inhibitors of glycolysis, as well as anoxic and/or ischemic states. The rate of cell injury and cell death following total ischemia or total anoxia is dependent on the ability of a particular cell to initiate anaerobic glycolysis.

A commonly used model of ischemia <u>in vitro</u> is the application of cyanide (CN) (approximately 1 mM) plus iodoacetate acid (IAA) (0.01 - 1 mM) to block glycolysis. We have studied this extensively in renal proximal tubule

epithelium (PTE) and in Ehrlich ascites tumor cells (EATC). Such injury is followed by an initial reversible phase, which can last from 30-60 min, characterized by shape changes with cell membrane blebbing, dilatation of the endoplasmic reticulum (ER), and condensation of the mitochondria and the nuclear chromatin. As the cells pass the "point of no return" or irreversibility, the swollen mitochondria acquire flocculent densities (denatured matrical proteins), interruptions occur in cell membrane continuity, and karyolysis begins. Almost immediately after adding KCN, there is a rise in $[Ca^{2+}]_i$, as measured with Fura 2, which increases t_o a new steady state of 400-500 nM. This precedes membrane blebbing and dilatation of the ER and is soon followed by a loss of $[K^+]_i$ and increases of $[Na^+]_i$ and $[Cl^-]_i$. In this case, the rate of membrane blebbing is relatively slow and the size of the blebs relatively small. Using DIFM, the increase in $[Ca^{2+}]_i$ is not homogeneous, but occurs initially in the perinuclear endoplasmic region. Since the increase of $[Ca^{2+}]_i$ is independent of extracellular calcium ($[Ca^{2+}]_e$), i.e., it does not occur if $[Ca^{2+}]_e$ is lowered to less than 5 uM, we infer that it is arising predominantly from redistribution of intracellular stores, in this case from the mitochondria. Essentially similar results are seen when cells are treated with uncouplers, such as CCCP or anoxia (Fig. 1).

B. Damage to Membrane Permeability with Complement

Following the sequential assembly of C5b-8 and C5b-9 channels, collectively termed terminal complement complexes (TCC), severe cell damage leading to severe cell injury and cell lysis occurs. When such complexes are formed in myelin,

there is a resulting hydrolysis in myelin basic protein through, in part, inactivation of calcium-dependent neutral proteases, resulting from Ca^{2+} influx through the C5b-8 and C5b-9 channels (Vanguri and Shin, 1988). A variety of events are stimulated, including lipid hydrolysis in part through activation of phospholipase C. This is presumably triggered by the increase in $[Ca^{2+}]_i$ with activation and translocation of protein kinase C to the cell membrane, possibly through the mediation of diacylglycerol (DAG). A variety of inflammatory mediators, such as arachidonic acid (AA) and its products, leukotriene B4, can be stimulated to be released from rat oligodendrocytes by TCC and that AA released in the presence of C5b-9 failed to induce AA release in the absence of $[Ca^{2+}]_e$ or with inhibitors for phospholipase A2 or protein kinase C. Somewhat similar results have been found by Kim et al. (1987), who, studying complement cytolysis in EATC, found a marked reduction in the rate of cytolysis or cell death when $[Ca^{2+}]_e$ was lowered from 1.5 mM to 0.015 mM. It is interesting that when fewer C5b-9 complexes are present, i.e., when they become limiting, the cell is able to remove the complexes and repair the membrane defects, probably through endocytic clearance of affected portions, presumably through endocytosis (Carney et al., 1986). In contrast to the cell killing response, this process is dependent on $[Ca^{2+}]_e$ and thus a paradoxical effect exists (Currin et al., 1989).

In addition to possible roles for calcium-activated proteases and lipases, calcium-activated nucleases may be important in certain types of immunologic and other cell injuries. For example, cell killing with cytotoxic T cells or NK cells is often accompanied by DNA fragmentation, changes in the morphology of

nuclear chromatin, and so-called apoptosis occurring at the cell surface. In this case, other channel-forming proteins, such as perforin or cytolysin discharged from effector cells and somewhat related to C9 may occur. Such DNA fragmentation can be readily stimulated by treating target cells with calcium ionophores, such as A23187 (Smith et al., 1989).

C. Calcium Ionophores

The most widely used calcium ionophores are ionomycin and A23187. Ionomycin has been much more useful in our studies as it does not interfere with the measurement of Fura 2 fluorescence. When such compounds are applied to the cell in the presence of normal levels of $[Ca^{2+}]_e$, there is rapid cell swelling, striking bleb formation at the cell surface, and rapid cell killing. If, however, $[Ca^{2+}]_e$ levels are lowered, preferably in the presence of EGTA, there is a marked delay of cell killing over long time periods. In the presence of normal $[Ca^{2+}]_e$, there is a very rapid rise of $[Ca^{2+}]_i$, which precedes the formation of blebs. The $[Ca^{2+}]_i$ accumulates in a very striking fashion with levels eventually exceeding 1 uM. The blebs, themselves, often detach and drift away into the medium as they do into the nephron lumen <u>in vivo</u> where they may contribute to acute renal failure. In the absence of $[Ca^{2+}]_e$, there is a striking increase in $[Ca^{2+}]_i$, which then rapidly returns to normal as Ca^{2+} leaks from the cell and is trapped by the EGTA (Fig. 2). At these concentrations, the steady-state calcium levels actually return to lower than the normal 100 nM concentration. In fact, it is possible to confer protection against anoxic injury by adding calcium ionophores to low calcium medium containing EGTA, the

inference being that lowering of $[Ca^{2+}]_i$ protects against calcium-mediated lethal effects.

In addition to ionophores, such as ionomycin and A23187 used as toxic chemicals, ionophorous compounds can be generated during the course of cell injury from endogenous substrates. Phosphatidic acid, formed during the hydrolysis of membrane phospholipids, is a possible candidate for an endogenous ionophore which can perpetuate initiated cell injury in the presence of normal $[Ca^{2+}]_e$.

D. Sulfhydryl-Reactive Compounds

SH-reactive compounds are a very important class of toxins containing such compounds as heavy metals, (e.g., mercury and cadmium) and a variety of organic compounds, such as N-ethylmaleimide (NEM). We have studied $HgCl_2$, organic mercurials including PCMB and PCMBS, and NEM (Phelps et al., 1989; Ambudkar et al., 1988; Smith et al., 1987; Trump et al., 1989). These are extremely important compounds <u>in vivo</u>, both in the CNS and in the kidney.

Using Fura 2 as a probe, changes in $[Ca^{2+}]_i$ were measured in cultured PTE cells from rat, rabbit, and human. In the rabbit, treatment with 2.5-10 mM $HgCl_2$ results in a $[Ca^{2}]_e$-independent 12-fold increase of $[Ca^{2+}]_i$ above resting levels of about 100 nM. Because of the magnitude of this increase, much greater than that observed when mitochondrial Ca is redistributed, we infer that this is from another intracytoplasmic pool, probably the ER or a specialized portion of the ER. The dependence of this response on interactions of SH groups is suggested

by the fact that exposure to SH protective agents, such as dithiothreitol, abolishes the response (Smith et al., 1987).

Exposure of PTE to higher concentrations of $HgCl_2$ (25-100 mM) resulted in a $[Ca^{2+}]_e$-independent transient of $[Ca^{2+}]_i$ reaching 1-2 mM, which is then buffered back to near normal levels followed by a secondary increase, which is dependent on $[Ca^{2+}]_e$ (Smith et al., 1987) (Fig. 3). Therefore, the initial transient increase is believed to represent release of Ca^{2+} from the ER or related structures and is independent of the rate of cell killing while the second increase is clearly due to influx from the extracellular space and clearly correlates with the rate of cell killing, which is reduced by decreasing $[Ca^{2+}]_e$ (Fig. 4). Likewise, the rate and size of blebbing was greatly diminished with low $[Ca^{2+}]_e$ (Fig. 5). All of these changes in $[Ca^{2+}]_i$ subsequent to $HgCl_2$ exposure could not be modified with the calmodulin inhibitors 48/80 or W7 and trifluoroperazine, nor did calcium-channel blockers, including verapamil, nifedipine, and nitrendipine, have any effect (Smith et al., 1987). Inhibitors of mitochondrial function, e.g., antimycin, oligomycin, IAA, hypoxia, and CCCP did not block the rise in $[Ca^{2+}]_i$ (Fig. 1). We also investigated neomycin, which has been used as a non-specific inhibitor of phospholipase C, thus blocking IP3 release, but it had no effect. Dantrolene, presumed to block release of Ca^{2+} from the ER and caffeine, allegedly releasing Ca^{2+} from ER, also had no effects before or after $HgCl_2$ treatment. It is thus possible that the Hg ion itself was either interacting with the membranes of the ER, stimulating the release of Ca^{2+}, or inhibiting the ER calcium-dependent ATPase. In fact, Abramson et al., (1983) reported that many heavy metals, including Hg, induce

both the rapid release of Ca^{2+} and also the activation of Ca^{2+}-Mg^{2+}-ATPase from rabbit skeletal muscle sarcoplasmic reticulum. Other SH modifiers, e.g., NEM, PCMB, and PCMBS, were also studied. These likewise produced a $[Ca^{2+}]_e$ independent rise of $[Ca^{2+}]_i$, resembling low $HgCl_2$ concentration again implying release from intracellular stores. It is of great interest that different SH modifiers may act in somewhat different ways.

In correlating the increases of $[Ca^{2+}]_i$ with cell morphology, it was observed that the increases of $[Ca^{2+}]_i$ always preceded the occurrence of the earliest morphologic changes, including blebbing at the cell surface, condensation of the mitochondria, and dilatation of the ER (Figs. 6, 7). The occurrence of blebs occurred after a threshold of approximately 400 nM $[Ca^{2}]_i$ was reached and as concentrations rose higher, both more numerous and larger blebs occurred (Fig. 8).

E. Oxidative Stress

Recently, Nitta et al. (1989) have utilized the xanthine-xanthine-oxidative system to investigate the effects of externally applied oxidative stress on cell injury in relation to $[Ca^{2}_{+}]_i$. The system generates $O_2.^-$ and H_2O_2 extracellularly which reacts presumably initially at the plasma membrane, resulting in acute and lethal cell injury. In the presence of normal $[Ca^{2+}]_e$, there is an initial rapid transient increase in fluorescence followed by a slower secondary sustained increase. While the initial increase was not seen with low $[Ca^{2+}]_e$, the sustained increase was apparently due to redistribution

from intracellular stores.

III. Consequences of Increased $[Ca^{2+}]_i$

Figure 9 depicts our current working hypothesis of the consequences and interactions of the deregulation of $[Ca^{2+}]_i$ in cell injury, cell division, and cell differentiation. This hypothesis is based on previous and current work in our laboratory and, at the moment, is under study in terms of several of the branch points. However, much can, already be said about the consequences of $[Ca^{2+}]_i$ deregulation as outlined above in the several model systems. In this section of the paper, we will to present the consequences of such deregulation and the resulting increase of $[Ca^{2+}]_i$ on several key regulatory systems as they relate to cell injury.

A. Deregulation of $[Ca^{2+}]_i$ by the Model Systems

In the previous section, we outlined the experimental results of several model injuries encompassing the major types of injury encountered in human and animal disease. Uniformly, these result in deregulation of $[Ca^{2+}]_i$ although by different mechanisms; their consequences, however, may or may not reach a final common pathway. In this section, we will consider the pathways of deregulation, the consequences of deregulation, and the specific targets of $[Ca^{2+}]_i$ deregulation in animal cells.

1. Cell Membrane

The cell membrane is a principal target of a number of important injurious stimuli. These include inhibition of the Ca-Mg or Na-K ATPases and/or increased membrane permeability resulting from oxidative stress, insertion of complement components, especially the C5-9 sequence, calcium ionophores such as ionomycin and A23187, SH agents such as $HgCl_2$, and covalent binding by electrophiles. As will be discussed below, it is difficult in practice to find agents that selectively and only affect the cell membrane, however, some components of this category seem to act primarily at this level. In experimental spinal cord injury, for example, Balentine (1988) found increases of Ca within 30 min and found that treatment with ionophores reproduced many of the features of spinal cord injury, including vesiculation of myelin. Similarly, Emery and coworkers (1987), studying development of damage gradients after dendrite transection in normal and ion-substituted media, found that calcium-free media was significantly protective over short-term, such as 2-6 hr, and that choline substitution for sodium had similar effects. Our interpretation of this is that sodium-calcium exchange is playing a role, as mentioned above, and since the sodium increase prevented damage, it probably also protected against a rise in $[Ca^{2+}]_i$.

2. Mitochondria

Mitochondria have the ability to transport Ca^{2+} and phosphate and to regulate $[Ca^{2+}]_i$ with a low affinity but high capacity. In some cases, if phosphate is present and a mitochondrial membrane potential exists, mitochondria can

accumulate and precipitate this in the form of calcium phosphate and later, calcium hydroxyapatite. However, treatment of cells with uncouplers including CCCP, and inhibitors such as antimycin or CN can inhibit the mitochondrial membrane potential and foster the release or unloading of $[Ca^{2+}]_i$ into the cytosol. In contrast to category 1 above where $[Ca^{2+}]_i$ can reach 1-2 uM, total unloading of mitochondria, according to data from our laboratory, can only reach levels approximating 400-500 nM. Therefore, some of the early effects are attenuated since mitochondrial uncoupling or inhibition apparently does not affect the cell membrane. These effects are reversible for 1-2 hr after injury and, accordingly, the early changes including cytoplasmic blebbing are minimized. In the case of mitochondrial calcium unloading, influx of Ca^{2+} from high $[Ca^{2+}]_e$ media, as opposed to low $[Ca^{2+}]_e$ media with EGTA does not occur. Mitochondrial inhibition, however, is extremely important in many important human diseases such as myocardial infarction, renal failure, and stroke and is one of the areas in which interventions may be most efficacious since the integrity of the cell membrane and cell membrane transport systems is longest preserved. Using an in vitro model of cerebral ischemia that employed 3-week-old basal ganglia culture, Goldberg (1986) observed severe damage to neurons, but longer survival in astrocytes and the use of low sodium, low calcium, and high potassium media were all found to be protective against the progression of acute injurious effects.

3. Endoplasmic Reticulum (ER)

The endoplasmic reticulum in a variety of cells has been shown to be an

important and high affinity sequestration site for Ca^{2+} and one that is modulated if not activated by a variety of stressors including membrane ligand interactions of the cell membrane and interactions with the ER itself. At the present time, it is unknown whether this component of intracellular cytoplasmic store regulation is generally distributed to the ER or is only confined to the "calciosome" portion of that system (Malgaroli et al., 1988). It still appears that, at least in some cells, including the PTE, this represents a major repository of Ca^{2+} within the intact cell. Furthermore, this repository is one that, according to a variety of current experiments, is susceptible to modulation if not activation by a variety of ligand receptor interactions at the cell membrane and direct interactions by several agents including heavy metals such as Pb, Hg, and Cd. This particular pathway appears to be involved in intracellular signalling and may represent a key link between cell injury, at least reversible cell injury, and cell proliferation and/or differentiation. Release of Ca^{2+} from the ER can, therefore, result not only from IP3 simulation, but also by inhibition of Ca-ATPase, ATP deficiency, and probably oxidative stress. In the models presented above, NEM and PCMBS particularly appear to be agents that directly interact with this organelle. In the case of $HgCl_2$, important as a toxin in many cells including the CNS, the mechanism is currently unknown, although it is possible that IP3 is released and also that Hg^{2+}, interacting with Ca-ATPase in the ER or specialized portions thereof, releases the Ca^{2+}.

B. Effects of Models on $[Ca^2]_i$ Regulation

Therefore, based on the above results, we have divided the deregulatory stimuli, including toxic agents, involving $[Ca^{2+}]_i$ into the following three categories. These are: (1) Those models that primarily effect influx of $[Ca^{2+}]_i$. The clearest example of these are calcium ionophores such as A23187 and ionomycin. Therefore, in this case, reduction of $[Ca^{2+}]_e$ is dramatically protective against cell injury and cell death (Fig. 10). (2) Those agents that primarily effect redistribution from intracellular stores. These include: inhibition of mitochondrial metabolism with IAA + CN, uncouplers such as FCCP, unloaders of the ER such as NEM and PCMBS, and oxidative stress with xanthine-xanthine oxidase. And (3) Those agents that effect both (1) and (2). This includes $HgCl_2$ which, as mentioned above, leads to an early $[Ca^{2+}]_e$ independent release from the ER, followed by a progressive increase dependent on $[Ca^{2+}]_e$ which is correlated with cell death. In all cases, the appearance of early changes including cytoplasmic blebbing correlates with the increase of $[Ca^{2+}]_i$.

Modulation of the rate of cell death in the above three categories is, therefore, dependent on the circumstance. We have found that reduction of $[Ca^{2+}]_e$ is most protective in (1), not at all in (2), and partially in the latter stages in (3).

C. Specific Targets

In this section, we will discuss the consequences on specific targets in the cell relating to deregulation of $[Ca^{2+}]_i$. The recent introduction of DIFM and other techniques has made it possible to examine $[Ca^{2+}]_i$ in detail in the whole

living cell or even in parts of the cell (Fig. 7).

1. Activation of Phospholipase A_2

Phospholipase A_2 (PLA_2) is a calcium-dependent enzyme, often embedded in the cell membrane, and capable of releasing a variety of products. Some of these products can be introduced into the AA pathway, leading to a variety of other mediators. The role of metabolites of PLA_2 hydrolysis is under study. These metabolites can be modified by many enzyme systems to lead to a variety of cell effects. However, one thing is inescapable and that is that PLA_2 activation can lead to breakdown of cell membranes. In our own laboratory, we have observed the appearance of breakdown products, possibly from PLA_2, activation that represent reversible products of cell membrane hydrolysis (Smith et al., 1980). In the absence of ATP, however, the acetyl-CoA reactivation pathway cannot be totally excluded; however, it is apparent that phospholipase in human disease, including gas gangrene, can be devastating to the cell. Furthermore, it is apparent from several recent studies that inhibitors of PLA_2 can be protective in the sense they can change the kinetics of cell death following deregulation of $[Ca^{2+}]_i$.

2. Calcium-Activated Proteases or Calpains

The area of calpains is under intense study. The calpains have been related to many phenomena ranging from memory to cell death. They can interact with the cytoskeleton, including keratin, actin, and tubulin and can modulate many other

important intracellular phenomena. In some experiments, calpain inhibitors, such as leupeptin, have been shown to modulate the kinetics of cell death. Experiments from our laboratory have shown that these inhibitors can modify the results of PTE injury to $HgCl_2$ or CN + IAA (Elliget et al., 1988). The interactions of calpains with the cell membrane may be related to blebs in the sense that calpain inhibition can lower the rate of bleb formation and reduce the rate of cell death. Calpains also influence the degradation of intermediate filaments. A well characterized example in the nervous system involves the turnover of intermediate filaments at the axonal terminus, when calcium is deregulated after cell injury, activation of calpains is often dramatic, and calcium influx dependent. This seems to lead to progressive collapse and fragmentation of neurons and the changes seen in Wallerian degeneration and can be studied by immunoelectrophoresis of products of intermediate filament hydrolysis.

3. Calcium-Activated Nucleases

This is a new area for the study of $[Ca^{2+}]_i$-regulated injury mechanisms; however, Wyllie et al. (1980) have been studying this with the apoptosis mechanism (Kerr et al., 1972) for some years and recent studies suggest that, at least in some types of injury including T cell injury, ladder-type formations of DNA breakdown are seen prior to the formation of total cytoplasmic blebbing (Smith et al., 1989). It is known, for example, that removal of the nucleus and inhibition of DNA synthesis are compatible at cell life for much longer than with the acute injuries of the type mentioned above. However, it appears that

these nucleases can produce single strand breaks, which could result in deregulation of transcription, leading to altered growth and differentiation. This is a major area of research at the current time and is one which could link cell injury, cell activation, cell division, and cell differentiation.

4. Calmodulin-Mediated Events

Increases of $[Ca^{2+}]_i$ lead to the activation of mechanisms related to the cytoskeleton, including tubulin and actin. These events can range from interaction with the mitotic spindle, as with asbestos, to minor alterations as with ionomycin. It is clear from recent data that deregulation of $[Ca^{2+}]_i$ can lead to cell division and/or differentiation in B lymphocytes, can be involved in the C5-9 activation pathway, and can be involved in the induction of differentiation as with serum-induced treatment of human bronchial epithelium (HBE). Current imaging analysis using DIFM may reveal the changes that are apparent on morphologic analysis of sections of normal vs. tumorigenic cell lines. It is also clear that calmodulin can modulate a variety of changes in the cytoskeleton which could relate to the shape changes seen in the early stages of cell injury.

5. Gene Activation

Increased $[Ca^{2+}]_i$ in a variety of cells can be associated with the activation of a series of oncogenes such as c-fos and c-myc, which are related to cell division, and possibly to terminal differentiation and differential effects in

normal vs. transformed cells. The mechanism of this activation or deactivation is currently unknown. We suspect that it is related to membrane cytoskeletal events that articulate the signalling between protein kinase C, the PI pathway, and possibly other unknown events. It is certainly clear that increased $[Ca^{2+}]_i$ can be associated with terminal differentiation. In cultured human bronchial epithelium (HBE), which can be terminally differentiated when activated by serum, $^{a}_{n}$ increase is not necessary to initiate differentiation activated by TGF-B or phorbol esters including TPA (Miyashita et al., 1989).

6. Protein Kinase C

Protein Kinase C (PKC) is a calcium-activated enzyme which is translocated when activated from the cytosol to the membrane and is a key to the interaction between tumor promoters such as TPA and the PI pathway, and the increase of $[Ca^{2+}]_i$ followed by reversible cell injury. At the present time, it is difficult to assess a particular role for PKC in its process, although PKC activation is assumed to result from TPA activation. It appears from our experiments that an additional pathway must be present, whereby PKC either activates or deactivates cell division or cell differentiation because in tumor vs. normal cells, PKC activation may have totally different effects.

7. Cell-Cell Communication

When $[Ca^{2+}]_i$ increases in cells, Loewenstein (1981) has found that cell-cell communication, putatively through gap junctions, decreases. This decrease can

have a number of effects and Trosko and Chang (1984) have put forward the hypothesis that decreased cell-cell communication correlates with tumor promotion. While it is true that connect signs in the gap junctions can close down with increased $[Ca^{2+}]_i$, the consequences of such are unknown, although current experiments from our laboratory suggest that the correlation may occur in cells other than fibroblasts (Albright et al., 1988).

8. Sodium-Proton Exchange

The area of sodium-proton (Na^+/H^+) exchange and alkalinization of the cytoplasm has become a very important focus of study during the last several years. Moolenaar et al. (1984) proposed that Na^+/H^+ exchange and alkalinization of the cytoplasm represented a simulation of growth factors in several cultured cell lines. At the same time our laboratory had documented that reduction of pH was protective against cell injury (Penttila and Trump, 1974) which has been recently confirmed by a variety of authors, including Currin et al. (1989). Therefore, it has been proposed that Na^+/H^+ exchange seems to be an important factor in cell death and cell division although the mechanism of this effect is unknown. This effect of sodium/calcium exchange can be even more striking in excitable cells. In a recent study, Morris et al. (1989) observed that inhibition of sodium/potassium ATPase with ouabain resulted in 20-30-fold increases of $[Ca^{2+}]_i$ approximately 10 times greater than that produced by inhibition of energy metabolism with CN_+ deoxyglucose.

Recently, however, the increased intracellular pH (pH_i) hypothesis has been

questioned (Thomas, 1989) because the work of Moolenaar and colleagues (1984) was performed in the absence of bicarbonate. Ganz et al. (1989) have recently shown that growth factors stimulate bicarbonate transport more than they stimulate Na^+/H^+ exchange. Also, in other studies, alkalinization was found to increase cell death dramatically. The effects of modification of pH_i on DNA transcription and translation are currently obscure. The areas of PKC activation, pH_i activation, and Na^+/H^+, or Cl^-/HCO_3^- exchange are not only not understood, but may be a key, at our current level of understanding, to the evalution of this process.

IV. Summary

We have thus reviewed available data to attempt to answer the question, "Is deregulation of $[Ca]_i$ important in the progress of cell injury"? It is clear from current data in a variety of systems in vivo and in vitro and a variety of toxic agents that the answer to this question is clearly "yes." The reasons for deregulation of $[Ca^{2+}]_i$ fall into three classes. These are: (1) influx from the extracellular space, (2) redistribution from intracellular stores, such as ER and/or mitochondria; and (3) combinations of both (1) and (2). Different toxic interactions or injurious agents result in different mechanisms and often more than one mechanism is involved. Several possible sites of action for the mechanism of calcium effects were reviewed. This is an area currently under study and one which hopefully will result in development of therapeutic interventions. Furthermore, it is now becoming clear that calcium can be involved in gene regulation and control of division and differentiation, and

thus may ultimately represent a link between acute and chronic cell injury including proliferative states. Work on this problem and the CNS is also beginning and results so far, some of which were reviewed here, suggest a very similar role for calcium deregulation in elements of the nervous system.

Acknowledgements

This is contribution No. 2799 from the Cellular Pathobiology Laboratory.

Supported by NIH grants DKAM15440 and N01-CP-51000 and by Navy N00014-88-K-0427.

V. References

Abramson JJ, Trimm JL, Weden L, and Salama G (1983). Heavy metals induce rapid calcium release from sarcoplasmic reticulum vesicles isolated from skeletal muscle. Proc Natl Acad Sci USA 80: 1526-1530.

Albright CD, Grimley PM, Jones RT, and Resau JH (1989). Intercellular communication (IC), cell growth and differentiation of normal and SV40 transformed human tracheobronchial cells (TBE). J Cell Biol 107: 554a.

Ambudkar IS, Smith MW, PHelps PC, Regec AL, and Trump BF (1988). Extracellular Ca^{2+}-dependent elevation in cytosolic Ca^{2+} potentiates $HgCl_2$-induced renal proximal tubular cell damage. Toxicol Ind Health 4: 107-123.

Balentine JC (1988). Spinal cord trauma: In search of the meaning of granular axoplasm and vesicular myelin. J Neuropath Exp Neurol 47: 77-92.

Carney DF, Hammer CH, and Shin ML (1986). Elimination of terminal complement complexes in the plasma membrane of nucleated cells: Influence of extracellular Ca^{2+} and association with cellular Ca^{2+}. J Immunol 137: 263-270.

Currin RT, Gores GJ, Thurman RG, and Lemasters JJ (1989). Protection by acidic pH against anoxic injury in perfused rat liver: Evidence for a "pH" paradox. FASEB J 3: A626.

DiGuiseppi J, Inman R, Ishihara A, Jacobson K, and Herman B (1985). Applications of digitized fluorescence microscopy to problems in cell biology. Biotechniques 3: 394-403.

Elliget KA, Phelps PC, and Trump BF (1988). Rat primary proximal tubule (RPPT) cells treated with $HgCl_2$ and calpain inhibitors, antipain and leupeptin. J Cell Biol 107: 394a.

Emery DJ, Lucas JH, and Gross GW (1987). The sequence of ultrastructural change sin cultured neurons of the dendrite transection. Exp Brain Res 67: 41-51.

Ganz MB, Boyarsky G, Sterzel RB, and Boron WF (1989). Arginine vasopressin enhances pH_i regulation in the presence of HCO_3- by stimulating three acid-base transport systems. Nature 337: 648-651.

Goldberg WJ, Kadingo RM, and Barrett JN (1986). Effects of ischemia-like conditions on cultured neurons: Protection by low Na^+, low Ca^{2+} solutions. J Neurosci 6: 3144-3151.

Grynkiewicz G, Poenie M, and Tsien RY (1985). A new generation of Ca^{2+} indicators with greatly improved fluorescence properties. J Biol Chem 260: 3440-3445.

Kerr JFR, Wyllie AH, and Currie AR (1972). Apoptosis: A basic biological phenomenon with wide-ranging implications in tissue kinetics. Br J Cancer

26:239.

Kim SH, Carney DF, Hammer CH, and Shin ML (1987). Nucleated cell killing by complement: Effects of C5b-9 channel size and extracellular Ca^{2+} on the lytic process. J Immunol 138: 1530-1536.

Lowenstein WR (1981). Junctional intercellular communication: The cell to cell membrane. Physiol Rev 61: 829-913.

Lucas JH, Gross GW, Trump BF, Balentine JD, Berezesky IK, Young W, Gilad GM, and Bernstein JJ (1988). Introduction: An international Symposium: Cellular and molecular correlates of central nervous system trauma. J Neurotrauma 5: 209-214.

Malgaroli A, Hashimoto S, Grohovaz F, Fumagalli G, Pozzan T, and Meldolesi J (1988). Intracellular source(s) of $[Ca^{2+}]_i$ transients in nonmuscle cells. Ann NY Acad Sci USA 551: 159-166.

Miyashita M, Smith MW, Willey JC, Lechner JF, Trump BF, and Harris CC (1989). Effects of serum, transforming growth factor beta or 12-O-tetradecanoylphorbol-13-acetate on ionized cytosolic calcium concentration in normal and transformed human bronchial epithelial cells. Cancer Res 49: 63-67.

Moolenaar WH, Tertoolen LG, and DeLaat SW (1984). Phorbol ester and diacylglycerol mimic growth factors in raising cytoplasmic pH. Nature 312: 371-

374.

Morris AC, Hagler HK, Willerson JT, and Buja LM (1989). Relationship between calcium loading and impaired energy metabolism during Na^+, K^+ pump inhibition and metabolic inhibition in cultured neonatal rat cardiac myocytes. J Cell Immunol, in press.

Nitta N, Maki A, Smith M, Phelps P, Elliget K, Berezesky I, and Trump B (1989). The effects of oxidative stress on rat proximal tubular epithelium (PTE): A role for cytosolic calcium ($[Ca^{2+}]_i$). Twelfth Annual Conference on Shock, submitted.

Pentilla A and Trump BF (1974). Extracellular acidosis protects Ehrlich ascites tumor cells and rat renal cortex against anoxic injury. Science 185: 277-278.

Phelps PC, Smith MW, and Trump BF (1989). Cytosolic ionized calcium and bleb formation after acute cell injury of cultured rabbit renal tubule cells. Lab Invest 60:000-000.

Schlaepfer WW (1987). Neurofilaments: Structure, metabolism and implications in disease. J Neuropath Ex Neurol 46: 117-129.

Smith CA, Williams GT, Kingston R, Jenkinson EJ, and Owen JJT (1989). Antibodies to CD3/T-cell receptor complex induce death by apoptosis in immature T cells in thymic cultures. Nature 337: 181.

Smith MW, Ambudkar IS, Phelps PC, Regec AL, and Trump BF (1987). $HgCl_2$-induced changes in cytosolic Ca^{2+} of cultured rabbit renal tubular cells. Biochem Biophys Acta 931(1): 130-142.

Smith MW, Collan Y, Kahng MW, and Trump BF (1980). Changes in mitochondrial lipids of rat kidney during ischemia. Biochim Biophys Acta 618: 192-201.

Thomas RC (1989). Bicarbonate and pH_i response. Nature 337: 601.

Trosko JE and Chang CC (1984). Adaptive and nonadaptive consequences of chemical inhibition of intercellular communication. Pharmacol Rev 36: 1375-1445.

Trump BF and Berezesky IK (1985a). Cellular ion regulation and disease. An hypothesis. In: Shamoo AE, editor. Regulation of Calcium Transport in Muscle, Vol. 25, New York: Academic Press, Inc., pp. 279-319.

Trump BF and Berezesky IK (1985b). The role of calcium in cell injury and repair: A hypothesis. Surv Synth Path Res 4: 248-256.

Trump BF and Berezesky IK (1987a). The role of ion regulation in respiratory carcinogenesis. In: McDowell EM, editor. Lung Carcinomas. New York: Churchill Livingstone, pp. 162-174.

Trump BF and Berezesky IK (1987b). Mechanisms of cell injury in the kidney: The role of calcium. In: Fowler BA, editor. Mechanisms of Cell Injury: Implications for Human Health. Dahlem Konferenzen. Chichester: John Wiley & Sons, Ltd. pp. 135-151.

Trump BF and Berezesky IK (1987c). Ion regulation, cell injury and carcinogenesis. Carcinogenesis 8: 1027-1031.

Trump BF and Berezesky IK (1987d). Calcium regulation and cell injury: A heuristic hypothesis. Ann NY Acad Sci USA 494: 280-282.

Trump BF and Berezesky IK (1989). Ion deregulation in injured proximal tubule epithelial cells. In: Bach PH and Lock EA, editors. Nephrotoxicity: Extrapolation from In Vitro and In Vivo, and Animals to Man. London: Plenum Press, pp. 731-742.

Trump BF and Ginn FL (1969). The pathogenesis of subcellular reaction to lethal injury. In: Bajusz E and Jasmin G, editors. Methods and Achievements in Experimental Pathology, Volume IV. Basel: Karger, pp. 1-29.

Trump BF, Berezesky IK, and Phelps PC (1981). Sodium and calcium regulation and the role of the cytoskeleton in the pathogenesis of disease: A review and hypothesis. Scan Electron Microsc 2: 34-454.

Trump BF, Croker BP Jr, and Mergner WJ (1971). The role of energy metabolism,

ion, and water shifts in the pathogenesis of cell injury. In: Richter GW and Scarpelli DG, editors. Cell Membranes: Biological and Pathological Aspects. Baltimore, Williams and Wilkins, pp. 84-128.

Trump BF, Strum JM, and Bulger RE (1974). Studies on the pathogenesis of ischemic cell injury. I. Relation between ion and water shifts and cell ultrastructure in rat kidney slices during swelling at 0-4°C. Virchows Arch Abt B Zellpath 16: 1-34.

Trump BF, Berezesky IK, Chang SH, Pendergrass RE, and Mergner WJ (1979). The role of ion shifts in cell injury. Scan Electron Microsc 3: 1-14.

Trump BF, Berezesky IK, Laiho KU, Osornio AR, Mergner WJ, and Smith MW (1980). The role of calcium in cell injury. A review. Scan Electron Microsc 3: 437-462.

Trump BF, Berezesky IK, Smith MW, Phelps PC, and Elliget KA (1989). The relationship between cellular ion deregulation and acute and chronic toxicity. Toxicol Appl Pharmacol 97: 6-22.

Trump BF, Smith MW, Phelps PC, Regec AL, and Berezesky IK (1988). The role of ionized cytosolic calcium ($[Ca^{2+}]_i$) in acute and chronic cell injury. In: Lemasters JJ, Hackenbrook CR, Thurman RG, and Westerhoff, HV, editors. Integration of Mitochondrial Function. New York: Plenum Press, pp. 437-444.

Vanguri P and Shin ML (1988). Hydrolysis of myelin basic protein in human

myelin by terminal complement complexes. J Biol Chem 263: 7228-7234.

Wyllie AH, Kerr JF, and Currie AR (1980). Cell death: The significance of apoptosis. Int Rev Cytol 68: 251-306.

Figure Legends

Figure 1. The effect of pre-exposure to several inhibitors of cellular energy production on the fluorescence response of Fura 2-loaded cells exposed to $HgCl_2$ in the presence of 1.37 mM $CaCl_2$. Inhibitors (antimycin 5 uM, oligomycin 5 ug/ml, CCCP 4 uM) of various mitochondrial functions (A) do not alter the $HgCl_2$-induced $[Ca^{2+}]_i$ changes. Anoxia and CCCP cause a 2-fold increase in cytosolic calcium before $HgCl_2$ is added and this response is independent of $[Ca^{2+}]_e$. (B) shows that both the glycolysis inhibitor iodoacetic acid (IAA) (0.1 mM) and mitochondrial uncoupler CCCP (4 uM) cause some increase in $[Ca^{2+}]_i$ but do not affect $HgCl_2$-induced $[Ca^{2+}]_i$ changes. CCCP quenches the fluorescence signal and apparently affects the calculation of $[Ca^{2+}]_i$. The values for $[Ca^{2+}]_i$ given on the ordinate are adjusted to estimate 100 nM $[Ca^{2+}]_i$ immediately after CCCP additions. The full scale represents fluorescence from F_{min} to F_{max}. (Reprinted with permission from Smith et al., 1987.)

Figure 2. Relative size of intracellular pools of Ca^{2+} compared to release of Ca^{2+} by 50 uM $HgCl_2$. In (A), addition of 4 uM CCCP to cells in low $[Ca^{2+}]_e$ plus 20 uM EGTA causes immediate quenching of the fluorescence signal followed by an increase in fluorescence attributed to unloading of mitochondrial Ca^{2+}. Addition of 1 uM 4-bromo-A23187 causes release of remaining intracellular Ca^{2+} stores. The elevated $[Ca^{2+}]_i$ then greatly decreases, probably due to equilibration with the external medium in the presence of ionophore. (B) shows the fluorescence response of cells in normal $[Ca^{2+}]_e$ treated first with 4 uM CCCP (to unload mitochondrial Ca^{2+}) and then with 50 uM $HgCl_2$. The fluorescence

maxima of both the ionophore- and $HgCl_2$-treated cells are very similar. The scale is adjusted to reflect quenching by CCCP and is based on $[Ca^{2+}]_i$ calculated following addition of bromo-A23187 or $HgCl_2$ alone. (Reprinted with permission from Smith et al., 1987.)

Figure 3. Fluorescence response of Fura 2-loaded cells to 50 uM $HgCl_2$ in low (<5 uM) or normal (1.37 mM) $[Ca^{2+}]_e$. The initial increase and decrease is virtually the same with either low or normal $[Ca^{2+}]_e$ indicating intracellular redistribution. After about 3 min, $[Ca^{2+}]_i$ increases in the presence of normal but not low $[Ca^{2+}]_e$, indicating the increase is due to entry of extracellular Ca^{2+}. (Reprinted with permission from Smith et al., 1987.)

Figure 4. Cell viability, as measured with propidium iodide, after treatment with 50 uM $HgCl_2$ in the presence of low or normal $[Ca^{2+}]_e$. Percent viability was determined by comparing the fluorescence of each sample before and after cell lysis with 0.07% Triton X-100. The ordinate represents decreasing fluorescence intensity from 60-0%. (Reprinted with permission from Smith et al., 1987.)

Figure 5. Phase micrographs of monolayer cells exposed to 50 uM $HgCl_2$ at 37°C with low $[Ca^{2+}]_e$ for 6 min (A) and 14 min (C), and with normal $[Ca^{2+}]_e$ for 4 min (B) and 14 min (D). In the presence of normal $[Ca^{2+}]_e$, there are at least twice as many blebs as in low $[Ca^{2+}]_e$ at similar times (x193). (Reprinted with permission from Phelps et al., 1989).

twice as many blebs as in low $[Ca^{2+}]_e$ at similar times (x193). (Reprinted with permission from Phelps et al., 1989).

Figure 6. Phase image (taken from Tracor Northern computer monitor) of a rabbit proximal tubule cell at 0 time (A) and 17 min following treatment with 100 uM $HgCl_2$ (B). (Courtesy of P.C. Phelps.)

Figure 7. Cultured rabbit kidney proximal tubule cell loaded with Fura 2. Fluorescent images were acquired using a DIFM system consisting of: a Nikon inverted microscope; a chopper-based Tracor Northern Fluoroplex III providing alternating xenon excitation light of 340/380 nm; a high resolutio.. intensified Newvicon video camera; and a Tracor Northern TN-8502 image analysis system for grabbing, storing and processing images. Paired 340/380 images were ratioed and the $[Ca^{2+}]_i$ represented by a grey scale ranging from lower (light) to higher (dark) concentrations. (A) The ratioed image of the cell at 0-time. The mean ratio is 0.97 and approximately 90 nM $[Ca^{2+}]_i$. (B-D) Ratioed images after addition of 100 uM $HgCl_2$. (B) Ratioed image at 0.5 min. The mean ratio is 1.29. (C) Ratioed image at 5 min. The mean ratio is 1.17. (D) Ratioed image at 16 min. The mean ratio is 1.3. At this time, there are obvious blebs present which contained elevated $[Ca^{2+}]_i$. (Courtesy of P.C. Phelps.)

Figure 8. Representative curves showing the effect of toxic agents on bleb formation, rate, number and size in monolayer PTE cells at 37°C after exposure to: 50 uM $HgCl_2$, 250 uM NEM, 1 mM PCMBS, 5 uM ionomycin, 10 uM A23187, 4 uM

CCCP, 5 mM KCN, and 5 mM KCN + 100 uM IAA with normal and low $[Ca^{2+}]_e$. Note that blebbing is similar with normal or low $[Ca^{2+}]_e$ for NEM and PCMBS. Solid circles represent smaller bleb sizes in the range of 0.5-2.0 um; open circles represent larger bleb sizes in the range of 3.0-4.0 um. (Reprinted with permission from Phelps et al., 1989.)

Figure 9. Flow chart illustrating our hypothesis and the relationships between $(Ca^{2+}]_i$ deregulation, cell injury and carcinogenesis. (Reprinted with permission from Trump and Berezesky, 1987c.)

Figure 10. Representative curves showing the loss of monolayer PTE cell viability at 37°C as determined by trypan blue staining during exposure to 50 uM $HgCl_2$, 250 uM NEm, 1 mM PCMBS, 5 uM ionomycin, 10 uM A23187, 4 uM CCCP, 5 mM KCN, 5 mM KCN + 100 uM IAA with normal and low $[Ca^{2+}]_e$. Note that cell death is similar with normal or low $[Ca^{2+}]_e$ for NEM, KCN + IAA, and PCMBS. (Reprinted with permission from Phelps et al., 1989).

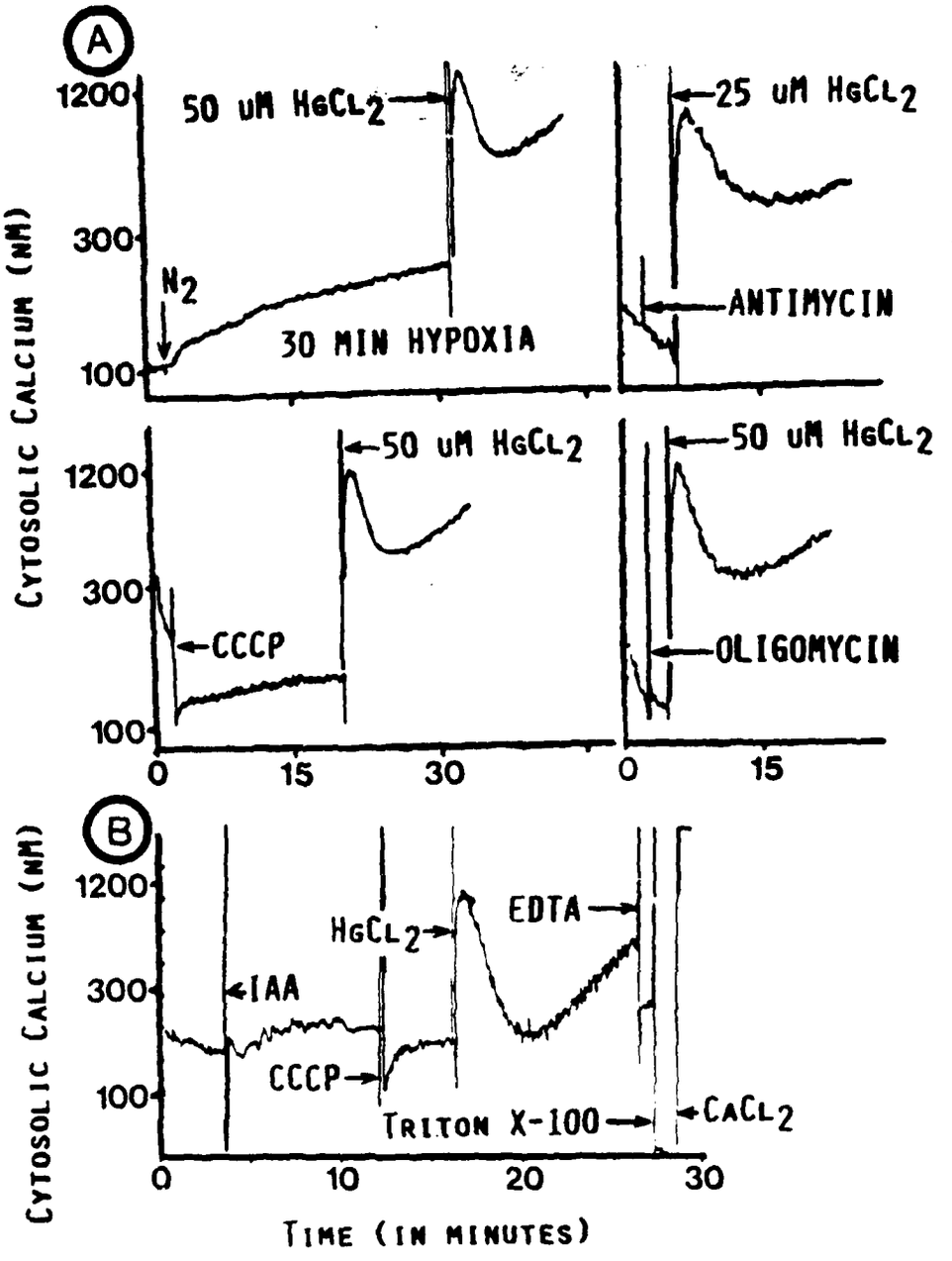
A
1200
300
100
50 uM HgCl2
25 uM HgCl2
N2
30 MIN HYPOXIA
ANTIMYCIN
50 uM HgCl2
50 uM HgCl2
CCCP
OLIGOMYCIN
0
15
30
0
15
Cytosolic Calcium (nM)
B
1200
300
100
HgCl2
EDTA
IAA
CCCP
Triton X-100
CaCl2
0
10
20
30
Cytosolic Calcium (nM)
Time (in minutes)

Fig 1

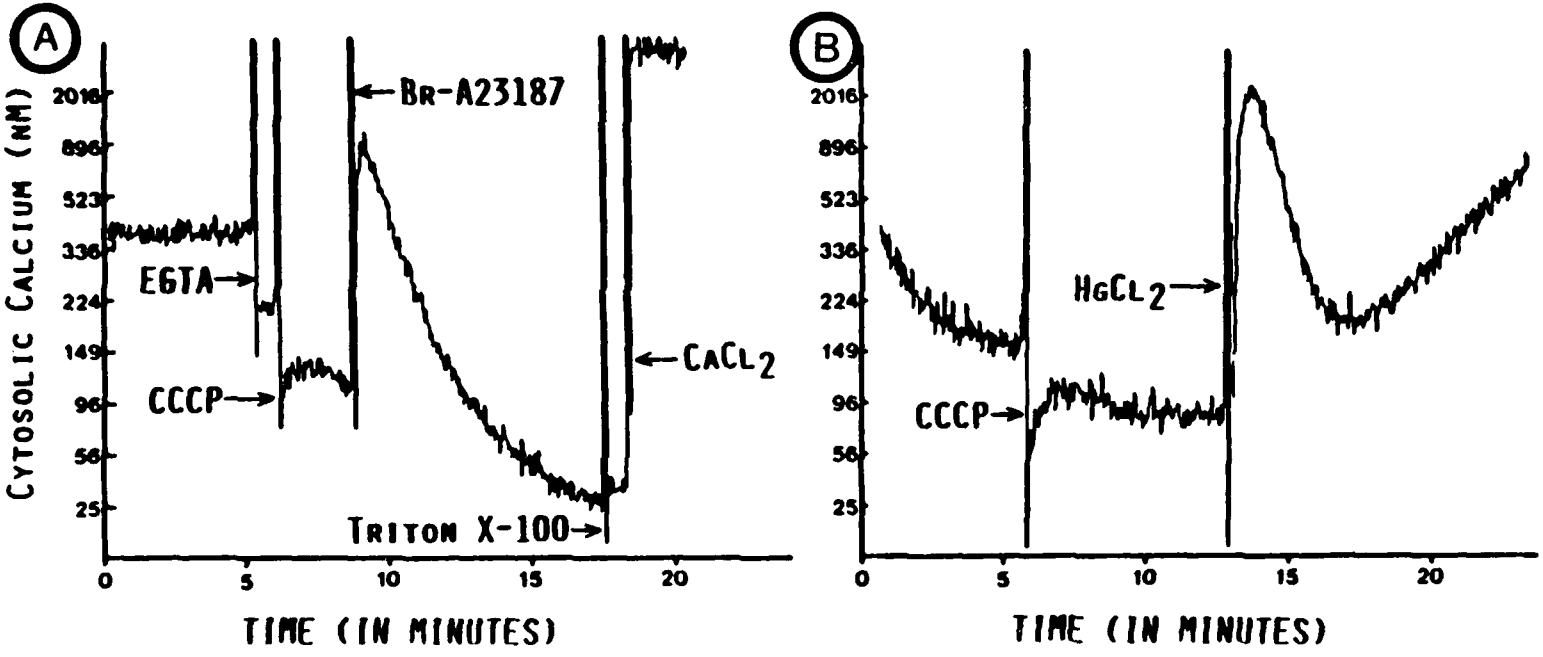
A
CYTOSOLIC CALCIUM (NM)
2016
896
523
336
224
149
96
56
25
EGTA
CCCP
BR-A23187
CACL2
TRITON X-100
0
5
10
15
20
TIME (IN MINUTES)
B
2016
896
523
336
224
149
96
56
25
HGCL2
CCCP
0
5
10
15
20
TIME (IN MINUTES)

Fig 21

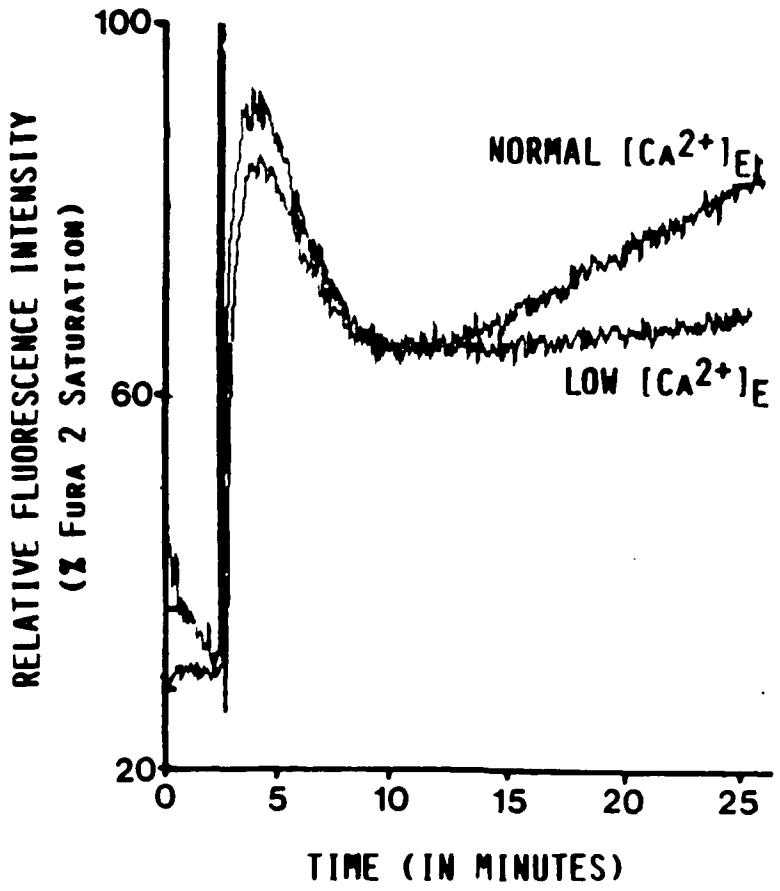
100
60
20
0
5
10
15
20
25
RELATIVE FLUORESCENCE INTENSITY
(% FURA 2 SATURATION)
TIME (IN MINUTES)
NORMAL $[Ca^{2+}]_E$
LOW $[Ca^{2+}]_E$

Fig 3

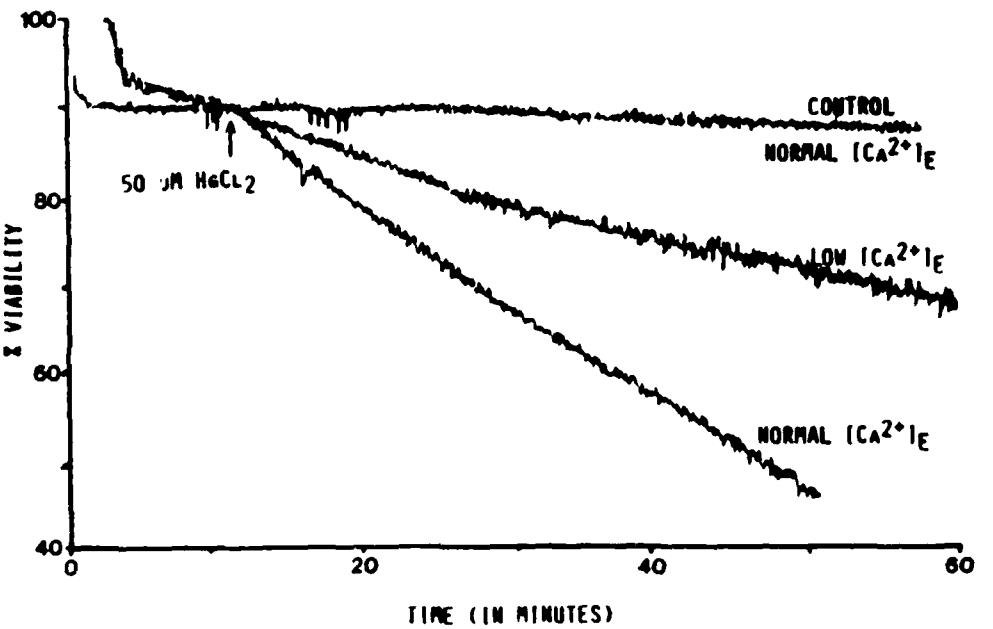
100
80
60
40
% VIABILITY
50 μM HgCl2
CONTROL
NORMAL [Ca2+]E
LOW [Ca2+]E
NORMAL [Ca2+]E
0
20
40
60
TIME (IN MINUTES)

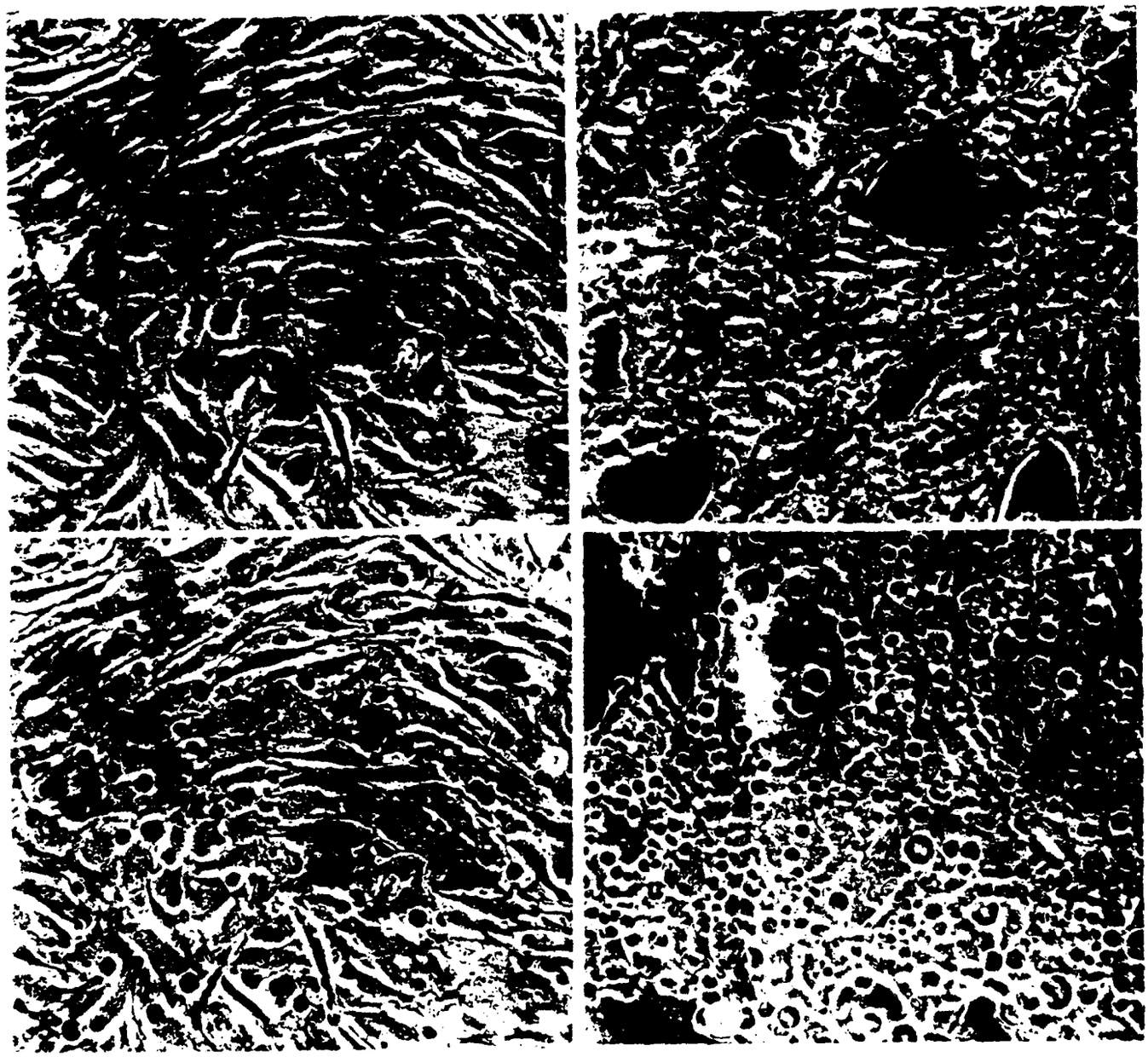

FIG. 5

Fig 6

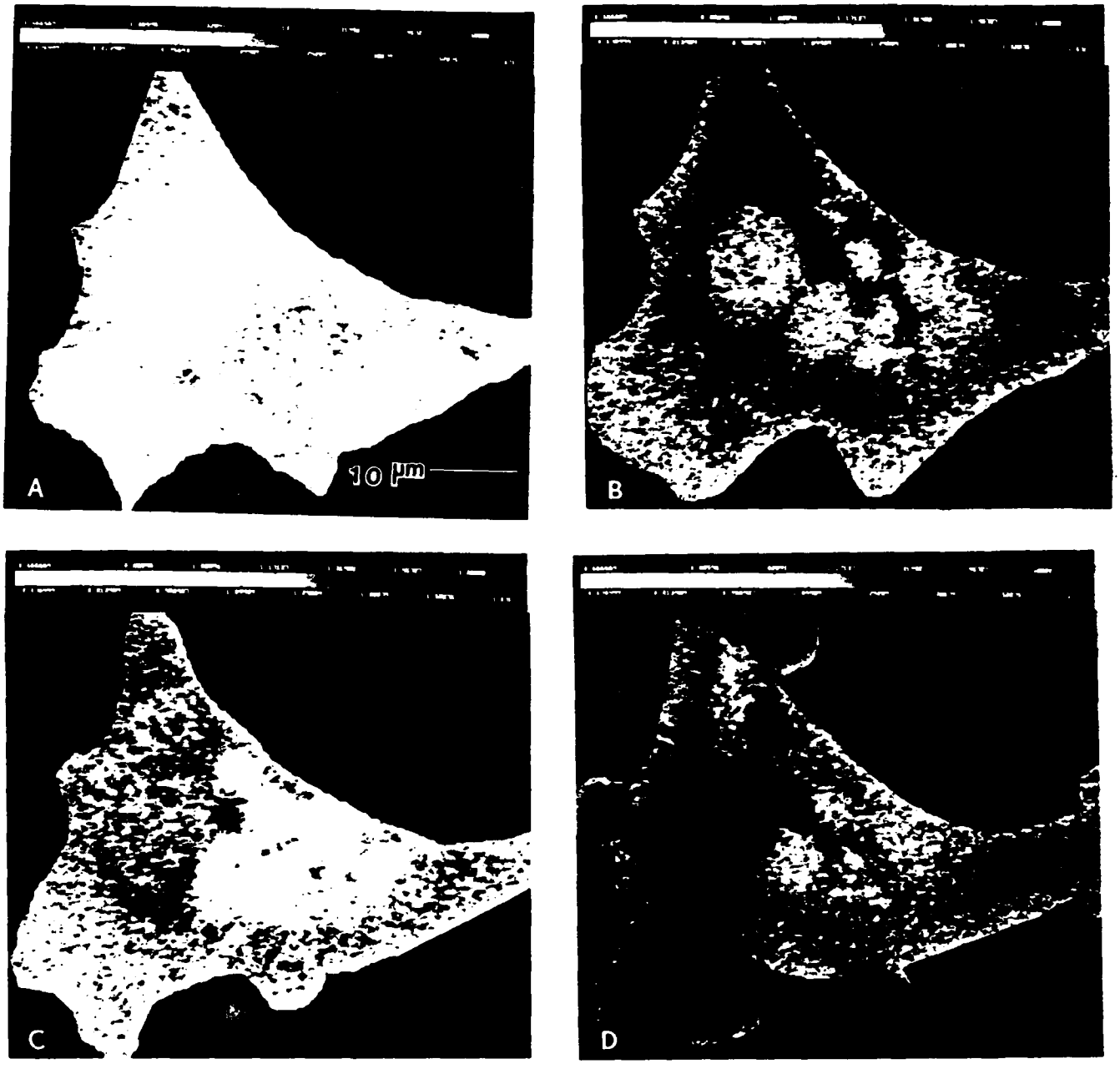

Fig 7

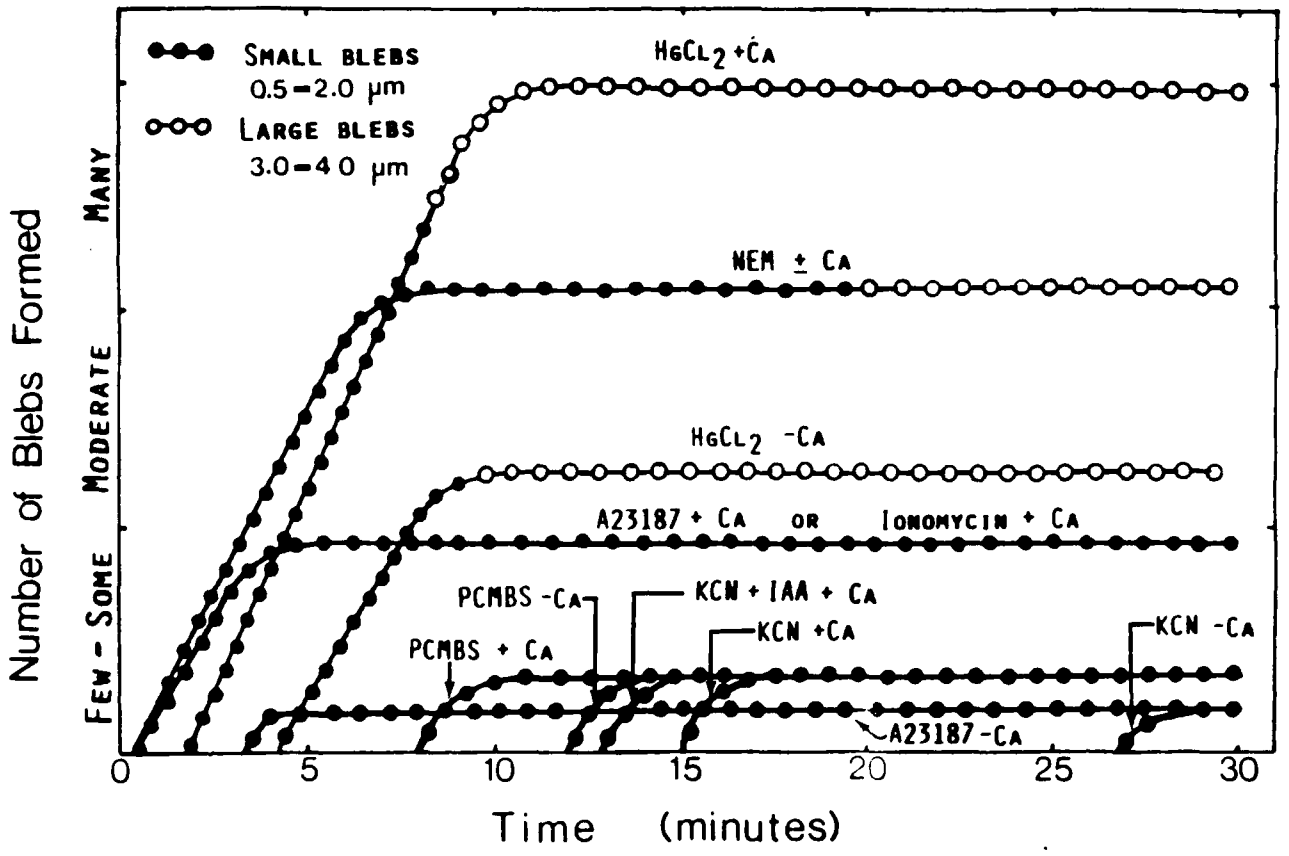
SMALL BLEBS
0.5–2.0 μm
LARGE BLEBS
3.0–4.0 μm
HgCl2 +Ca
NEM ± Ca
HgCl2 -Ca
A23187 + Ca OR Ionomycin + Ca
PCMBS -Ca
KCN + IAA + Ca
KCN +Ca
KCN -Ca
PCMBS + Ca
A23187 -Ca
Number of Blebs Formed
FEW - SOME MODERATE MANY
0
5
10
15
20
25
30
Time (minutes)

Fig 8

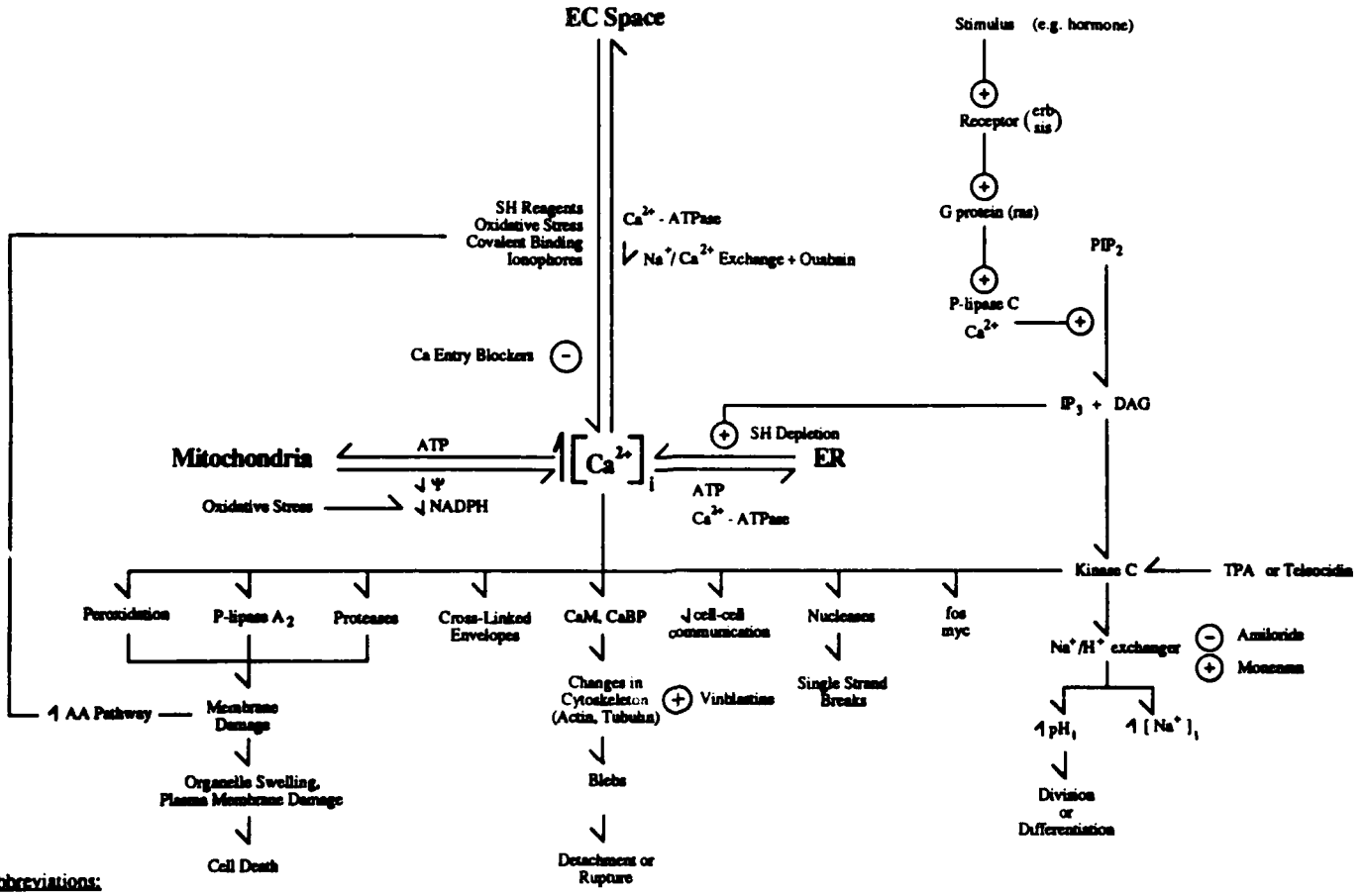

Abbreviations:

PIP = Phosphatidylinositol 4, 5 - diphosphate
Ψ = Mitochondrial membrane potential
CaM = Calmodulin
CaBP = Other calcium-binding proteins
TPA = 12 - O - Tetradecanoylphorbol - 13 - acetate

Fig 9

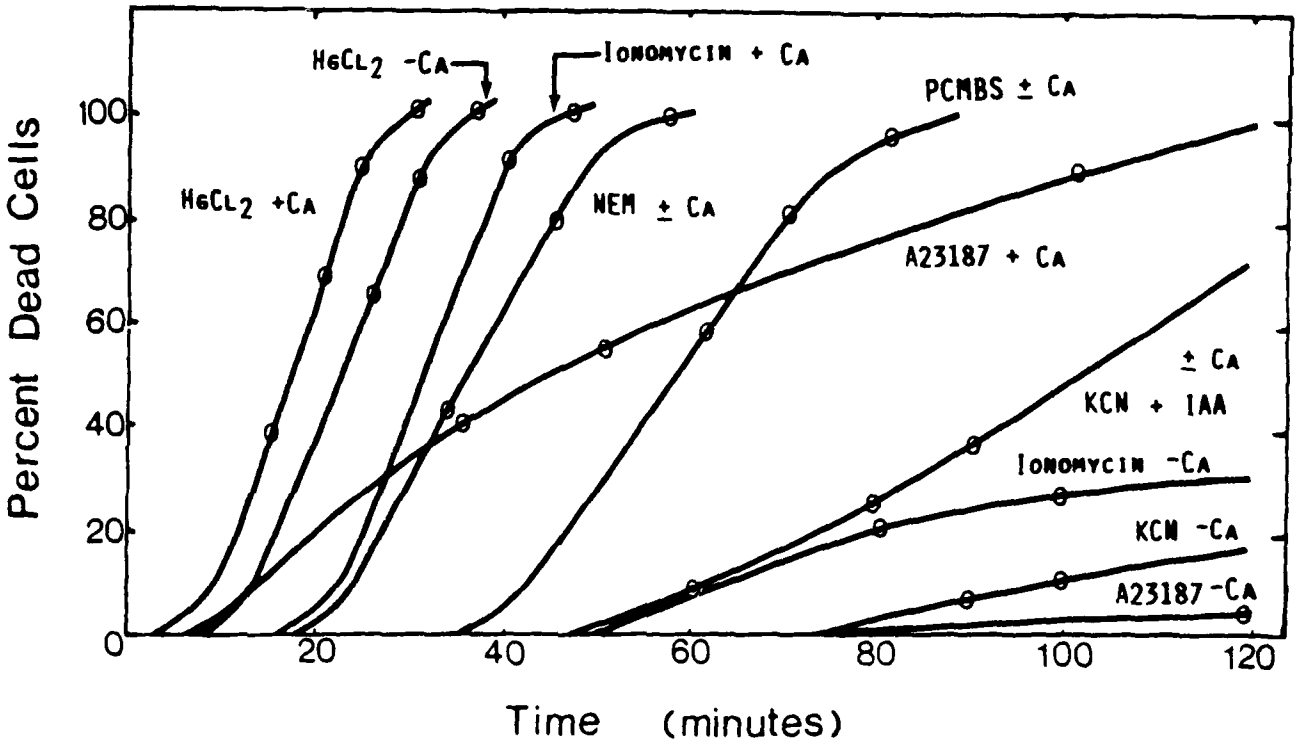
Percent Dead Cells
100
80
60
40
20
0
20
40
60
80
100
120
Time (minutes)
HgCl2 -Ca
Ionomycin + Ca
PCMBS ± Ca
HgCl2 +Ca
NEM ± Ca
A23187 + Ca
± Ca
KCN + IAA
Ionomycin -Ca
KCN -Ca
A23187 -Ca

Fig 10

CULTURE AND CHARACTERIZATION OF NORMAL RAT KIDNEY PROXIMAL TUBULE EPITHELIAL CELLS IN DEFINED AND UNDEFINED MEDIA

KATHRYN A. ELLIGET and BENJAMIN F. TRUMP

Department of Pathology

University of Maryland School of Medicine

and

Maryland Institute for Emergency Medical Services Systems

Baltimore, Maryland 21201

Running Title: Rat Proximal Tubule Cells

Address for Correspondence: Benjamin F. Trump, M.D.

Department of Pathology

University of Maryland School of Medicine

10 South Pine Street

Baltimore, Maryland 21201

SUMMARY

Normal rat kidney proximal tubule (NRKPT) epithelial cells were isolated by collagenase-pronase digestion of renal cortex and studied in primary culture for 10 d. The tubule suspension was seeded in Dulbecco's Modified Eagle Medium 50%:Ham's F12 50% (DME:F12) with 10% fetal bovine serum and at 24 h the medium was changed to compare three media: 1) DME:F12 with 10% FBS (DF-S); 2) serum-free DME:F12 (DF-SF); and 3) serum-free DME:F12 supplemented with insulin, hydrocortisone, transferrin, and epidermal growth factor (DF-SF+). Results of this study indicate that NRKPT cells proliferate more rapidly in medium with serum than in serum-free or growth factor-supplemented medium. Proliferation was assessed by cell count and total protein. Growth curves showed that by 4 d, cells in DF-SF+ and DF-SF were 57% and 42%, respectively, of those in DF-S. Total protein profiles correlated with changes in cell number. By light microscopy, the cells were squamous with numerous mitochondria, a central nucleus, and a rather well-defined homogeneous ectoplasm. By electron microscopy, the cells were polarized with microvilli and cell junctions at the upper surface and a thin basal lamina toward the culture dish. They stained positively for keratin and negative for Factor VIII and vimentin, and expressed activities of the microvillar hydrolases γ-glutamyltranspeptidase and leucine aminopeptidase. Day 7 cells exhibited Na^+-dependent glucose transport activity which was inhibited by 0.1 mM ouabain. Multicellular domes were evident in the second week of culture. These studies demonstrated that NRKPT cells represent a satisfactory model for studies of normal and abnormal biology of the renal proximal tubule epithelium.

Key Words: proximal tubules, primary culture, domes, glucose transport, proliferation

INTRODUCTION

Primary renal proximal tubule epithelial (PTE) cell cultures are essential for the study of renal cell responses to injury and mechanisms of toxicity because the PTE is a major target of cell toxicity and *in vitro* methods, and cell monolayers are an essential part of current evaluation of intracellular effects. Such studies involve the critical evaluation of toxic compounds. If serum is present in the medium, effects can be decreased or enhanced by the presence of endogenous serum components such as proteins, steroid hormones, mitogens, antibodies, or toxins. Moreover, in some epithelia, serum fosters the occurrence of terminal differentiation. For this reason, it is important to use a serum-free defined culture medium which both satisfies the nutritional requirements of cells and does not interfere with the experimental design.

Defining a hormone- and growth factor-supplemented medium often requires systematic and lengthy studies (16,17). Moreover, growth requirements of primary cultured cells have been studied less extensively than those of continuous tumorigenic or non-tumorigenic cell lines. It is known that growth requirements for primary cell cultures are more complex and typically demand more rigorous definition of culture conditions when compared to continuous cell lines (3,4). Indeed, many laboratories have been working to define and maintain a normally differentiated state in primary cultured epithelia through manipulation of the culture environment (9,10,21). Chung et al. (10) have formulated a serum-free growth factor-supplemented medium to maintain primary rabbit proximal tubule cells for several days. Hormone and growth factor deletion studies revealed that these cells require insulin, hydrocortisone and

transferrin for proliferation but did not respond to epidermal growth factor or triiodothyronine. A complex medium composed of hormones and growth factors was developed by Lechner et al. (22,23) for culturing normal human bronchial epithelium. In addition to hormones and hormone-like components, this medium has trace elements and bovine pituitary extract, an undefined factor. Although much has been learned regarding the growth requirements of some types of primary cultured cells (11,12,28), complete growth requirements are not understood for normal rat kidney proximal tubule (NRKPT) cells. Because of this fact, we have set out to characterize NRKPT cells in culture and to study the serum-free conditions for optimal proliferation and expression of differentiated function.

MATERIALS AND METHODS

Media and Solutions. The basal medium was Dulbecco's Modified Eagle Medium 50%:Ham's F12 50% (DME:F12, GIBCO Laboratories, Grand Island Biological Co., Grand Island, NY) containing 1.2 mg/ml $NaHCO_3$, 15 mM HEPES buffer, and 50 µg/ml gentamycin sulfate (Sigma Chemical Co., St. Louis, MO). To this medium was added (1) 10% fetal bovine serum (FBS, Hazelton Biologics, Inc., Lenexa, KS) or (2) 10 µg/ml insulin, 10 µg/ml transferrin, $2x10^{-7}$ M hydrocortisone (all three from Sigma Co.), and 10 ng/ml epidermal growth factor (Collaborative Research, Inc., Bedford, MA). Growth supplements were added immediately prior to use.

The digestion solution was HBSS Ca^{2+}-, Mg^{2+}-free (GIBCO) with the following additions: 350 mg/L $NaHCO_3$, 15 mM HEPES buffer, 700 mg/L $CaCl_2$, 200 mg/L sodium pyruvate, 1 g/L glucose, 0.125 mg/ml collagenase (Type I, Sigma), 1 g/L protease, neutral Dispase (Boehringer Mannheim Biochemicals, Indianapolis, IN), and 0.0025% soybean trypsin inhibitor (Sigma Co.).

Proximal Tubule Cell Isolation. Kidneys from 150-200 g male Fischer 344 rats were surgically removed and placed in HBSS at 0-4°C. Whole kidneys were washed 3X in HBSS (0-4°C), decapsulated and washed again in complete DME:F12. The cortex and outer stripe of the outer medulla were removed, washed with complete DME:F12 (0-4°C), cut into 1-2 mm^3 pieces, and washed a final time with serum-free DME:F12 (0-4°C). Tissue pieces were transferred to a Tekmar (Tekmar Company, Cincinnati, OH) sterile plastic bag to which 20 ml digestion solution was added. The bag was placed in a Tekmar Stomacher Lab Blender and agitated at room temperature for 10 sec, the supernatant was discarded and 20 ml fresh digestion solution added. The first digestion served as a wash.

Tissue was then agitated in the stomacher for 10-20 sec and all contents put into a 50 ml centrifuge tube. The suspension was centrifuged at 50 X g for 3 min, supernatant discarded, pellet resuspended in 50 ml digestion solution and put into a spinner flask for a final 20 min digestion at 37°C. The digested cortex was then centrifuged at 50 X g for 3 min and the pellet resuspended in complete DME:F12, quartered, and subjected to two 10 min sedimentation periods at 1 x g and room temperature (RT). The final pellet was proximal tubule-rich and the yield could easily accommodate 120, 35 mm culture dishes. Cultures were maintained in a humidified environment of 95% room air:5% CO_2.

MDCK Cell Line. The Madin-Darby canine kidney (MDCK) cell line was obtained from the American Type Culture Collection (Rockville, MD). Cell stocks were maintained in Eagle's minimum essential medium in Earle's balanced salt solution with 10% fetal bovine serum. Cells were subcultivated once a week at a 1:4 dilution. Because of their distal tubule characteristics, MDCK cells were used as the negative control for the Na^+-glucose co-transport study.

Seeding Efficiency. Proximal tubules (PT) were inoculated into 60 mm culture dishes at ~ 0.5 mg protein/ml medium in DME:F12 with 10% FBS. Seeding efficiency was determined by measuring the amount of protein attached at 12 h per unit protein inoculated. At 12 h, attached and unattached tubule/cell protein approximated the amount of protein in the inoculate.

Cell Viability. Viability of tubule fragments was determined with trypan blue dye exclusion and neutral red dye uptake. Four drops of a 1:10 dilution of trypan blue dye (0.4%, GIBCO) were added to each 60 mm culture dish and incubated for 5-10 min at room temperature. A visual count was then made of unstained and stained cells.

Neutral red dye (Sigma Co.) was used as a 50 µg/ml solution in phenol red-free Hank's balanced salt solution, pH 7.2. Prior to use, the dye was centrifuged at 1,000 x g for 5 min and the supernatant used for the assay. Culture medium on test cells was replaced with neutral red solution and left for 3 h at 37°C. Neutral red dye accumulated into lysosomes of live cells (6).

Laminin Biomatrix. Thawed laminin (Sigma Co.) was diluted with sterile tissue culture medium. Culture dishes were coated with 1.5 µg laminin/cm^2 culture dish by allowing them to stand at room temperature for 45 min. Following the incubation period, the laminin solution was aspirated, dishes washed once with culture medium, and cells inoculated into the vessels.

Cell Proliferation. On designated days, cells were counted by dispersing the monolayer with 0.25% trypsin-EDTA (GIBCO) and counting with a hemocytometer. Proliferation, as determined by total cell protein, was determined by the Coomassie blue protein assay (Bio-Rad Laboratories) based on the Bradford method (7). Cell monolayers were washed 5X with PBS and lysed with 0.1 N NaOH for 2 hr at 37°C. A 1:6 dilution of Bio-Rad protein reagent was added to the lysates and 30 min later the solutions were read at 630 nm with a Titertek Multiscan spectrophotometer (Flow Laboratories, McLean, VA).

Microvillar Hydrolases. Leucine aminopeptidase (LAP) enzyme activity was measured by the method of Appel (2) and calculated as μmoles per mg protein per minute of formation of p-nitroaniline from L-leucine-p-nitroanilide. γ-glutamyltranspeptidase (GGT) enzyme activity was measured by the method of Glossman and Neville (14) and calculated as μmoles per mg protein per hour of the liberation of p-nitroaniline from γ-L-glutamyl-p-nitroanilide. Absorbance changes were read at 405 nm for both assays and protein was estimated by the Lowry method (29).

Keratin. Immunohistochemical staining of keratin was performed according to the peroxidase-antiperoxidase method of Schlegel et al. (38). Briefly, 60-80% confluent monolayers were rinsed in PBS and fixed in absolute ethanol for 1 hr at room temperature (RT). Cells were treated with methanolic hydrogen peroxide, washed, and incubated with a 1:10 dilution of normal bovine serum. Cells were then incubated with rabbit antihuman keratin antiserum (1:20 dilution) for 1 hr at RT, washed, and incubated with peroxidase-conjugated antirabbit IgG (1:20 dilution) for 1 hr at RT. After extensive washing, cells were then incubated with 3,3'-diaminobenzidine tetrahydrochloride for 15 min at RT. Antibody localization was determined by detection of peroxidase activity, a brown reaction product.

Factor VIII and Vimentin. Indirect immunofluorescence was performed on cells previously fixed in 100% acetone at -20°C for 5 min and stored at -70°C on coverslips (36). Coverslips were warmed to room temperature and rinsed in phosphate buffered saline (PBS: 171 mM NaCl, 3 mM KCl, 1 mM $CaCl_2$, 0.5 mM $MgCl_2$, in 20 mM phosphate buffer, pH 7.2). Cells were then incubated with either anti-Factor VIII or anti-vimentin monoclonal primary antibodies

(Transformation Research, Inc., Framingham, MA; diluted 1:20 in PBS) for 45 min at 37°C. Following three 10 min rinses with PBS, cells were incubated with affinity purified goat anti-mouse fluorescein isothiocyanate (FITC)-labeled secondary antibodies (Cooper Biomedical, Inc., Malvern, PA; diluted 1:20 in PBS) for 45 min at 37°C. Cells were then rinsed with five 10 min changes in PBS and mounted on glass slides in a non-quenching medium. Preparations were viewed with a Zeiss Photomicroscope III with epifluorescence.

Electron Microscopy. Cells cultured for transmission electron microscopy were seeded into 60 mm culture dishes. At the end of the experiment, monolayers were washed 3X with PBS and fixed in 3% glutaraldehyde in 0.1 M cacodylate buffer, pH 7.4. Cells were post-fixed in 1% osmium tetroxide, en bloc stained with uranyl acetate, dehydrated in 2 graded series of alcohols and propylene oxide, infiltrated with ratios of Polybed 812/propylene oxide, and embedded with Polybed 812 (Polysciences, Warrington, PA). Ultrathin sections were cut and mounted on 200 mesh, coated grids. Sections were stained with uranyl acetate and lead citrate and examined in a JEOL CX1 transmission electron microscope.

Na^+-glucose Co-transport. Seven day cultures in 35 mm plastic culture dishes were used for measurement of the uptake of α-methylglucoside (AMG), by the method of Chung et al. (10). Monolayers were washed X3 with a modified Kreb's Ringer solution where Na_2HPO_4 replaces $NaHCO_3$. Cells were incubated at room temperature (RT) in modified Kreb's Ringer solution with 0.5 mCi/mmol methyl α-D-glucopyranoside, [glucose-^{14}C(U)]-(New England Nuclear, Boston, MA) and 1 mM unlabeled AMG (1-O-methyl α-D-glucopyranoside, Sigma Co.). At the

end of the uptake period, cells were washed 3X with modified Kreb's Ringer solution and solubilized overnight with 0.1 N NaOH. Two hundred µl of each sample were taken for protein determination and the remainder of each sample for scintillation counting. The radioactive counts in each sample were normalized with respect to protein and corrected for zero-time uptake. The uptake was measured in 1) modified Kreb's Ringer; 2) Na^+-free modified Kreb's Ringer; 3) after a 20 min preincubation of cultures with 0.1 mM ouabain in Na^+-containing modified Kreb's Ringer; 4) after a 20 min preincubation of cultures with 0.1 mM ouabain in Na^+-free modified Kreb's Ringer; and 5) in the Madin-Darby canine kidney (MDCK) cell line in Na^+-containing modified Kreb's Ringer. For the Na^+-free assay, the Na_2HPO_4 and NaCl were replaced by K_2HPO_4 and sucrose, respectively. Values are expressed as nanamoles of AMG per mg protein. Protein was determined by the Coomassie blue protein assay (Bio-Rad Laboratories) based on the Bradford method (7).

RESULTS

Growth Characteristics. The seeding efficiency of tubule fragments is routinely 60%. By our calculations, this estimation of recovery was done at a time when a maximum number of tubules had attached and before mitosis. It was performed only as a crude estimation to determine the percent of tubules that attach at any given isolation. The population doubling time during log growth was found to be 21.8 h in DF-S, 25.9 h in DF-SF+, and 27.4 h in DF-SF. When the DF-SF+ medium was used to isolate NRKPT cells, seeding efficiency decreased 40% compared to DF-S. A laminin biomatrix did not increase the seeding efficiency when used in conjunction with the growth factor-supplemented medium.

Morphology. Figure 1A shows a NRKPT cell culture at 24 h. The cells appeared to be growing from the open ends of tubule fragments to form small colonies at 24 h and a confluent monolayer by 5-7 d. The majority of the tubule fragments, though prominent at 24 h, eventually diminished in size to become part of the monolayer (Fig. 1B). These tubule remnants excluded trypan blue dye, incorporated the vital dye neutral red, and stained positively for GGT enzyme activity.

The ultrastructure of the NRKPT cells was studied at day 4. By transmission electron microscopy (Figs. 2A,B), the polarized nature of the epithelium was evident. The apical cell surface was at the medium interface and was covered with a rudimentary microvillus border. Junctional complexes were present toward the apical surface (Fig. 2A) while desmosomes and gap junctions appeared along the lateral cellular interdigitations. Though cultured cells are often described as monolayers, we have observed cell

overlapping, often up to 3 layers with extensive lateral cellular interdigitations. Bundles of microfilaments coursed parallel to a thin basal lamina (Fig. 2A). The cytoplasm contained a centrally located nucleus, a well-defined supranuclear Golgi apparatus (Figs. 2C), lysosomes, autophagic vacuoles and numerous coated vesicles and vacuoles which made up the endocytic apparatus. There were abundant mitochondria, rough and smooth endoplasmic reticulum and free polysomes. Lipid droplets were seen in some cells (presumably from the P_3 segment).

Multicellular domes were present in the second week of culture. More domes were apparent in cultures incubated in DF-SF+ compared to cells grown in serum-containing medium.

Cell Markers. Cultures were analyzed immunohistochemically for keratin on days 1, 4 and 7 and the characteristics of staining were unchanged through this time frame. Day 4 cells were negative for vimentin and Factor VIII. Analysis of γ-glutamyltranspeptidase (GGT) and leucine aminopeptidase (LAP) enzyme activities (Table 1) indicate that these parameters were significantly reduced over the 10 d culture period. Both GGT and LAP were markedly reduced between days 2 and 4. GGT activity spiked at day 2, decreased between days 2 and 4, and remained low through day 10 (day 10 activity is 16% of day 1). LAP activity steadily declined from day 1 to day 4 and remained low through day 10 (day 10 activity is 27% of day 1).

Proliferation and Media Comparison. Continuous growth of NRKPT cells was evaluated by comparing three different media. Tubules were inoculated in DF-S and at 24 h the medium changed to either DF-S, DF-SF+ or DF-SF. Cells were counted on days, 1, 2, 3, 4, 7, and 10. Figure 3A represents the growth

curves of NRKPT cells in each of the three media. The curves are a semilogarithmic plot of cell density (cells per milliliter of culture medium) as a function of time. Cells in DF-S and DF-SF+ were in the exponential phase of growth between days 1 and 4. Cells in DF-S reached the stationary growth phase at day 4 and remained in the non-proliferative state through day 10. Cells in DF-SF+ appeared to be in the stationary phase between days 7 and 10. Under serum-free growth factor-free conditions, a lag phase was apparent between days 1 and 2, exponential growth between days 2 and 4, and a stationary phase from day 4 through 10. Media were changed on days 3, 5, 7, and 9. Figure 3B shows cell growth as a function of time as determined by protein measurements on days 1, 4, 7, and 10. While in serum-containing medium (DF-S), cellular protein increased between days 1 and 4 (log phase of growth), and steadily decreased between days 4 and 10. Growth factor-supplementation of DME:F12 basal medium (DF-SF+) resulted in increase in protein between days 1 and 4, no increase between days 4 and 7, and a minor surge between days 7 and 10 (possibly a reflection of the medium change on day 7). Serum-free medium (DF-SF) caused a gradual increase in cell protein concentration from day 1 to 4, and gradual decline from day 4 to day 10.

Figures 4A-C are light micrographs of cultures at 7 days in three medium formulations. At 24 h, the cultures were washed 3X with HBSS and refed with either DF-S, DF-SF+ or DF-SF. The morphology of the cells was dependent on the medium. In the presence of serum (Fig. 4A), some cells became pleomorphic and lost the pavement-like appearance of those in a tight epithelial sheet, such as those grown in serum-free growth factor-supplemented medium (Fig. 4B). The

loss of pavement-like morphology was especially evident at the edge of colonies. Under serum-free conditions (Fig. 4C), there were fewer cells and cell spreading was more prominent.

Na^+-glucose Co-transport. As a functional marker of the proximal tubule cells, we tested their ability to transport glucose in an Na^+-dependent manner. The Na^+-glucose transporter is located on the apical surface of the proximal tubule cells and does not function in other nephron segments. The transport of α-methylglucoside (AMG), a non-metabolizable sugar, was studied in 7 d cultures. Figure 5 illustrates the uptake of 1 mM AMG into 7 d cultures over a 210 min period at room temperature. After 210 min in the absence of Na^+, AMG uptake was inhibited by 70%. Ouabain at 0.1 mM inhibited AMG uptake in the presence and absence of Na^+ by 51% and 85%, respectively. No uptake of AMG was evident in the MDCK cell line.

DISCUSSION

NRKPT cells are stimulated to proliferate by insulin, hydrocortisone, transferrin and epidermal growth factor in basal DME:F12. Cell proliferation in DF-SF was significantly different than that in DF-S at 2 d, 7 d ($p < 0.01$), and 10 d ($p < 0.05$). After 3 d, DF-SF+ was not significantly different than DF-S ($p < 0.01$). Ongoing studies in our laboratory indicate that NRKPT proliferation may be enhanced by the presence of selenium, triiodothyronine and cholesterol in the medium. With these additional supplements, the medium would then be similar to that which has been developed for the LLC-PK1 cell line (9), which was derived from a normal Hampshire pig kidney and has characteristics of proximal tubule epithelial cells. We expect that the growth requirements for NRKPT cells will be more complex than the LLC-PK1 cell line. Short-term cultures of NRKPT epithelial cells are not growth inhibited by the presence of serum as are other cultured epithelial cells (30,41), including mouse keratinocytes (5,19) and human bronchial epithelial cells (24). In addition, a high Ca^{2+} concentration in the medium was not found to be inhibitory to growth, as was reported for mouse epidermal cells (18,20,44) and bronchial epithelial cells (24). Indeed, it has been shown that not all epithelia respond in the same fashion to serum or calcium in the medium (15,43); in mouse keratinocytes and human bronchial epithelium, serum induces terminal differentiation.

Epithelial cell growth from the ends of broken tubule fragments is a characteristic of renal tubule cultures and has been described by others (13,21,40). Within the first 24 h of culture, distinct outgrowths are seen. There are two morphological populations of cells present in the cultures. The

differences are seen with phase microscopy, where one population is flatter than the other. Both populations stain positively for keratin and GGT. We feel that the two populations may represent proximal straight and proximal convoluted tubules. Suzuki et al. (40) report a distinct morphological difference between the proximal convoluted (PCT) and straight tubules (PST) in cultured rabbit tubule cells. PCT are columnar while PST are flattened, when viewed by vertical sections at the TEM level.

The NRKPT cell brush border is not well developed when compared to in vivo proximal tubule epithelia. These results are in agreement with others who have described in vitro proximal tubule brush borders as rudimentary or sparse (9,12,37) which is suggestive of the less differentiated state of cultured epithelial cells. We have found that the degree of brush border development in vitro is not consistent from cell to cell and varies over the monolayer.

Multicellular domes are characteristic of confluent monolayers of transporting epithelia in vitro. They are focal, fluid-filled spaces between the basolateral surface and substrate on which the cells are attached. Dome formation is thought to be dependent on three major characteristics: 1) an impermeable substrate, 2) occluding junctions, and 3) unidirectional transport. Domes have been observed in both epithelial cell lines (8,27) and primary cultures (37,39,40). We observed dome formation in the second week of culture. These results are consistent with the demonstration of Na^+-glucose co-transport, morphological polarity, and the presence of junctional complexes

in NRKPT cells. Though domes were not abundant under our growth conditions, there appeared to be more in cultures grown in growth factor-supplemented media as opposed to serum-supplemented media.

The activities of two brush border enzymes were studied in primary rat proximal tubule cells. In both cases, enzyme activities declined over the culture period. Low enzyme activities correlate with underdeveloped brush border. These results are in agreement with others who found a similar time-dependent decline in microvillar enzyme activity in cultured epithelia (10,42).

Glucose transport in proximal tubule cells is driven by the Na^+ electrochemical gradient across the membrane. The gradient is maintained by the active extrusion of Na^+ at the basolateral membrane and is ouabain inhibited. The Na^+:glucose ratio is 2:1 (25). The LLC-PK1 cell line has a Na^+-dependent glucose co-transport system characteristic of renal proximal tubules (31,34). In these cells, the expression of the co-transport is dependent on several conditions. For instance, they do not express the transporter in trypsin EDTA-treated confluent monolayers or exponentially growing cells; confluency is a requirement (1). Several studies show that the transport property can be manipulated by culture conditions (32,33), such as cell density, where transport increases with density. NRKPT epithelial cells express a Na^+:glucose co-transport that is inhibited by ouabain and is Na^+-dependent. Ouabain (0.1 mM) inhibited AMG uptake in the presence and absence of Na^+. In our experimental system, ouabain inhibition in the presence of Na^+ was only 51%. This low inhibition is likely due to the plastic substrate. Transepithelial transport is best measured in cells on a

porous substratum. Thus, the cell-substrate relationship is a great factor influencing in vitro transport. Indeed, Cereijido et al. (8) have discussed the importance of the substrate in ion fluxes and suggest that the pumps are working against an impermeable plastic substrate which has a detrimental affect on transport. The MDCK cell line was used as a negative control for the Na^+:glucose transport because it has previously been found to lack AMG uptake activity (35).

We have examined short-term NRKPT cell cultures and conclude that they exhibit functional and structural properties of proximal tubules. Our impression is that they are less differentiated over time in culture. Though the in vitro conditions for induction of proliferation and/or differentiation of NRKPT cells are unknown, our studies indicate that combinations of growth factors and hormones are capable of supporting proliferation in serum-free medium. In this study, we have focused on improvement of growth and have not specifically tried to formulate a medium for improving expression of differentiated function. Further studies are necessary, however, to establish optimal growth requirements as well as maintenance of a differentiated state. The NRKPT cell culture system is a credible model with which to study the in vitro cellular responses to injury in the kidney.

REFERENCES

1. Amsler, K.; Cook, J. S. Development of Na^+-dependent hexose transport in a cultured line of porcine kidney cells. Am. J. Physiol. 242: C94-C101; 1982.

2. Appel, W. Leucine aminopeptidase. Bergmeyer, H. V. ed. Methods of enzymatic analysis. Vol. 2. New York: Verlag Chemie Weinheim, Academic Press; 1974: 954-963.

3. Barnes, D.; Sato, G. Methods for growth of cultured cells in serum-free medium: Review. Anal. Biochem. 102: 255-270, 1980.

4. Barnes, D. W.; Sato, G. H. Serum-free cell culture: an underlying approach. Cell 22: 649-655; 1980.

5. Bertolero, F.; Kaighn, M. E.; Camalier, R. F.; Saffiotti, U. Effects of serum and serum-derived factors on growth and differentiation of mouse keratinocytes. In Vitro 22: 423-428; 1986.

6. Borenfreund, E.; Puerner, J. A. Cytotoxicity of metals, metal-metal and metal-chelator combinations assayed in vitro. Toxicology 39: 121-134; 1986.

7. Bradford, M. A rapid and sensitive method for the quantitation of microgram quantities of protein utilizing the principle of protein-dye binding. Anal. Biochem. 72:248-254; 1976.

8. Cereijido, M.; Ehrenfeld, J.; Fernandez-Castelo, S.; Meza, I. Fluxes, junctions, and blisters in cultured layers of epithelioid cells (MDCK). Ann. N.Y. Acad. Sci. 81: 422-441; 1981.

9. Chuman, L.; Fine, L. G.; Cohen, A. H.; Saier, M. H., Jr. Continuous growth of proximal tubular kidney epithelial cells in hormone-supplemented serum-free medium. J. Cell Biol. 94: 506-510; 1982.

10. Chung, S. D.; Alavi, N.; Livingston, D.; Hiller, S.; Taub, M. Characterization of primary rabbit kidney cultures that express proximal tubule functions in a hormonally defined medium. J. Cell Biol. 95: 118-126; 1982.

11. Detrisac, C. J.; Sens, M. A.; Garvin, J.; Spicer, S. S.; Sens, D. A. Tissue culture of human epithelial cells of proximal tubule origin. Kidney Int. 25: 383-390; 1984.

12. Fine, L. G., Sakhrani, L. M. Proximal tubular cells in primary culture. Mineral Electrolyte Metab. 12: 51-57; 1986.

13. Frielle, T.; Tong, J.; Curthoys, N. P. Changes in rat renal glutaminase activity studied in vivo and in primary cultures of proximal convoluted tubular cells. Contr. Nephrol. 47: 150-156; 1985.

14. Glossmann, H.; Neville, D. M., Jr. γ-glutamyltransferase in kidney brush border membranes. FEBS Lett. 19: 340-344; 1972.

15. Grisham, J. W.; Smith, J. D.; Tsao, M. S. Colony forming ability in calcium-poor medium in vitro and tumorigenicity in vivo coupled in clones of transformed rat hepatic epithelial cells. Cancer Res. 44: 2831-2834; 1984.

16. Ham, R. G. Survival and growth requirements of nontransformed cells. Baserga, R. ed. Tissue growth factors. New York: Springer-Verlag Berlin; 1981: 13-83.

17. Ham, R. G.; St. Clair, J. A.; Webster, C.; Blau, H. M. Improved media for normal human muscle satellite cells: serum-free clonal growth and enhanced growth with low serum. In Vitro Cell Devel. Biol. 24: 833-844; 1988.

18. Hennings, H.; Michael, D.; Cheng, C.; Steinert, P.; Holbrook, K.; Yuspa, S. H. Calcium regulation of growth and differentiation of mouse epidermal cells in culture. Cell 19: 245-254; 1980.

19. Kaighn, M. E.; Camalier, R. F.; Bertolero, F.; Saffiotti, U. Spontaneous establishment and characterization of mouse keratinocyte cell lines in serum-free medium. In Vitro Cell Devel. Biol. 24: 845-854; 1988.

20. Kulesz-Martin, M. F.; Koehler, B.; Hennings, H.; Yuspa, S. H. Quantitative assay for carcinogen altered differentiation in mouse epidermal cells. Carcinogenesis 1: 995-1006; 1980.

21. Larsson, S.; Aperia, A.; Lechner, C. Studies on final differentiation of rat renal proximal tubular cells in culture. Am. J. Physiol. 251: C455-C464; 1986.

22. Lechner, J.F.; Haugen, A.; Autrup, H.; McClendon, I. A.; Trump, B. F.; Harris, C. C. Clonal growth of epithelial cells from normal adult human bronchus. Cancer Res. 41: 2294-2304; 1981.

23. Lechner, J.F.; Haugen, A.; McClendon, I.A.; Pettis, E. W. Clonal growth of normal adult human bronchial epithelial cells in a serum-free medium. In Vitro 18: 633-642; 1982.

24. Lechner, J. F. Interdependent regulation of epithelial cell replication by nutrients, hormones, growth factors, and cell density. Fed. Proc. 43: 116-120; 1984.

25. Lever, J. E. Expression of a differentiated transport function in apical membrane vesicles isolated from an established kidney epithelial cell line: sodium electrochemical potential-mediated active sugar transport. J. Biol. Chem. 257: 8680-8686; 1982.

26. Lever, J. E. Expression of differentiated functions in kidney epithelial cell lines. Mineral Electrolyte Metab. 12: 14-19; 1986.

27. Lever, J. E.; Sari, C. E. Effect of tunicamycin on polarized membrane functions of an established kidney epithelial cell line. Biochim. Biophys. Acta 762: 215-271; 1983.

28. Lipman, R. D.; Harris, R. C.; Seifter, J. L.; Brenner, B. M.; Lechner, C. Growth of rat proximal tubular cells (RPTC) occurs at the periphery of a colony, where cells are more alkaline and have a higher K/Na ratio. Kidney Int. 29: 402-408; 1986.

29. Lowry, O. H.; Rosebrough, N. J.; Farr, A. L.; Randall, R. J. Protein measurement with the Folin phenol reagent. J. Biol. Chem. 193: 269-275; 1951.

30. Masui, T.; Wakefield, L. M.; Lechner, J.F.; LaVeck, M. A.; Sporn, M. B.; Harris, C. C. Type β transforming growth factor is the primary differentiation-inducing serum factor for normal human bronchial epithelial cells. Proc. Natl. Acad. Sci. USA 33: 2438-2442; 1986.

31. Moran, A.; Handler, J. S.; Turner, J. R. Na^+-dependent hexose transport in vesicles from cultured renal epithelial cell line. Am. J. Physiol. 243: C293-C298; 1982.

32. Mullin, J. M.; Diamond, L.; Kleinzeller, A. Effects of ouabain and orthovanadate on transport-related properties of the LLC-PK1 renal epithelial cell line. J. Cell Physiol. 105: 1-6; 1980.

33. Mullin, J. M.; Weibel, J.; Diamond, L.; Kleinzeller, A. Sugar transport in the LLC-PK1 renal epithelial cell line: similarity to mammalian kidney and the influence of cell density. J. Cell Physiol. 104: 375-389; 1980.

34. Rabito, C. A. Localization of the Na^+-sugar cotransport system in a kidney epithelial cell line (LLC-PK1). Biochim. Biophys. Acta 649: 286-296; 1981.

35. Rabito, C. A. Sodium co-transport processes in renal epithelial cell lines. Mineral Electrolyte Metab. 12: 32-41; 1986.

36. Resau, J. H.; Phelps, P. C.; He', A.; Anthony, R. L.; Jones, R. T. Long-term culture of hamster duodenal explants and cells. Digestion 41: 9-21; 1988.

37. Sakhrani, L. M.; Badie-Dezfooly, B.; Trizna, W.; Mikhail, N.; Lowe, A. G.; Taub, M.; Fine, L. G. Transport and metabolism of glucose by renal proximal tubular cells in primary culture. Am. J. Physiol. 246: F757-F764; 1984.

38. Schlegel, R.; Banks-Schlegel, S.; Pinkus, G. S.; Immunohistochemical localization of keratin in normal human tissues. Lab. Invest. 42: 91-96; 1980.

39. Sugahara, K.; Caldwell, J. H.; Mason, R. J. Electrical currents flow out of domes formed by cultured epithelial cells. J. Cell Biol. 99: 1541-1546; 1981.

40. Suzuki, M.; Capparelli, A.; Jo, O.; Kawaguchi, Y.; Ogura, Y.; Miyahara, T.; Yanagawa, N. Phosphate transport in the in vitro cultured rabbit proximal convoluted and straight tubules. Kidney Int. 34: 268-272; 1988.

41. Takehara, K.; LeRoy, E. C.; Grotendorst, G. R. TGF-β inhibition of endothelial cell proliferation: alteration of EGF binding and EGF-induced growth-regulatory (competence) gene expression. Cell 49: 415-422; 1987.

42. Trifillis, A. L.; Regec, A. L.; Trump, B. F. Isolation, culture and characterization of human renal tubular cells. J. Urology 133: 324-329; 1985.

43. Trump, B. F.; Berezesky, I. K. Ion regulation, cell injury and carcinogenesis. Carcinogenesis 8: 1027-1031; 1987.

44. Yuspa, S. H.; Koehler, B.; Kulesz-Martin, M.; Hennings, H. Clonal growth of mouse epidermal cells in medium with reduced calcium concentration. J. Invest. Dermatol. 76: 144-146; 1981.

ACKNOWLEDGEMENTS

The authors would like to thank Mr. Wayne J. Ivusich for his professional assistance in preparing the manuscript and Dr. Raymond T. Jones for his reading and critical review. This project was supported by NIH, #2-R01-DK15440-16A1 and Department of the Navy, #N00014-88-K-0427.

TABLE 1

MICROVILLAR HYDROLASE ACTIVITIES IN NRKPT EPITHELIAL CELLS[a]

Day	Enzyme[b]	
	γ-glutamyltranspeptidase (GGT)	leucine aminopeptidase (LAP)
0 (tubule suspension)	13.6±0.3	45.4±1.4
1	30.6±2.4	14.7±1.2
2	79.3±3.9	12.3±0.5
4	7.7±0.3	3.5±0.2
7	5.7±0.5	4.2±1.1
10	5.0±0.7	4.0±0.3

[a]Experiments were performed at 37°C. [b]Both enzyme activities are expressed as nmoles p-nitrophenyl x mg^{-1} x min^{-1}. Values are mean ± SEM, n=6.

FIGURE LEGENDS

Figure 1: Phase contrast micrographs of normal rat kidney proximal tubule epithelial cells (A) growing from tubule fragments (arrow), 24 h post-isolation, and (B) at 4 days, where whole tubule fragments are less prominent than at 24 h (arrow). A & B X149.

Figure 2: Transmission electron micrographs of normal rat kidney proximal tubule epithelial cells at 4 days in culture. (A) Vertical section shows a polarized cell with microvilli at the apical surface and a thin basal lamina toward the dish (arrow). A junctional complex is seen near the apical surface, cellular interdigitation, and a cytoplasmic lipid droplet. (B) There are numerous mitochondria, rough and smooth endoplasmic reticulum, and abundant free polysomes. Coated vesicles and vacuoles make up the endocytic apparatus. (C) The supranuclear Golgi apparatus is well-defined (g), and cellular interdigitation is prominent (arrows). A x33,800; B x10,600; C x20,000.

Figure 3: Growth curves showing normal rat kidney proximal tubule cell proliferation through 10 days. Proximal tubules were seeded in DME:F12 with 10% FBS (DF-S). After 24 h, the cells were washed and the medium changed to compare (1) DME:F12 with 10% FBS (DF-S) (square); (2) DME:F12 supplemented with 10 ug/ml insulin, 10 ug/ml transferrin, $2x10^{-7}$ M hydrocortisone and 10 ng/ml epidermal growth factor (DF-S+) (circle); and (3) DME:F12 serum-free (DF-SF) (triangle). Media were changed on days 3, 5, 7, and 9. Both cell number (A) and total cellular protein (B) were analyzed. Each

value is mean ± SEM for three separate experiments, n=3 for each experiment. After 72 h (A), the curves for DF-S and DF-S+ were not significantly different ($p<0.01$).

Figure 4: Phase contrast micrographs of 7 day normal rat kidney proximal tubule cells grown in (A) DME:F12 with 10% FBS (DF-S); (B) DME:F12 supplemented with 10 µg/ml insulin, 10 µg/ml transferrin, 5×10^{-7} M hydrocortisone and 10 ng/ml epidermal growth factor (DF-S+); and (C) DME:F12 serum-free (DF-SF). A. X147, B. X154, C. X141.

Figure 5: α-methylglucoside (AMG) uptake in normal rat kidney proximal tubule cells 7 d in culture in the presence of Na^+ (open square), absence of Na^+ (solid square), in the presence of 0.1 mM ouabain in Na^+-containing solution (solid circle), 0.1 mM ouabain in Na^+-free solution (open circle), and in the MDCK cell line (solid triangle). NaCl and $NaHPO_4$ were replaced by 0.3 M sucrose and K_2HPO_4, respectively, in the Na^+-free modified Kreb's Ringer solution. AMG uptake was measured after incubation in medium containing (^{14}C) AMG at room temperature. Values are mean ± SEM, n = 9.


A
g
B'
C

Figure 3A

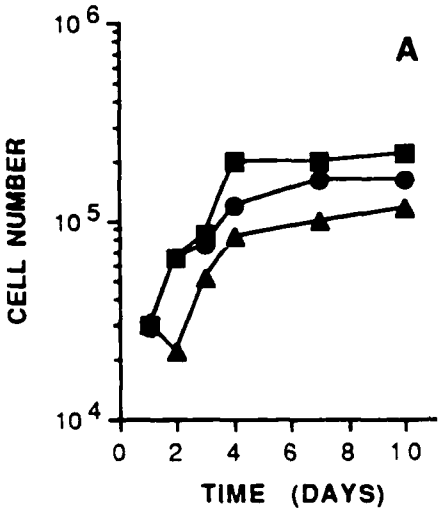

Figure 3B

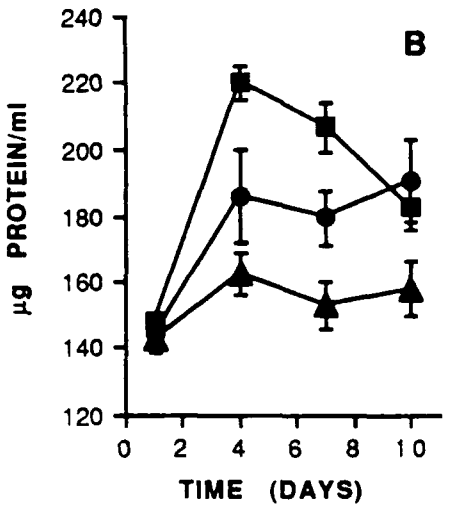

Figure 5

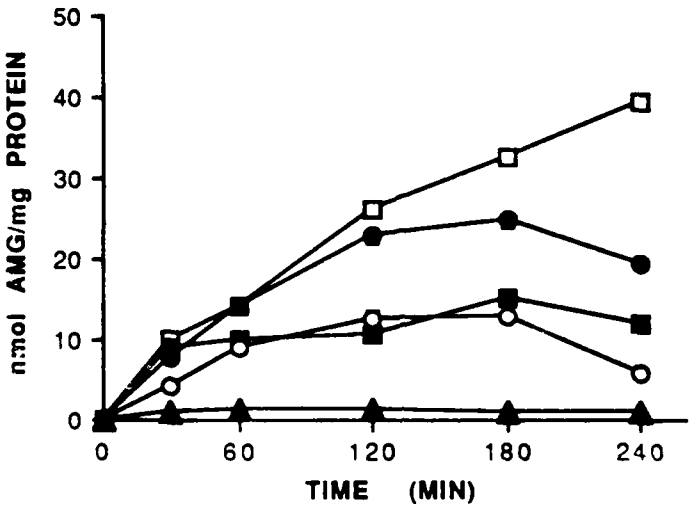

HOW IS INTRACELLULAR IONIZED $[Ca^{2+}]_i$ IN PROXIMAL TUBULE EPITHELIUM (PTE) RELATED TO NEPHROTOXICITY DIGITAL IMAGING FLUORESCENCE MICROSCOPY (DIFM) STUDIES?

B.F. Trump, M.W. Smith, P.C. Phelps, K.A. Elliget, T.W. Jones, and I.K. Berezesky, Dept. of Pathology, University of Maryland School of Medicine, and MIEMSS, Baltimore, MD 21201, U.S.A.

With the advent of DIFM and fluorescent probes e.g., Fura-2 for $[Ca^{2+}]_i$, it is now possible to study $[Ca^{2+}]_i$ following injury in living cells. Changes of $[Ca^{2+}]_i$ precede early changes such as cytoplasmic blebbing, mitochondrial condensation, and dilatation of the ER and can result from redistribution of intracellular stores such as mitochondria or ER or from Ca^{2+} influx. In many cases, both phenomena occur. We have grouped a series of nephrotoxins in 3 categories: 1) agents causing influx of $[Ca^{2+}]_e$ e.g., the ionophores, ionomycin and A23187, and ouabain which inhibits Na/Ca exchange (in this category, protection or delay of cell killing is enhanced by reducing $[Ca^{2+}]_e$); 2) agents that predominantly result in redistribution of $[Ca^{2+}]_i$ e.g., PCMB, PCMBS, NEM, cyanide, CN^- + IAA, CCCP, and HCBD conjugates; and 3) agents causing both redistribution and influx e.g., $HgCl_2$ which at first causes a roughly 10- to 20-fold, $[Ca^{2+}]_e$-independent increase of $[Ca^{2+}]_i$ to 2 uM, followed by a secondary increase which is dependent on normal $[Ca^{2+}]_e$. Reduction of $[Ca^{2+}]_e$, therefore, delays blebbing and killing in the case of $HgCl_2$. Increases of $[Ca^{2+}]_i$ often begin in perinuclear locations but, as blebbing develops, $[Ca^{2+}]_i$ reaches extremely high levels in the blebs. We visualize the blebbing as representing an interaction between the $[Ca^{2+}]_i$, the cytoskeleton, and the cell membrane. [Supported by NIH DK15440 and Navy N0001-88-K-0427.]

Fourth International Nephrotoxicity Symposium - Guildford, England, July 23-28, 1989.

1271

THE EFFECT OF $HgCl_2$ ON CYTOSOLIC CALCIUM ($[Ca^{2+}]_i$) AND BLEBBING OF RAT PROXIMAL TUBULE CELLS. P. C. Phelps, M. W. Smith, K. A. Elliget, and B. F. Trump. Dept. of Path., Univ. of MD Sch. of Med., and MIEMSS, Balto., MD 21201.

To study changes in $[Ca^{2+}]_i$ in response to $HgCl_2$-induced toxicity, primary cultures of rat proximal tubular epithelial cells were loaded with Fura 2-AM, and examined with digital imaging fluorescence microscopy (DIFM). Images were acquired at 0, 0.5, 1, 2, 3, 5, and up to 40 min of $HgCl_2$ (10, 50, 100 μM). Image analysis showed two dose-related patterns of $[Ca^{2+}]_i$ increase. With 10 μM $HgCl_2$, $[Ca^{2+}]_i$ starts to increase noticeably by 3 min and stabilizes at about 8X normal by 10 min. With 50 and 100 μM, $[Ca^{2+}]_i$ immediately increases, peaking at 1 min to 8X normal and then declines for the next 3-5 min to 4X normal. The $[Ca^{2+}]_i$ then undergoes another period of elevation, plateauing at 6-10X normal by about 15 min. Well before cells die, but after $[Ca^{2+}]_i$ is greatly elevated, large blebs form at the cell surface (as early as 6 min with 100 μM and generally after 30 min with 10 μM). These blebs retain Fura 2 better than the cell proper and always have very high Ca^{2+} concentrations. Blebs readily detach from living cells but are also found on trypan blue stained (dead) cells. Through DIFM, we have been able to demonstrate a sequence of changes following $HgCl_2$ which shows that an elevation of $[Ca^{2+}]_i$ precedes blebbing which occurs prior to cell death. [Supported by NIH DK15440 and Navy grant #N00014-88.]

FASEB J 3:A445, 1989

4042

CELL INJURY ON CULTURED RAT PROXIMAL TUBULE EPITHELIUM (PTE) BY PARAQUAT (PQ)-INDUCED OXIDATIVE STRESS. N. Nitta, K. A. Elliget, M. W. Smith, P. C. Phelps, I. K. Berezesky, and B. F. Trump. Department of Pathology, Maryland Institute for Emergency Medical Services Systems and University of Maryland School of Medicine, Baltimore, MD 21201.

PQ cytotoxicity in cultured rat PTE was investigated after exposure to 1 mM and 10 mM PQ for 1, 3, 6 and 24 h. It was also done at each time point after changing cells to PQ-free medium following initial 1 and 10 mM PQ exposure. Toxicity was determined by neutral red assay and cellular ATP concentration. PQ caused a time- and dose-dependent decrease in cell viability and ATP levels, which did not recover after PQ was removed from the medium. Observation by phase microscopy after 6 h exposure to 10 mM PQ showed a disoriented growth pattern and evidence of cell contraction. Addition of superoxide dismutase, catalase or mannitol to the medium was not protective. Increase in cytosolic calcium $[Ca^{2+}]_i$ may mediate cell injury by PQ; however, use of the ionized probe "Fura-2" was not possible because PQ interacts with Fura-2 and interferes with Ca^{2+}-Fura-2 binding. We are currently studying calcium flux on PQ treated cells by using ^{45}Ca. These results suggest that PQ caused prolonged and irreversible PTE injury associated with a decrease in energy. Changes in calcium homeostasis, possibly involving $[Ca^{2+}]_i$ redistribution, may be important in injury caused by oxidative stress. [Supported in part by Navy Grant #N00014-88-K-0427 and NIH #DK15440.]

FASEB J 3:A922, 1989

•UM#2822

PRACTICAL IN VITRO TOXICOLOGY
ABSTRACT REPRODUCTION FORM

Deadline 20 January 1989 **Type Abstract within guidelines**

Please read instructions carefully before typing abstract. DO NOT FOLD this form.

Indicate preference: Oral Presentation ☐ **Poster** ☑ **Ref No.**

Session No. (see Scientific Programme) ☐

Principal author's name Benjamin F. Trump, M.D.

Address Dept. of Pathology, University of Maryland School of Medicine, 10 S. Pine Street

City/Town Baltimore, Maryland **Code** 21201 **Country** USA

Telephone (301) 328-7070 **Fax** (301) 328-8414

NEPHROTOXICITY *IN VITRO*: ROLE OF ION DEREGULATION IN SIGNAL TRANSDUCTION FOLLOWING INJURY - STUDIES UTILIZING DIGITAL IMAGING FLUORESCENCE MICROSCOPY (DIFM)

Benjamin F Trump, Irene K Berezesky, Kathryn A Elliget, Mary A Smith and Patricia C Phelps

Department of Pathology, University of Maryland School of Medicine and Maryland Institute for Emergency Medical Services Systems
Baltimore, MD 21201

Over the years, many approaches have been utilized for studying *in vitro* toxicity in the kidney. These have included isolated perfused kidneys, renal slices, isolated explanted nephrons and cultured tubular epithelium. Current technology utilizing DIFM for the study of intracellular ions such as $[Ca^{2+}]_i$, $[Na^+]_i$, $[K^+]_i$, and $[H^+]_i$ requires the use of *in vitro* systems - either primary cultures or cell lines. We have developed methods for the primary culture of rat, rabbit, and human proximal tubular epithelium (PTE) and are employing such systems for the study of acute cell injury and the comparison of animal data to those obtained on human cells. In the current studies, we have utilized Fura 2 to observe changes in $[Ca^{2+}]_i$ as they relate to cell injury. Changes in $[Ca^{2+}]_i$ begin very early after a variety of lethal and sublethal toxic injuries. The changes can increase $[Ca^{2+}]_i$ from its normal 100 nM to 2 uM. The changes precede early bleb formation and may activate enzymes such as lipases and proteases that lead to cell death.

(Supported by NIH DK15440 and Navy N00014-88-K-0427.)

Phelps P C, Smith M W, and Trump B F: Cytosolic ionized calcium and bleb formation after acute cell injury of cultured rabbit renal tubule cells. Lab Invest 60: 630-642, 1989.

Smith M W, Ambudkar I S, Phelps P C, Regec A L, and Trump B F: $HgCl_2$-induced changes in cytosolic Ca^{2+} of cultured rabbit renal tubular cells. Biochem Biophys Acta 931(1): 130-142, 1987.

Trump B F, Berezesky I K, Smith M W, Phelps P C, and Elliget K A: The relationship between cellular ion deregulation and acute and chronic toxicity. Toxicol Appl Pharamcol 97: 6-22, 1989.

Second International Congress on Practical In Vitro Toxicology - Nottingham, England
July 23-27, 1989.

UM#2796

Society of Toxicologic Pathologists

VIII International Symposium
Cincinnati, Ohio
May 21-25, 1989

ABSTRACT FORM
For Poster Session
Deadline for Submission: March 15, 1989

TYPE name, address, and telephone number of FIRST AUTHOR to whom all correspondence will be sent.

Name Kathryn A. Elliget, M.S.

Address Department of Pathology, Sch. of Med.
University of Maryland
10 S. Pine St.
Baltimore, MD 21201

Telephone (301) 328-6588

[X] Please consider this abstract for 1989 Junior Investigator Award (separate application required)

Abstracts must be typed on this original form and will be used as camera-ready copy. Proofread abstract carefully. Single space and indent paragraphs. Use authors' last names and initials without degrees. For more forms, call Dr. W. O. Iverson (201) 277-7409

All accepted abstracts will be published in *Toxicologic Pathology*. Senior author will be notified by April 10, 1989, of abstract acceptance. DO NOT FOLD THIS SHEET. Use cardboard backing when mailing.

Mail original typed abstract and two (2) photocopies to:

Nancy M. Streett
Planning Unlimited
P.O. Box 220
New London, PA 19360

IN VITRO TOXIC EFFECTS OF MERCURIC CHLORIDE ON PRIMARY RAT PROXIMAL TUBULE EPITHELIAL CELLS.

K.A. Elliget, M.W. Smith, P.C. Phelps, I.K. Berezesky, and B.F. Trump, Dept. of Path. Univ. of Md. Sch. of Med. and MIEMSS, Baltimore, MD 21201

Exposure of rat proximal tubule epithelial cells to $HgCl_2$ results in a marked drop in viability that is accompanied by increased cytosolic calcium ($[Ca^{2+}]_i$) and formation of plasma membrane blebs. This response is augmented when the $CaCl_2$ concentration in the culture medium is increased. The viability after exposure to 25 uM $HgCl_2$ in the presence and absence of extracellular calcium (1.37 mM) was 28 and 81%, respectively. Similar results are seen with doses of 10, 50, and 100 uM $HgCl_2$. We are also using digital imaging fluorescence microscopy (DIFM) to visualize the cellular responses to injury and further clarify the mechanisms involved. By using the probe for $[Ca^{2+}]_i$, Fura 2, we have determined that one cellular manifestation of $HgCl_2$ toxicity is a biphasic increase in $[Ca^{2+}]_i$; the second, sustained rise is attributed to Ca^{2+} influx from the extracellular space. These results suggest a major function for Ca^{2+} in $HgCl_2$-induced cell injury, and demonstrate the utility of combinations of studies, such as toxicity/viability assays and DIFM.

(Supported by NIH AM15440 and Navy N00014-88-K-0427.)

103 THE EFFECTS OF OXIDATIVE STRESS ON RAT PROXIMAL TUBULAR EPITHELIUM (PTE): A ROLE FOR CYTOSOLIC CALCIUM ($[Ca^{2+}]_i$). N. Nitta*, A. Maki*, M. Smith*, P. Phelps*, K. Elliget*, I. Berezesky* and B. Trump. Maryland Institute for Emergency Medical Services Systems and Dept. of Path., U. of MD School of Medicine, Balto., MD 21201

Oxidative stress from a variety of sources, including PMN infiltrates and reperfusion injury appears to be a significant source of cell injury in shock. We investigated this in cultured rat PTE using the xanthine/xanthine oxidase (X/XOD) system. This system generates $O_2^{\cdot-}$ and H_2O_2 extracellularly which reacts first at the cell surface. Cell viability was measured after exposure to serum-free medium containing xanthine (500 μM) and XOD (2.5-25 mU/ml) for 1, 2 and 3 hr by using the neutral red (vital dye) assay and presented as % of control. Viability at 1, 2 and 3 hr following 5 mU/ml XOD was 71, 48 and 36%, respectively. X/XOD caused time- and dose-dependent decreases in viability. Pre-addition of catalase protected the cells significantly; however, superoxide dismutase had only a slight protective effect. Changes in $[Ca^{2+}]_i$ following X/XOD (25 mU/ml) were determined by spectrofluorometric measurement of Fura 2-loaded cells. In the presence of normal $[Ca^{2+}]_e$ (1.37 mM), there was an initial rapid transient increase in fluorescence followed by a slower secondary sustained increase. The initial $[Ca^{2+}]_i$ increase which was observed in normal $[Ca^{2+}]_e$ was not seen with low $[Ca^{2+}]_e$ (< 5 μM). The transient increase was prevented with low $[Ca^{2+}]_e$ but the sustained increase was not. These data suggest that both influx of Ca^{2+} (early transient) and redistribution of Ca^{2+} from intracellular stores, e.g. mitochondria and ER (secondary sustained) play a major role in the deregulation of $[Ca^{2+}]_i$. [NIH AM15440 and Navy N00014-88K-0427.]

Circ Shock 1989 27:333-334

Fourth Aspen Cancer Conference - Carcinogenesis: From Molecular Mechanisms to Molecular Epidemiology - Aspen, CO, July 23-26, 1989.

$[Ca^{2+}]_i$ Does Relate to Cell Injury, Cell Death, Cell Differentiation, and Cell Division: Studies Using Digital Imaging Fluorescence Microscopy (DIFM)

BENJAMIN F. TRUMP, IRENE K. BEREZESKY, MARY W. SMITH, PATRICIA C. PHELPS, AND KATHRYN A. ELLIGET, Department of Pathology, University of Maryland School of Medicine and the Maryland Institute for Emergency Medical Services Systems, Baltimore, MD 21201

For many years, we have been impressed with the fact that cell injury and cell death are preceded by a series of events involving deregulation of cellular ion control including $[Na^+]_i$, $[K^+]_i$, and $[Ca^+]_i$ (7), although not knowing how these events could relate to the processes of cell death, cell regeneration, and neoplasia. Therefore, our laboratory has been working on characterizing the nature of this link which appears to involve a relationship between ion deregulation, and cell toxicity, cell injury, cell death, cell division, and cell differentiation. Recently, it has become possible, using DIFM and fluorescent probes, to measure ions such as $[Ca^{2+}]_i$ or $[H^+]_i$ in living cells. We have used this new technology on cultures of rat, rabbit, and human kidney and the human bronchus to examine the following series of events (6):

<u>The Relationship Between $[Ca^{2+}]_i$ and Acute Cell Injury.</u>

1. <u>Prelethal injury</u>. We have observed that $[Ca^{2+}]_i$ increases very rapidly (4), precedes the development of blebbing at the cell surface (3), the contraction of mitochondria, and the condensation of nuclear chromatin (5). We have hypothesized that $[Ca^{2+}]_i$ interacting with cytoskeletal elements and other ions within the cell, leads to these phenomena (5).
2. <u>Lethal injury</u>. Following a period of reversible change, the cell enters a period of irreversible change. This is characterized by breakdown of membrane units including mitochondria, ER, and the cell membrane, and by alterations in the already clumped nuclear chromatin. This phase of

cell injury appears to involve calcium-activated proteases, nucleases, and phospholipases (5, 6).

The Relationship Between $[Ca^{2+}]_i$ and Chronic Cell Injury.

A possible role for $[Ca^{2+}]_i$ in the control of differentiation and division in the human bronchial epithelium (HBE) is under study. Experiments have shown that normal levels (1.3 mM) of $[Ca^{2+}]_e$ result in the initiation of a terminal differentiation program leading to keratinization and cell death. It had been previously proposed by Yuspa and colleagues (1) that normal $Ca^{2+}]_e$, approximately 1.3 mM, results in terminal differentiation of normal but not neoplastic keratinocytes. We, therefore, asked the question of whether or not the signalling for terminal differentiation produced by serum, formaldehyde, acrolein, or hydrogen peroxide would or would not lead to a $[Ca^{2+}]_i$ signal. We examined this question using HBE and BEAS-2B cells and found that, in the case of formaldehyde, acrolein, and serum, there not only was a $[Ca^{2+}]_i$ transient but also that TGF-B and TPA were not associated with a $[Ca^{2+}]_i$ transient (2). We, therefore, are currently examining the relationship between the stimuli and the action on $[Ca^{2+}]_i$. In some cases, e.g., protein kinase C activation, normal $[Ca^{2+}]_i$ may be sufficient or there may be alternate pathways.

In summary, it appears that ion deregulation is pivotal in the reaction of cells to acute injury as well as in their response to chronic injury. Current technology finally permits careful study of this question. As a result of such data, it is now possible to postulate that sublethal injuries may result in the activation of genetic responses leading to regeneration and even to neoplasia. [Supported by Navy N00014-88-K-0427, NIH DK15440, and NLM LMD 04411.]

References

1. Hennings H, Micheal D, Cheng C, Steinert P, Holbrook K, and Yuspa SH (1980). Calicum regulation of growth and differentiation of mouse epidermal cells in culture. Cell 19: 245-254.

2. Miyashita M, Smith MW, Willey JC, Lechner JF, Trump BF, and Harris CC (1989). Effects of serum, transforming growth factor beta or 12-O-tetradecanoylphorbol-13,acetate on ionized cytosolic calcium concentration in normal and transformed human bronchial epithelial cells. Cancer Res. 49: 63-67.

3. Phelps PC, Smith MW, and Trump BF (1989). Cytosolic ionized calcium and bleb formation after acute cell injury of cultured rabbit renal tubule cells. Lab. Invest. 60: 630-642.

4. Smith MW, Ambudkar IS, Phelps PC, Regec AL, and Trump BF (1987). $HgCl_2$-induced changes in cytosolic Ca^{2+} of cultured rabbit renal tubular cells. Biochem. Biophys. Acta. 931(1): 130-142.

5. Trump BF and Berezesky IK (1985). Cellular ion regulation and disease. A hypothesis. In: Regulation of Calcium Transport in Muscle, Vol. 25, AE Shamoo (ed). Academic Press, Inc., New York, pp. 279-319.

6. Trump BF, Berezesky IK, Smith MW, Phelps PC, and Elliget KA (1989). The relationship between cellular ion deregulation and acute and chronic toxicity. Toxicol. Appl. Pharmacol. 97: 6-22.

7. Trump BF, Croker BP Jr, and Mergner WJ (1971). The role of energy metabolism, ion, and water shifts in the pathogenesis of cell injury. In: Cell Membranes: Biological and Pathological Aspect. GW Richter and DG Scarpelli (eds). Williams & Wilkins, Baltimore, pp. 84-128.

CALCIUM SIGNALLING IN CELL INJURY: THE EFFECTS OF ANOXIA AND SHOCK MODELS ON KIDNEY PROXIMAL TUBULE EPITHELIUM (PTE) IN VITRO. B.F. Trump, I.K. Berezesky, M.W. Smith, P.C. Phelps, and K.A. Elliget, Department of Pathology, University of Maryland School of Medicine and Maryland Institute for Emergency Medical Services Systems, Baltimore, Maryland 21201

Acute cell injury is characterized by a series of reversible and irreversible subcellular changes. Prominent among these is the deregulation of cellular ions including Na^+, Cl^-, Mg^{2+}, Ca^{2+} and H^+. In our laboratory, we have been focusing on the role of Ca regulation as this ion plays an important role in both physiological and pathological cell structure and function. Current technology permits the measurement of cytosolic ionized calcium ($[Ca^{2+}]_i$) in living cells using digital imaging fluorescence microscopy and fluorescent probes such as Fura-2. We have employed this technique to examine changes in $[Ca^{2+}]_i$ following several model injuries in the rat, rabbit and human PTE. These changes were studied as a function of time following the initial injury and correlated with changes in morphology by phase microscopy on living cells and electron microscopy on fixed cells, with Ca-mediated effects on proteases, lipases, and nucleases and with changes in transcription of genes related to division and differentiation. Following anoxia or chemical models thereof, such as KCN + iodoacetate, $[Ca^{2+}]_i$ rapidly rises to approximately 400-600 nM. This rise is associated with blebbing at the cell surface, mitochondrial condensation, dilatation of the endoplasmic reticulum (ER) and chromatin clumping. At this point, the cells are reversibly injured and can recover if the cell is re-oxygenated. The rise in $[Ca^{2+}]_i$ is related to intracellular redistribution since the use of low extracellular calcium ($[Ca^{2+}]_o$) and/or medium containing EGTA do not prevent the increase. The mechanism(s) of these effects include alterations in the cytoskeleton and possible activation of Ca-mediated proteases. Cytosolic pH (pH_i) was measured using the probe BCECF following anoxia or KCN. Following treatment with anoxia, a reversible increase of pH_i (approximately 0.1 unit) occurred; a similar increase occurred with KCN (1-5 mM). In conclusion, modification of $[Ca^{2+}]_i$ and pH_i may represent events in cell injury which relate not only to cell death, but also to cell proliferation and differentiation. [Supported by Navy N00014-88-K-0427, NIH AM15440, and NLM LMD 04411.]

Biology of Cellular Transducing Signals '89 - Ninth International Washington Spring Symposium - Washington, DC, May 8-12, 1989.

A NEW TECHNIQUE FOR THE ASSESSMENT OF CELLULAR INJURY: DIGITAL IMAGING FLUORESCENCE MICROSCOPY (DIFM)

BENJAMIN F. TRUMP, IRENE K. BEREZESKY, AND ALAN C. MORRIS

DEPARTMENT OF PATHOLOGY

UNIVERSITY OF MARYLAND SCHOOL OF MEDICINE

AND

MARYLAND INSTITUTE FOR EMERGENCY MEDICAL SERVICES SYSTEMS

BALTIMORE, MARYLAND 21201

This is contribution No. 2812 from the Cellular Pathobiology Laboratory.

Supported by NIH Grants DK15440 and NO1-CP-51000 and by Navy N00014-88-K-0427.

1.1 Introduction

The purpose of this chapter is to introduce the technology involved in digital imaging fluorescence microscopy (DIFM) and its application to the study of toxic cell injury. A compelling issue in toxicologic pathology is the characterization of cellular and molecular events as they occur in the living cell following injury. The development of phase and Nomarski techniques for light microscopy has greatly improved the solution to this problem and certainly the development of electron microscopy (EM) and analytical electron microscopy has enabled visualization of cell membranes and organelles at fixed points in time following an injury and has permitted correlation with observations of living cells in real time using phase or Nomarski microscopy often coupled with time-lapse cinematography or video microscopy. An important limitation of microscopy of living cells, however, has been that low levels of illumination and contrast problems have been difficult to solve and that information on chemical changes in the cell during phase microscopy has not been possible. Even the introduction of fluorescent probes has alone not solved these problems because of the phenomenon of photo bleaching at normal levels of illumination. Moreover, the problems of contrast in examining the faint images of organelles were difficult to overcome even with advances in the sensitivity of photographic techniques. The development of DIFM has provided new opportunities for studying dynamic cellular events, particularly when coupled with traditional methods of fluorescence microscopy (for review, see Taylor and Salmon, 1988).

During the past several years, aided by the efforts of investigators such as Robert D. Allen (1985) and Shinya Inoué (1986) and abetted by developments in microcomputers, a quiet revolution in microscopy has occurred, whereby the microscopic image can now be amplified with intensified video cameras,

digitized, and then manipulated by various software programs on modern microcomputers (DiGuiseppi et al., 1985; Arndt-Jovin et al., 1985; Wick, 1986). Such manipulations permit modulation of gamma and intensify selected areas of the image.

Following these developments in image intensification and computer-assisted microscopy, a group of chemists led by Roger Tsien and his colleagues (Grynkiewicz et al., 1985; Tsien, 1989) succeeded in developing a series of fluorescent dyes such as Fura 2 for $[Ca^{2+}]_i$, SBFI for $[Na^+]_i$, PBFI for $[K^+]_i$, BCECF for $[H^+]_i$, and Furapta for $[Mg^{2+}]_i$, which could enter cells and respond to intracellular signals. At the same time, developments in EM have proceeded-especially developments in analytical electron microscopy, whereby total elemental levels can be measured.

Our laboratory has, for some years, been investigating the role of cellular ion deregulation in the mechanism of the pathophysiologic response of cells to injury (for reviews, see Trump and Berezesky, 1985, 1987, 1988; Trump et al., 1989a). Although we had hypothesized in our papers over 20 years ago (Trump and Bulger, 1968) that $[Na^+]_i$, $[H^+]_i$, $[K^+]_i$, and $[Ca^{2+}]_i$ were intimately involved in this process, the precise tools for assessing this involvement had not yet been developed. Because of the developments in DIFM, it is now possible to examine this response in detail in living cells with phase microscopy, to correlate these responses with morphologic and other changes in fixed cells with EM, and to evaluate such with modern molecular biologic techniques. This approach, therefore, has become an essential methodology in modern toxicology. In this review, we will describe the instrumentation, the technique, and give several examples of current applications.

1.2 Methodology

1.2.1 Fluorescence Microscopy

Fluorescence epiillumination microscopy includes an optical path in which the objective lens of the microscope serves both as condenser and objective of the system (Fig. 1A). The feature which makes this possible is the dichroic mirror placed in the light path between the objective lens and the detection device. The dichroic mirror serves as an interference filter which has a high reflectance for desired excitation wavelengths, but not for emission wavelengths passed by the selected barrier filter (Fig. 1B). The desired emission wavelengths pass through the dichroic mirror. This configuration produces a simple and efficient optical path since the excitation wavelengths do not have to pass through the specimen. In addition, the epiillumination method of fluorescence microscopy can be combined with conventional bright field methods, e.g., phase and Nomarski, allowing one to compare the distribution of the fluorophore of interest to the bright field view of the specimen (Taylor and Salmon, 1989), thus permitting analysis of both fluorescence and phase images of the same cell. Furthermore, the specimen can then be analyzed by scanning electron microscopy (SEM), transmission electron microscopy (TEM), or analytical EM.

1.2.1. (a) Fluorescence microscopy requires a broad range of excitation illumination from the ultraviolet to the infrared. While spectral output can be manipulated with different filter configurations, such control is limited by the spectral characteristics of the lamp chosen. The lamps most frequently used are: tungsten; quartz-halogen; 50 and 100 W mercury arcs; and 75 or 150 W

xenon arcs (Taylor and Salmon, 1989). The arc lamps are the most useful for fluorescence work because of their intensities and uniformity of illumination (Fig. 2). While the mercury lamps offer great intensities in certain regions of their spectral output (Fig. 2), we and others believe that the 75 W xenon lamp is the light source of choice not only because of its intensity but because of its linear output in the UV ranges (Taylor and Salmon, 1989; Wampler et al., 1989).

1.2.1. (b) Ratio Fluorescence Microscopy

Quantifying a fluorescent signal from a biological specimen viewed with a microscope is difficult. Problems such as variations of fluorochrome concentration, variations in the optical path length, changes in autofluorescence, and temporal and spatial variation within the sample must be dealt with when using a single excitation, single emission probe (Grynkiewicz et al., 1985; Bright et al., 1989). By using fluorescence ratio microscopy, however, most of the problems related to quantifying cellular fluorescence are overcome.

The basic requirement of ratio fluorescence microscopy is that the probe be sensitive to the parameter of interest in at least two excitation or emission wavelengths (Bright et al., 1989). The excitation or emission at one of the wavelengths should

be either nonsensitive, much less sensitive, or sensitive in the opposite direction when compared to the other excitation or emission wavelength. This relationship between the two signals allows ratioing, thus providing a measured response (Bright et al., 1989). Since the excitation or emission signal arises from the same cellular space, the ratio relationship normalizes for changes in optical pathlength, concentration of indicator, or photobleaching (Bright et al., 1989).

When using ratio fluorescence microscopy with a video camera coupled to an image analysis system, it is easiest to use a dual excitation, single emission probe; however, if photon counting is the sole detection method, it is easier and more cost effective to use a single excitation, dual emission probe. In this discussion, we will address some of the requirements for the use of the dual excitation, single emission probe of ionic Ca^{2+} activity, Fura-2.

1.2.1. (c) Equipment necessary for fluorescence ratio microscopy

The microscope used in fluorescence ratio microscopy can be any one whose optical path can be modified to accommodate the necessary monochromatic excitation and emission detection devices (Fig. 3). The optical path within the microscope should be checked for efficiency in transmitting efficiency in the U.V. range and the

excitation source should be a 75 W or 150 W xenon lamp for reasons presented earlier. Between the lamp and the microscope, there must be a means of producing alternating excitation wavelengths that can be rapidly controlled from a peripheral device such as a computer or an image analyzer. These devices can be a filter wheel or sliding filters under the control of a stepper motor or a chopping mirror which can transmit or reflect the xenon lamp output into tunable monochromators (Fig. 4A). The output of the monochromators is directed into a bifurcated quartz fiber optic using collimating lenses and the fiber optic is coupled to the epiilluminator of a microscope. The advantages of this system, as opposed to filter wheels or shutters attached to the microscope, are the isolation of the microscope from vibration resulting from mechanical events providing alternating excitation, and the higher time resolution provided by using a chopping mirror (5 msec) versus that achieved with a filter wheel (100 msec) (Bright et al., 1989).

Whatever system of alternating excitation is used, the purpose is to produce linear output of alternating excitation wavelengths (Fig. 4B). Using Fura 2 as an example, one must alternate excitation between 340 nm and 380 nm light, producing emission maxima in the range of 510 nm; then, by ratioing 340/380, one can determine $[Ca^{2+}]_i$ concentration. However, no matter what speed of alternation is used, there exists a transition period between wavelengths during which non-linear illumination from both excitation

wavelengths is mixed, producing a period during which data sampling should not take place (Fig. 4B). Using a microprocessor-controlled chopper wheel, the phase angle between the two signals can be controlled and a known period of linear, usable illumination established for integration no matter what type of detector is being used.

To make quantitative measurements in fluorescence ratio microscopy, two types of detectors are used: photomultiplier tubes and a variety of imaging devices (Fig. 5) (Wampler and Kutz, 1989). Photomultiplier tubes are the detector of choice for temporal resolution of fluorescence emission; however, they provide no spatial information. Nevertheless, they can resolve very rapid events which will be presented elsewhere in this text.

To characterize spatial information in a fluorescent sample, a two-dimensional detection system must be used such as a low light level video camera system (Bright et al., 1987, 1989). There are a number of such devices available with different characteristics; however, there are factors to consider when gathering low light level images that apply to all types of acquisition devices.

Under many conditions, photon fluxes which produce different levels of illuminance are so low that usable video information cannot be gathered in a single frame, but must be averaged over a certain period of time to produce a usable image (Spring and Lowy, 1989). The improvements in spatial information is at the cost of temporal information due to the period of integration. The camera system chosen should, therefore, be sensitive enough to allow the shortest integration time possible to provide optimal spatial and temporal information. The two approaches to low light video cameras have employed the use of charge-coupled devices or the use of photoemissive devices such as image

intensifiers (Spring and Lowy, 1989). With both types of technology, the quality of image provided is determined by the noise characteristics of the detector and the sensitivity is limited by the signal to noise ratio of the camera (Spring and Lowy, 1989). The higher the signal to noise ratio, the cleaner the video signal; therefore, the only way to improve on the signal under conditions of very low light is by extended signal averaging or integration, again, sacrificing temporal resolution for spatial resolution (Spring and Lowy, 1989; Inoué, 1986). Spatial resolution is also a function of the incoming light intensity at the face plate of the detection device (Spring and Lowy, 1989). Therefore, the resolution of images obtained at low light levels is less than those produced with high intensity, thus, once again, requiring the averaging or integration of successive video frames to produce an image of sufficient spatial resolution.

An additional consideration with low light level cameras is temporal resolution or its response speed. Response speed is expressed as the lag of the image or percentage of a signal remaining in the next field, thus overlapping a new incoming field (Inoué, 1986; Spring and Lowy, 1989). The video camera is serving the same role as a photomultiplier tube; therefore, the investigator must know when the signal at the detector faceplate is a valid one. Thus, experimental sampling rate cannot exceed the lag-time of the camera chosen. Inoue (1986) has recently reviewed available cameras in detail; therefore, they will not be discussed here. Presented here are the basic features of the major classes of detectors (Spring and Lowy, 1989). The Silicon Intensified Target Camera (SIT) can be used for moderately low light levels but generally cannot detect those levels which are not visible to the dark-adapted eye. The SIT camera has good resolution and moderately low lag (50 msec). The Intensified

Silicon Target Camera (ISIT) consists of a SIT fiber, optically coupled to an image intensifier. These cameras have 600 line resolution and moderate lag times (40 msec) but exhibit gain nonuniformity and geometric distortion (Bright et al., 1989).

Image intensifiers, built recently, use microchannel plates as electron multipliers and do not introduce geometric distortion or gain inhomogenetics into the resultant image (Spring and Lowy, 1989). These devices can approach the theoretical limit for photon detection and resolution, and have extremely fast response times (usec). New modular intensifiers coupled by relay lens optics can be used with another detector of choice such as a SIT camera (Spring and Lowy, 1989; Spring and Smith, 1987). Recently, cooled solid state cameras (CCDs), which were originally developed for use in astronomy and other physical sciences, are being tested for video microscopy. CCDs are especially well suited for low light level microscopy, exhibit high resolution, great dynamic range, and on-chip integration of light input. Their main disadvantage is slow read-out of the chip to keep noise to a minimum. All of the above cameras are available in a wide range of configurations, costs, and performance levels. Each application will determine the best system for its needs.

1.2.2 Fura 2 Measurements of Ionic Calcium

Fura 2 is a dual excitation, single emission fluorescent probe that can be used to measure $[Ca^{2+}]_i$ concentrations in living cells (Grynkiewicz et al., 1985). This compound, developed by Tsien and his co-workers, binds calcium in a 1 to 1 ratio and undergoes an excitation maxima shift upon binding calcium with little or no change in emission maxima. In the cytoplasm of a living cell, calcium-free Fura 2 has an excitation maxima of 380 nm, upon binding with calcium that maxima shifts to 340 nm (Grynkiewicz et al., 1985). This

characteristic shift allows one to take the ratio of emission at 340 nm excitation to that of emission at 380 nm excitation and calculate $[Ca^{2+}]_i$ concentration using the following equation:

$$[Ca^{2+}]_i = K_D \left(\frac{R - R_{min}}{R_{max} - R}\right) \beta$$

where R = an experimental measurement of 340/380, R_{min} = that minimal 340/380 emission when fura is calcium-free, R_{max} = calcium saturated fura or maximal fluorescence, β = emission at 380 excitation under calcium-free conditions over emission at 380 excitation under calcium saturating conditions (Grynkiewicz et al., 1985). The value of K_D can, in theory, be affected by viscosity, e.g., nucleus vs. cytosol or between different organelles. The possible errors, if any, that might result from this have not been resolved.

Fura 2 can be loaded in cells in its AM (acetoxymethylester) form which is lipid soluble and membrane permeant. Upon entry into the cytosol, the ester groups are cleaved by native cytosolic esterases leaving the hydrophobic molecule trapped in the cell (Fig. 6) (Grynkiewicz et al., 1985). The pentasodium salt can also be microinjected into cells (See Tank et al., 1988). While Fura 2 is the most popular of the fluorescent calcium indicators, there are potential problems with its use. When the AM form enters a cell, it is possible for several species of the indicator to exist in stages of partial deesterification producing calcium-insensitive fluorescent signals (Scanlan et al., 1987). There have been reports of Fura 2 compartmentalization within subcellular organelles or cell types that readily pump Fura 2 out of the cytosol (for review, see Tsien, 1989). In our experience, this needs to be carefully assessed prior to measurement, but does occur as a function of time.

1.3 Examples of DIFM Applications

1.3.1 Kidney

We have been studying the effects of injury on ion regulation in the kidney using proximal tubule epithelium (PTE) isolated from the rat (Elliget and Trump, 1987; 1989), rabbit (Smith et al., 1987), and human (Trifillis et al., 1986). For the following experiments, rabbit and rat PTE were isolated and cultured as previously described (Smith et al., 1987; Elliget and Trump, 1989), including loading of Fura 2 and subsequent measurements of ionized intracellular calcium ($[Ca^{2+}]_i$) concentrations. Cells were incubated in Hank's buffered salt solution (HBSS) with 1.37 mM $CaCl_2$ (pH 7.2 with 10 mM HEPES). For imaging studies, to utilize high resolution inverted light microscopy for epifluorescence, 20 mm diameter holes were drilled in the bottoms of 60 mm plastic culture dishes and glass coverslips attached with aquarium silicone sealant. The dishes were then sterilized with U.V. light and cells plated on the coverslips (Hennings et al., 1989). Cells were loaded with 3-5 uM Fura 2AM at 25-37°C in HBSS for 1 hr and then rinsed to remove extracellular fluorescent debris. Imaging data were acquired using a Tracor Northern FluoroPlex III (Middleton, WI) interacting with a Nikon Diaphot inverted microscope, an intensified Newvicon video camera and the Tracor Northern 8502 image analysis system for processing and storage (Fig. 5) (Trump et al., 1989a). Assays were carried out by collecting image pairs at alternating 340 and 380 nm excitation. Image pairs (10 frames each) were collected at serial time intervals, stored to disk, and processed for obtaining the ratioed images (Trump et al., 1989a). Backgrounds collected from cell-free areas were subtracted from the ratioed images. Calibration was performed by treating the cells with ionomycin for R_{max} or ionomycin + 5 mM EDTA for R_{min}. Simultaneous or alternate observation by

phase microscopy permitted correlation of morphologic changes with the changes in $[Ca^{2+}]_i$; viability was assessed using trypan blue or the fluorescent dye, propidium iodide.

Imaging studies were correlated with studies of cells in suspension using a spectrofluorometer (Smith et al., 1987). In this case, cells were grown in flasks for 8-14 days, rinsed with HBSS, and loaded for 1 hr with Fura 2AM as described above. Cells were then collected through mild digestion with trypsin and EDTA, gently removed, washed, and concentrations adjusted to 2-4 x 10^6 cells/ml. Fura 2 fluorescence was measured using a Perkin Elmer MPF-66 spectrofluorotometer by following the 510 emission with continuous 340 nm excitation.

1.3.1. (a) Conditions resulting in entry of Ca^{2+} with normal $[Ca^{2+}]_e$

The clearest example of this type of condition is treatment of cells with calcium ionophores, such as A23187 or ionomycin (Fig. 7C). In the presence of normal extracellular calcium ($[Ca^{2+}]_e$), this treatment is associated with a $[Ca^{2+}]_e$ rise to levels approximating 2 uM within less than a minute. In normal resting cells, $[Ca^{2+}]_i$ is approximately 100 nM. This marked increase in $[Ca^{2+}]_i$ Precedes, but is rapidly followed by the formation of large cytoplasmic blebs at the cell periphery (Phelps et al., 1989) (Figs. 8-10). The examination of 340/380 images indicates an initial burst of increased $[Ca^{2+}]_i$ in the perinuclear region followed by increased $[Ca^{2+}]_i$ in the large blebs as they

form and ultimately as they detach (Trump et al., 1989a,b) (Figs. 12A,B). Interestingly, Fura 2 can be retained even after the detachments of blebs. X-ray microanalysis of blebs in normal rat hepatocytes treated with A23187 for 30 min showed increased total calcium as compared to that measured in the cytoplasm (Fig. 11) (Trump and Berezesky, 1989).

1.3.1. (b) Events and conditions resulting predominantly in redistribution of Ca^{2+} from intracellular stores

Several sulfhydryl reactive agents, including the membrane permeant agents, PCMB and N-ethylmaleimide (NEM), and the putative impermeant mercurial, PCMBS, were utilized. NEM produced a rapid 8-12-fold increase in $[Ca^{2+}]_i$, which was totally independent of $[Ca^{2+}]_e$ (Fig. 7B). Both PCMB and PCMBS gave almost identical 3-6-fold increases, which plateaued after several minutes, and stabilized (Fig. 7B). In both cases, the increases in $[Ca^{2+}]_i$ were rapidly followed by changes in cell shape with the formation of blebs at the cell surface (Smith et al., 1987; Phelps et al., 1989).

Inhibition of energy metabolism using mitochondrial inhibitors or uncouplers, such as anoxia, CCCP, oligomycin, and antimycin were generally associated with significantly lesser increases of $[Ca^{2+}]_i$, approximating 2-3-fold (Fig. 7D). Again, in these cases, the increases were independent of $[Ca^{2+}]_e$. Imaging of

340/380 ratios resulted in a slight and mainly perinuclear increase by 60 min in human PTE treated with 5 mM KCN + 10 mM IAA (Fig. 12 C,D).

1.3.1. (c) Conditions resulting in both influx and redistribution of Ca^{2+}

For these studies, we have primarily utilized the potent nephrotoxin, $HgCl_2$, at doses of 2.5-100 uM (Smith et al., 1987). At low concentrations, $HgCl_2$ is associated with a rapid, dose-related increase in fluorescence, reaching a steady state after 3-4 min. At higher concentrations (25-75 uM), there is an initial phase of rapid increase, reaching a maximum after about 1 min, approximating 2 uM (Fig. 7A). $[Ca^{2+}]_i$ then consistently decreases rapidly to reach 1-to 3-fold steady state levels after 3-4 min, followed by a slower secondary sustained increase which is correlated with cell killing. The early transient increase is independent of $[Ca^{2+}]_e$ and is presumed to represent release from intracellular stores, probably primarily the endoplasmic reticulum (ER), or subsets thereof, since unloading of mitochondria is associated only with much lesser increases. Therefore, with these higher doses of $HgCl_2$, we observed a biphasic response: (1) an early release from intracellular stores; and (2) a later increase due to influx of $[Ca^{2+}]_e$ (Fig. 7A). We investigated the mechanism of this early release and observed that

calmodulin inhibitors, such as 48/80 and W7, had no effect on the changes in $[Ca^{2+}]_i$ (Smith et al., 1987). Trifluoperazine, at lower concentrations caused no change; however, higher concentrations accelerated the rise but may have involved a detergent effect. The calcium channel-blockers, verapamil, nifedipine, and nitrendipine had no effect. We attempted to investigate the role of the ER Ca^{2+}-ATPase by using neomycin, a nonspecific inhibitor, but this had no effect either; dantrolene, presumed to block release of Ca^{2+} from the sarcoplasmic reticulum (SR) or caffeine which supposedly facilitates release also had no effect (Smith et al., 1987). The mechanism of this early effect, therefore, remains unknown and may well involve direct interaction of $HgCl_2$ with the Ca^{2+}-Mg^{2+}-ATPase of the ER.

Using DIFM, it is possible to follow these responses in individual cells and to investigate the relationship to other organelles and to changes that occur, as well as to cell viability (Trump et al., 1989a). Typical examples of the response to 50 uM $HgCl_2$ are shown in Figs. 12E and 12F. Note the relatively homogeneous distribution of $[Ca^{2+}]_i$ in the normal cytosol (Fig. 12E). Within seconds after adding $HgCl_2$, there is a striking increase which is not uniform, but concentrated in the perinuclear region. This concentration increases further over the next few minutes and then begins to decline as it is presumably buffered either by reaccumulation into the ER or by extrusion at the cell membrane. Later, as Ca^{2+} influx occurs from the extracellular space, large blebs form which eventually have very high concentrations of $[Ca^{2+}]_i$ prior to

detachment (Fig. 12F) (Phelps et al., 1989).

1.3.2 Myocardium

Fura 2 can be used to accurately measure $[Ca^{2+}]_i$ under a variety of slow and rapid events using photon counting and image analysis methods (Tsien et al., 1985; Tsien, 1989; Wier et al., 1987). It is especially useful for measuring $[Ca^{2+}]_i$ transients associated with spontaneous contractions in neonatal rat ventricular myocytes. In experiments, in which dynamic changes in $[Ca^{2+}]_i$ were measured by quantitative microspectrofluorometry, myocytes were grown on laminin-coated, 25 mm diameter glass coverslips. The coverslips were treated with laminin (20 ug/ml medium) (Collaborative Research, Lexington, MA) for 1 hr before seeding with myocytes. After 3 or 4 days in culture, the myocytes were treated with phenol red-free medium 199 containing 1% fetal calf serum and 3.0 uM Fura 2/AM (Calbiochem-Behring Corp., La Jolla, CA) for 30 min at 37°C. After the Fura 2/AM loading period, the cells were equilibrated in Fura-free medium 199 for 30-60 min, at which time the experiments were performed.

The coverslips were mounted in Sykes-Moore chambers (Belco Glass Co., Vinewood, NJ) and examined with a Nikon Diaphot microscope equipped with UV light optics, a heated stage, and a perfusion pump. Calcium transients associated with spontaneous contractions of the myocytes were measured using alternating 340 and 380 nM excitation produced by a microspectrofluorometer (Tracor Northern, Middleton, WI) and coupled by a quartz bifurcated fiber optic to the microscope epiilluminator (see Fig. 5). Emission maxima at 510 nm were measured by photon counting. Data were collected from small groups of myocytes (approx. 10-20 cells) using a Nikon 40X Fluor objective lens. Control myocytes exhibited a contraction rate of 80-100 spontaneous contractions per minute. The

changes in $[Ca^{2+}]_i$ were resolved by alternating the appropriate excitation signals with a 10-segment chopper wheel at a rate of 40 revolutions per second. Background measurements at 340 and 380 nm were obtained from a sample not incubated with Fura 2/AM and were automatically subtracted from acquisitions obtained from Fura-2-loaded myocytes.

The experimental protocols were performed by superfusing the test solutions through the Sykes-Moore chamber at a rate of 1 ml/min. Fura 2 emission maxima were recorded at prescribed time intervals during the course of the experiments. Calibration of Fura 2 fluorescence was performed in the cells containing Fura 2 as recommended by Scanlan et al. (1987) and Peeters et al. (1987). R_{max} was determined at the end of an experimental protocol by treating the cells with the nonfluorescent ionophore, 4-bromo-A23187 (20 mM) (Calbiochem-Behring Corp.) and R_{min} was determined by treatment with 5.0 mM EGTA (Peeters et al., 1987). $[Ca^{2+}]_i$ was calculated according to the formula of Grynkiewicz et al. (1985) using a K_d of 225 nM. A series of cellular calibrations (n = 7) yielded R_{max} of 4.5 $\pm$ 0.16, R_{min} of 0.46 $\pm$ 0.03 and Sf2/Sb2 of 5.4 $\pm$ 0.30. The range of Fura 2 ratios and results were similar to those obtained with other microscope systems (Poenie et al., 1985, 1986).

Using the methods and calibration techniques described above, neonatal rat ventricular myocytes were observed under control conditions and conditions of metabolic inhibition with 20 mM 2-deoxy-d-glucose and 1 mM sodium cyanide. Using photon counting methods for emission detection, under control conditions the myocytes displayed spontaneous contractions with ionic calcium levels of 550 nM at peak contraction and 150 nM at maximal relaxation (Fig. 13). Metabolic inhibition caused cessation of contractions and calcium transients. In this experiment, restoration of normal medium after 1 hr of metabolic inhibition

resulted in resumption of contraction and ionic calcium transients (Morris et al., 1989). These data demonstrate that, using ratio fluorescence microscopy and Fura 2, the components of a rapid event can be resolved by photon counting.

1.3.3 Epidermal Cells

The epidermis, particularly that of the mouse, has been a widely used model for the study of carcinogenesis and, in many ways, more is known about the mechanism of carcinogenesis in the skin than in any other organ. Indeed, it was utilizing the skin model that the original concept of initiation and tumor promotion was developed (Berenblum and Shubik, 1947). More recently, the use of cultured keratinocytes from mouse as well as from other species has become an important model for the study of in vitro carcinogenesis. Tumorigenic cell lines have also been developed by Yuspa and his group (Hennings et al., 1980) from cultured keratinocytes using various methods. Cell division, cell differentiation and keratinization in keratinocytes cultured in vitro can be modulated by a number of factors including ($[Ca^{2+}]_e$), TPA, and other putative promoters (Hennings and Holbrook, 1983). When $[Ca^{2+}]_e$ is low, keratinocytes grow as a monolayer with a high proliferation rate, having many of the characteristics of basal cells, including the basal cell keratin phenotype (Roop et al., 1987). If, however, $[Ca^{2+}]_e$ levels are shifted to normal (1.2 mM), the cells change their gene expression program shifting to a program characteristic of differentiation including the expression of keratins, which are characteristic of the suprabasal keratinizing cells in vivo (Hennings et al., 1980; Hennings and Holbrook, 1983). Thus, $[Ca^{2+}]_e$ acts as a regulator of gene expression and differentiation. At the same time, it was noted that several tumorigenic cell lines developed from the keratinocytes did not respond to the high $[Ca^{2+}]_e$ signal by differentiation, but continued to divide and to

incorporate thymidine. This led Yuspa et al. (1982) to propose, at that time, a new concept of tumor promotion, whereby at least some tumor promoters may act by inducing terminal differentiation in normal, but not in initiated cells, thereby giving a growth advantage to the latter. Interestingly, data using various analytical EM techniques have also revealed that there is a gradient of $[Ca^{2+}]_e$ levels in skin in vivo, with very low $[Ca^{2+}]_e$ in the extracellular space around the basal cells and serum-like levels at the surface in the suprabasal and terminally differentiated cells in vivo. It thus became logical to ask the question of whether the increased $[Ca^{2+}]_e$ could be associated with signalling involving increase of $[Ca^{2+}]_i$ either through influx, intracellular redistribution or both. Furthermore, since the keratinocyte populations are heterogeneous and have a small population that does not respond to $[Ca^{2+}]_e$, the only appropriate method would be to utilize imaging techniques such as DIFM, rather than studies of cell populations in suspension.

Therefore, Hennings et al. (1989), using DIFM, studied the response of $[Ca^{2+}]_i$ in relation to increased $[Ca^{2+}]_e$ in both normal and neoplastic keratinocytes. They observed that most normal keratinocytes responded to increasing $[Ca^{2+}]_e$ by a gradual 2-3-fold increase in $[Ca^{2+}]_i$ for at least 28 min. The smaller subpopulation, possibly representing dividing cells, only displayed a sharp transient peak of $[Ca^{2+}]_i$ at 2 min. Experiments measuring phosphoinositides revealed that there was a sustained increase of IP_3 in the cells as they terminally differentiated which accompanied the prolonged increase of $[Ca^{2+}]_i$. They concluded that the $[Ca^{2+}]_i$ increase probably had an initial contribution from influx of $[Ca^{2+}]_e$ and an additional sustained contribution from release from the endoplasmic reticulum (ER) or parts thereof induced by IP_3. Totally in contrast, neoplastic cells had a 2-3-fold higher level of

resting $[Ca^{2+}]_i$ and a totally different response to increasing $[Ca^{2+}]_e$. In neoplastic keratinocytes, there was a rapid transient 4-9-fold elevation which then was regulated as the cells continued to divide. Thus, the use of DIFM has already permitted the investigator to begin approaching the problems of intracellular signalling with agents that modify division and differentiation.

1.3.4 Tracheobronchial Epithelium

As in the case of the cultured keratinocytes, cultured normal human bronchial epithelia (NHBE) respond to a variety of promoters and putative promoters by undergoing a program of terminal differentiation. This program involves altered keratin gene expression and the formation of cross-linked envelopes, or arrest of colony formation, and often tritiated thymidine incorporation, squamous differentiation, stratification, and ultimately cell death.

As in the case of the cultured keratinocytes mentioned above, normal $[Ca^{2+}]_e$ (approximately 1.3 mM) in the culture medium also initiates a similar program of terminal differentiation in normal or BEAS-2B cells (a non-tumorigenic cell line produced by transfection with adenovirus 12-SV40 hybrid virus) as compared with transformed cell lines (Miyashita et al., 1989). Therefore, normal levels of $[Ca^{2+}]_e$ also can act as a putative promoter. Furthermore, addition of ionophores, such as A23187, to the medium results in rapid formation of cross-linked envelopes.

We have, therefore, used DIFM, as well as spectrofluorometric studies of cells in suspension, to evaluate the possible modulation of $[Ca^{2+}]_i$ following these stimuli to evaluate our hypothesis. Resting concentrations of $[Ca^{2+}]_i$ in normal and BEAS-2B cells were found to be 63 $\pm$ 15 nM (standard deviation) and 44 $\pm$ 15 nM respectively. It was found that addition of 8% Ca-free fetal bovine

serum caused a significant increase in $[Ca^{2+}]_i$ which significantly preceded the induction of terminal squamous differentiation (Miyashita et al., 1989). When a serum-resistant cell line of BEAS-2B was tested, there was no calcium signal, thus compatible with our hypothesis. Analysis of the 340/380 ratioed images revealed a localized spike of $[Ca^{2+}]_i$ which lasted for < 3 min (Figs. 12G,H).

Similar results were observed with formaldehyde (Smith et al., 1989a). At concentrations of 1.5 mM, $[Ca^{2+}]_i$ increased 3-5-fold by 5 min and remained elevated following treatment. With 15 mM formaldehyde, $[Ca^{2+}]_i$ increased rapidly by 1 min and stabilized 3-8-fold higher than at 0 time. With 150 mM formaldehyde, $[Ca^{2+}]_i$ increased 5-10-fold within 1 min. None of these doses resulted in cell killing, as measured by trypan blue, during the 20 min treatment. Formaldehyde is a common environmental toxin resulting in squamous metaplasia of the tracheobronchial epithelium in humans and experimental animals and in nasopharyngeal carcinoma in rats.

A variety of peroxides are found in cigarette smoke and other pulmonary carcinogens and may act either as initiators, promoters, or both. Therefore, studies were carried out to investigate calcium signalling in the terminal differentiation induced by hydrogen peroxide (H_2O_2). The results were similar to those seen with formaldehyde. Using BEAS-2B cells grown in LHC8 without phenol red, cysteine, riboflavin, and folic acid which may interfere with the fluorescence, it was observed that 0.1 mM H_2O_2 had little effect on $[Ca^{2+}]_i$, while 1.0 mM H_2O_2 resulted in a 4-6-fold elevation which was sustained. At these doses, there was no cell killing and minimal or no cell blebbing (Smith et al., 1989b). Studies using DIFM on sub-populations have, however, not yet been done.

The tumor promoter TPA, inhibits growth of NHBE and induces terminal

squamous differentiation when added to the culture medium, but does not do so in tumor cell lines (Willey et al., 1984). TPA also produces terminal differentiation in mouse keratinocytes accompanied by DNA single-strand breaks first seen 12-24 hr after exposure. The similarity of this to the effects of high $[Ca^{2+}]_e$ medium suggests a possible role of Ca-activated nucleases; however, in NHBE, no increases in single-strand breaks using the alkalization technique were observed nor were increases in $[Ca^{2+}]_i$, as described above with serum, seen (Miyashita et al., 1989). This may be because normal $[Ca^{2+}]_i$ was adequate for protein kinase C activation or that some pathway other than that shown in Fig. 14 is involved. So far, no other mechanism other than protein kinase C activation was initiated in TPA activity in NHBE. Measurements using electron spin labelling failed to reveal the induction of oxyradicals in NHBE as occurs in other cells following TPA exposure. Similarly, we did not observe an increase in $[Ca^{2+}]_i$ after adding the growth factor TGF-B which also induces terminal differentiation. This suggests that both TPA and TGF-B act through different signalling pathways than H_2O_2, formaldehyde, and serum (Miyashita et al., 1989).

The tumor promoter, palytoxin, also did not induce a change in $[Ca^{2+}]_i$ although it did produce a slight increase in c-myc mRNA (Bonnard et al., 1988). Because palytoxin binds to Na^+-K^+ ATPase, the effects of ouabain were compared to palytoxin, but a ouabain-resistant cell line was as sensitive to the growth inhibitory effect as the parent cell line, suggesting different binding sites. Ouabain also increased the steady state level of c-myc and, because of Na^+-Ca^{2+} exchange, probably increased the level of $[Ca^{2+}]_i$. We have also observed such an increase in $[Ca^{2+}]_i$ in rabbit PTE following exposure to ouabain (Phelps et al., 1989). Other growth factors have other effects. In BALBc/3T3 cells,

Tucker et al. (1989) found that platelet-derived growth factor (PDGF) produced a larger and more prolonged increase of $[Ca^{2+}]_i$ than did fibroblast growth factor (FGF). In both cases, however, the increases occurred in < 2 min and were sustained for > 20 min. The initial increase was due to redistribution and the latter more prolonged increase to influx. Both correlated with mitosis. Inhibition of $[Ca^{2+}]_i$ treatment with Quin 2 inhibited PDGF stimulation of mitosis but did not affect that following FGF (Tucker et al., 1989).

1.3.5 Central Nervous System

Studies using DIFM are just beginning to be performed on the effects of toxic and other injuries in the central nervous system (CNS), but this area has by no means been exploited at the time of this writing. There are, however, several studies indicating a role for $[Ca^{2+}]_i$ in neuronal cell injury (Emery et al., 1987; Goldberg et al., 1986). One elegant study by Tank et al. (1988) examined the calcium dynamics of mammalian Purkinje cells in cerebellar slices. It has been known for some time that the spatial distribution of ion channels in the plasmalemma of neurons and associated compartmentation of biologic properties is a critical issue in CNS function. The delicate modulation of this regulation is important both in normal and abnormal function of neurons. Using electrophysiological methods, studies over the past several years have examined the nature of voltage-dependent ionic channels over the somatic and dendritic membranes of neurons. In the case of Purkinje cells from the cerebellum, degradation of voltage-dependent Na^+ and Ca^{2+} conductances were found, i.e., voltage-dependent Na^+ conductance was restricted to the soma and axon, whereas Ca^{2+} conductance was most prominently observed over the region of the dendrites (Llinas and Sugimori, 1980a,b). This, however, could not have been confirmed without direct imaging of neurons and imaging of $[Ca^{2+}]_i$ oscillations and

changes in distribution. Using the technique of ionophoretic injection of Fura 2 into Purkinje cells of cerebellar slices from adult Guinea pigs, Tank et al. (1988) first determined that the Fura 2 distribution resembled that of Lucifer yellow, a technique well-established to study dendrite distribution. Then, in experiments correlating cell electrical activity with imaging of $[Ca^{2+}]_i$ using DIFM, it was possible to test the hypothesis derived from the earlier electrophysiologic studies. It was found that $[Ca^{2+}]_i$ increased from 10 to 100-fold between the inactive and active phases of oscillation in the dendrites, whereas the levels in the soma remained essentially unchanged. Using high resolution, i.e., 300 x 500 pixel maps, clear delineation of the dendritic tree was obtained. An important feature of DIFM, however, is that when using the highest resolution, the acquisition time is of the order of 5 sec for the 340/380 image pairs. In order to increase the time resolution in DIFM, it is necessary to decrease the pixels that are written to disk. The authors accomplished this by reducing the spatial resolution to 125 x 175 pixels and were then able to study the oscillations within a 2 sec time resolution. These data then showed oscillation of the $[Ca^{2+}]_i$ in correlation with the fluxes.

In order to further test the observation, they studied the toxic response of the dendritic $[Ca^{2+}]_i$ to the funnel-web spider venom which blocks both spontaneous electrical oscillations, and is a specific blocker of voltage-dependent Ca^{2+} channels in central neurons. After administration of total blockage of oscillation, it was observed after 5 min and continued for 20-30 min with perfusion of toxin-treated saline. During this period, constant low levels of $[Ca^{2+}]_i$ were maintained for up to 30 min after the toxin was applied, totally consistent with the hypothesis of the activity of the dendrites in Ca^{2+} oscillations. Application of this technique to neurotoxicology and

neuropathology is clearly indicated.

1.4 Potential future applications for DIFM in toxicologic pathology

The future of the field of DIFM is one that is currently difficult to overestimate because of the power of the technology and the linkage of computer systems to microscopes. Along with the development of fluorescent probes and sensitive photon detectors, many new applications have been and continue to be developed. The reader is referred to a recent article by Wick (1989), in which some of the current and future applications are mentioned. Some of the points made in that paper will be summarized here with comments on specific applications to toxicology.

1.4.1 Image Luminometry

Because of the development of highly sensitive photon counting instrumentation, it has been possible to study a variety of phenomena, for example, ATP-induced bioluminescence, potentially even at the intracellular level (Maly et al., 1988). The possibility of such studies would mean that ATP measurements along with measurements of $[Ca^{2+}]_i$, $[Na^+]_i$, and $[H^+]_i$ could be correlated with phase microscopy and recorded on video tape or other media. Other applications of this technique include microtiter plate determination using luminescence assays (Hauber et al., 1988) and even measurements of respiratory bursts in leukocytes using Lucigenen-coupled respiratory burst bioluminescence, cell luminescence of B-lymphocytes and the luminescence immunoassay of IgE (Maly et al., 1989).

As the respiratory burst accompanying phagocytosis is accompanied by chemiluminescence, such technology potentially permits the study of this phenomenon using living cells and even time-lapse imaging. Unfortunately, the yield of photons is extremely low; however, Suematsu et al. (1987) have imaged the burst

in single cultured leukocytes stimulated with opsonized zymosan using luminol. This type of study will obviously lead to a much better insight into the kinetics and mechanisms of the inflammatory process in response to environmental and other toxins and also to sorting out the heterogeneity within a cell population.

1.4.2 Metabolic Imaging

Using photon counting imaging technology with frozen tissue sections covered with sections of frozen enzyme solutions, Mueller-Klieser et al. (1988), have described methods where the enzymes in such a sandwich are coupled to a luciferase-based light generating reaction. While the tissue is still frozen, a transmitted or reflected light image of the tissue is acquired and stored in memory. The microscope stage temperature is then raised and a luminescence image obtained by allowing the enzyme solution to diffuse into the tissue to initiate the reaction and to accumulate the emitted photons. As with other digitized images, these can then be pseudo-colored and overlayed on parallel sections to visualize localization. With this methodology, the spatial distribution of glucose, lactate, and ATP can be determined in normal and tumor tissues. Excellent illustrations of this technique are shown by Wick (1989) in his recent review.

1.4.3 Molecular Biology

Among the exciting new developments in this area is the characterization of genes from bacteria or the firefly that are engaged in bioluminescence. These have been cloned, transfected and can then be used as "reporter" systems which offer the opportunity to directly visualize transcription and translation in living cells (deWet et al., 1987). In the case of the firefly luciferase, the bioluminescence is produced through the oxidation

of D-luciferin in the presence of ATP (Koncz et al., 1987). In bacterial systems, aldehyde substrates, can be utilized in the vapor phase and readily penetrate living cells. Schmetterer et al. (1986) have utilized such technology at the microscope level and have actually visualized single isolated cells carrying the liciferase gene. In the field of toxicology, this has obvious and immediate applications, especially in heterogeneous populations of transfected cells in which some but not necessarily all may have altered growth or differentiation patterns.

1.5 Summary

The advent of digital imaging fluorescence microscopy (DIFM) and the development of fluorescent probes has opened up a new era in the study of reactions of cells to toxic injury. Measurements can now be performed on single living cells and correlated with standard methods of phase, Nomarski, TEM, SEM, and analytical EM. The concurrent development of in vitro techniques for the study of both animal and human tissues (Trump and Harris, 1979; Harris and Trump, 1983) permits these technologies to be applied to both animal and human cells and, thereby, extrapolation of animal data to man.

The many applications of DIFM to the study of toxic cell injury that we are utilizing in our laboratory are shown in Fig. 14 which represents our current working hypothesis on the effects of deregulation of $[Ca^{2+}]_i$ in a generic cell (Trump and Berezesky, 1987). This flow chart also emphasizes the relationship between acute, sublethal, or lethal cell injury and processes related to altered growth and differentiation. Note that $[Ca^{2+}]_i$ is regulated by three main mechanisms: (1) the plasma membrane; (2) the mitochondria, and (3) the endoplasmic reticulum (ER). Note also that signal transduction of the cell membrane is currently conceived of principally modifying the ER or subsets

thereof. Note also that the effects of increased $[Ca^{2+}]_i$ are diverse, including activation of phospholipases, nucleases, proteases, modification of cytoskeletal proteins, modifications of cell-cell communication through gap junctions, the activation of genes related to cell division including c-myc and c-fos, and modulation of protein kinase C. Note also the interaction with the Na^+/H^+ antiport, believed to play an important role in control of cell division and cell differentiation through modulation of cell pH. As mentioned above, new fluorescent probes are currently available for $[Na^+]_i$, $[Mg^{2+}]_i$, $[K^+]$, and pH_i and others are in the process of being developed. As indicated in the flow chart (Fig. 14), a variety of toxic compounds can interfere more or less specifically with many of the activities of ion deregulation - the plasma membrane, the mitochondria, the ER, the Na^+/H^+ antiport, and protein kinase C.

Therefore, the future of DIFM has great potential, indeed, for qualitative and quantitative studies on cells. This technology, coupled with standard LM, TEM, SEM, and analytical EM, along with laser scanning confocal microscopy, 3-dimensional reconstruction, and video intensification microscopy, represents a new exciting approach to the further understanding of the mechanisms of toxic cell injury, their prevention, and their treatment.

1.6 References

Allen, R.D. (1985), New observations on cell architecture and dynamics by video-enhanced contrast optical microscopy. Ann. Rev. Biophys. Chem. 14, 265-290.

Arndt-Jovin, D.J., Robert-Nicoud, M., Kaufman, S.J. and Jovin T.M. (1985), Fluorescence digital imaging microscopy in cell biology. Science 230, 247-256.

Berenblum, J. and Shubik, P. (1947), The role of croton oil applications associated with a single painting of a carcinogen in tumour induction of the mouse's skin. Brit. J. Cancer 1, 379.

Bonnard, C., Lechner, J.F., Gerwin, B.I., Fujiki, H. and Harris, C.C. (1988), Effects of palytoxin or ouabain on growth and squamous differentiation of human bronchial epithelial cells in vitro. Carcinogenesis 9, 2245-2249.

Bright, G.R., Fisher, G.W., Rogowska, J., and Taylor, D.L. (1989), Fluorescence microscopy of living cells in culture. Methods in Cell Biology 29: Part A, pp. 157-190.

Bright, G.R., Rogowska, J., Fisher, G.W., and Taylor, D.L. (1987), Fluorescence ratio imaging microscopy temporal and spatial measurements in single living cells. BioTechniques 5, 556-563.

deWet, J.R., Wood, K.V., DeLuca, M., Helinski, D.R. and Subramani, S. (1987), Firefly luciferase gene: Structure and expression in mammalian cells. Mol. Cell Biol. 7, 725-737.

DiGuiseppi, J., Inman, R., Ishihara, A., Jacobson, K., and Herman, B. (1985), Applications of digitized fluorescence microscopy to problems in cell biology. BioTechniques 3, 394-403.

Elliget, K.A. and Trump, B.F. (1987), Use of primary rat proximal tubular cells (PTC) in studies of nephrotoxicity. Fed. Proc. 46(4), 1411.

Elliget, K.A. and Trump, B.F. (1989), Culture and characterization of normal rat kidney proximal tubule epithelial cells in defined and undefined media. (Submitted)

Emery, D.J., Lucas, J.H., and Gross, G.W. (1987), The sequence of ultrastructural changes in cultured neurons of the dendrite transection. Exp. Brain Res. 67, 41-51.

Goldberg, W.J., Kadingo, R.M., and Barrett, J.N. (1986), Effects of ischemia-like conditions on cultured neurons: Protection by low Na^+, low Ca^{2+} solutions. J. Neurosci. 6, 3144-3151.

Grynkiewicz, G., Poenie, M. and Tsien, R. (1985), A new generation of Ca^{2+} indicators with greatly improved fluorescence properties. J. Biol. Chem. 260, 3440-3450.

Harris, C.C. and Trump, B.F. (1983), Human tissues and cells in biomedical research. Surv. Synth. Path. Res. 1, 165-171.

Hauber, R., Miska, W., Schleinkofer, L. and Geiger, R. (1988), The application of a photon-counting camera in very sensitive, bioluminescence-enhanced detection system for protein blotting. J. Clin. Chem. Clin. Biochem. 26, 147-148.

Hennings, H. and Holbrook, K. (1983), Calcium regulation of cell-cell contact and differentiation of epidermal cells in culture. Exp. Cell Res., 143, 127-142.

Hennings, H., Kruszewski, F.H., Yuspa, S.H. and Tucker, R.W. (1989), Intracellular calcium alterations in response to increased external calcium in normal and neoplastic keratinocytes. Carcinogenesis 10, 777-780.

Hennings, H., Michael, D., Cheng, C., Steinert, P., Holbrook, K. and Yuspa, S.H. (1980), Calcium regulation of growth and differentiation of mouse epidermal

cells in culture. Cell 19, 245-254.

Inoué, S. (1986), Video Microscopy. Plenum Press, New York and London.

Koncz, C., Olsson, O., Langridge, W., Schell, J., and Szalay, A.A. (1987), Expression and assembly of functional bacterial luciferase in plants. Proc. Natl. Acad. Sci. USA 84, 131-135.

Llinas, R. and Sugimori, M. (1980a), Electrophysiological properties of in vitro Purkinje cell somata in mammalian cerebellar slices. J. Physiol. (London) 305, 171-195.

Llinas, R. and Sugimori, M. (1980b), Electrophysiological properties of in vitro Purkinje cell dendrites in mammalian cerebellar slices. J. Physiol. (London) 305, 197-213.

Maly, F.E., Urwyler, A., Rolli, H.P., Dahinden, C.A., and de Weck, A.L. (1988), A single photon imaging system for simultaneous quantitation of luminescent emissions from multiple samples. Anal. Biochem. 168, 462-469.

Maly, F.E., Vittoz, M., Urwyler, A., Koshikawa, K., Schleinkofer, L., and de Weck, A.L. (1989), A dual microtiter plate luminometer employing computer-aided single photon imaging applicable to cellular luminescence and luminescence immunoassay. Submitted.

Miyashita, M., Smith, M.W., Willey, J.C., Lechner, J.F., Trump, B.F. and Harris, C.C. (1989), Effects of serum, transforming growth factor type B, or 12-O-tetradecanoylphorbol-13-acetate on ionized cytosolic calcium concentration in normal and transformed human bronchial epithelial cells. Cancer Res. 49, 63-67.

Morris, A.C., Hagler, H.K., Willerson, J.T., and Buja, L.M. (1989), Relationship between calcium loading and impaired energy metabolism during Na^+, K^+ pump inhibition and metabolic inhibition in cultured neonatal rat cardiac myocytes.

J. Clin. Invest. 83, 001-000, (in press).

Mueller-Klieser, W., Walenta, S., Paschen, W., Kallinowski, F., and Vaupel, P. (1988), Metabolic imaging in microregions of tumors and normal tissues with bioluminescence and photon counting. JNCI 80, 842-848.

Peeters, G.A., Hlady, V., Bridge, J.H.B., and Barry, W.H. (1987), Simultaneous measurement of calcium transients and motion in cultured heart cells. Am. J. Physiol. 22, H1400-H1408.

Phelps, P.C., Smith, M.W., and Trump, B.F. (1989), Cytosolic ionized calcium and bleb formation after acute cell injury of cultured rabbit renal tubule cells. Lab. Invest. 60, 630-642.

Poenie, M., Alderton, J., Tsien, R.Y., and Steinhardt, R.A. (1985), Changes of free calcium levels with stages of the cell division cycle. Nature (Lond.) 315, 147-149.

Poenie, M., Alderton, J., Steinhardt R., and Tsien, R. (1986), Calcium rises abruptly and briefly throughout the cell at the onset of anaphase. Science (Wash. DC) 233, 886-889.

Roop, D.R., Huitfeldt, H., Kilkenny, A. and Yuspa, S.H. (1987), Regulated expression of differentiation-associated keratins in cultured epidermal cells detected by monospecific antibodies to unique peptides of mouse epidermal keratins. Differentiation 35, 143-150.

Scanlan, M., Williams, D.A., and Fay, F.S. (1987), A Ca^{2+}-insensitive form of fura-2 associated with polymorphnuclear leukocytes: assessment and accurate Ca^{2+} measurement. J. Biol. Chem. 262, 6308-6312.

Schmetterer, G., Wolk, C.P., and Elhai, J. (1986), Expression of luciferases from Vibrio harveyi and Vibrio fischeri in filamentous cyanobacteria. J. Bacteriol. 167, 411-414, 1986.

Smith, M.W., Ambudkar, I.S., Phelps, P.C., Regec, A.L. and Trump, B.F. (1987), $HgCl_2$-induced changes in cytosolic Ca^{2+} of cultured rabbit renal tubular cells. Biochim. Biophys. Acta 931, 130-142.

Smith, M.W., Miyashita, M., Phelps, P.C., Jones, R.T., Harris, C.C. and Trump, B.F. (1989a), The effect of formaldehyde on cytosolic Ca^{2+} of transformed human bronchial epithelial cells as measured by digital imaging fluorescence microscopy. Proc. Amer. Assoc. Ca. Res. 30, 107.

Smith, M.W., Phelps, P.C., Jones, R.T., Trump, B.F., and Harris, C.C. (1989b), The effect of hydrogen peroxide on cytosolic Ca^{2+} of transformed human bronchial epithelial cells as measured by digital imaging fluorescence microsocpy. The Toxicologist 9, 160.

Spring, K.R. and Lowy, R.J. (1989), Fluorescence microscopy of living cells in culture. Methods in Cell Biology 29: Part A, pp. 269-289.

Spring, K.R. and Smith, P.D. (1987), Illumination and detection systems for quantitative fluorescence microscopy. J. Microscopy 147, 265-278.

Suematsu, M., Oshio, C., Miura, S. and Tsuchiya, M. (1987), Real time visualization of oxyradical burst from single neutrophil by using ultrasensitive video intensifier microscopy. Biochem. Biophys. Res. Commun. 149, 1106-1110.

Tank, D.W., Sugimori, M., Connor, J.A. and Llinas R.R. (1988), Spatially resolved calcium dynamics of mammalian Purkinje cells in cerebellar slice. Science 242, 773-777.

Taylor, D.L. and Salmon, E.D. (1989), Fluorescence microscopy of living cells in culture. Methods in Cell Biology 29: Part A, pp. 208-236.

Trifiliis, A.L., Regec, A., Hall-Craggs, M., and Trump, B.F.: Effects of cyclosporine on cultured human renal tubular cells. Toxicol. Pathol. 14, 210-

212, 1986.

Trump, B.F. and Berezesky, I.K. (1985), Cellular ion regulation and disease. A hypothesis. In: A.E. Shamoo (Ed), Regulation of Calcium Transport in Muscle, Vol. 25, Academic Press, New York, N.Y., pp. 279-319.

Trump, B.F. and Berezesky, I.K. (1987), Ion regulation, cell injury and carcinogenesis. Carcinogenesis 8, 1027-1031.

Trump, B.F. and Berezesky, I.K. (1989), Cell injury and cell death. The role of ion deregulation. Comments Toxicology 3, 47-67.

Trump, B.F. and Bulger, R.E. (1968), Studies of cellular injury in isolated flounder tubules. III. Light microscopic and functional changes due to cyanide. Lab. Invest. 18, 721-730.

Trump, B.F. and Harris, C.C. (1979), Human tissues in biomedical research. Hum. Pathol. 10, 245-248.

Trump, B.F., Berezesky, I.K., Smith, M.W., Phelps, P.C., and Elliget, K.A. (1989a), The relationship between cellular ion deregulation and acute and chronic toxicity. Toxicol. Appl. Pharmacol. 97, 6-22.

Trump, B.F., Berezesky, I.K., Smith, M.W., Phelps, P.C., Elliget, K.A., Miyashita, M., Harris, C.C., Tilliotson, T.T., Resau, J.R., and Jones, R.T. (1989b), The role of cytosolic ionized calcium in acute cell injury and neoplasia. Lab. Invest. 60, 111A.

Tsien, R.Y. (1989), Fluorescence microscopy of living cells in culture. Methods in Cell Biology 29: Part A, pp. 127-153.

Tsien, R.Y., Rink, T.J., and Poenie, M. (1985), Measurement of cytosolic free Ca^{2+} in individual small cells using fluorescence microscopy with dual excitation wavelength. Cell Calcium 6, 145-157.

Tucker, R.W., Chang, D.T., and Meade-Cobun, K. (1989), Effects of platelet-

derived growth factor and fibroblast growth factor on free intracellular calcium and mitogenesis. J. Cell Biochem. 39, 139-151.

Wampler, J.E. and Kutz, K. (1989), Quantitative fluorescence microscopy using photomultiplier tubes and imaging detectors. Methods in Cell Biology 29: Part A, pp. 239-265.

Wick, R.A. (1989), Photon counting imaging: applications in biomedical research. BioTechniques 7, 262-269.

Wier, W.G., Cannell, M.B., Berlin, J.R., Marban, E., and Zederer, W.J. (1987), Subcellular heterogeneity of $[Ca^{2+}]_i$ in single heart cells revealed by Fura-2. Science 235, 325-328.

Willey, J.C., Moser, C.E., Jr., Lechner, J.F. and Harris, C.C. (1984), Differential effect of 12-O-tetradecanoylphorbol-13-acetate on cultured normal and neoplastic human bronchial epithelial cells. Cancer Res. 44, 5124-5126.

Yuspa, S.H., Ben, T., Hennings, S., and Lichti, U. (1982), Divergent responses in epidermal basal cells exposed to the tumor promoter 12-O-tetradecanoylphorbol-13-acetate. Cancer Res. 42, 2344-2349.

1.7 Figure Legends

Fig. 1 Optical path for excitation (A) and emission (B) in an inverted epifluorescence microscope. Desired fluorescence emission above the dichroic cutoff passes through the dichroic mirror to a detection device while emission below the dichroic cutoff does not (B).

Fig. 2 Diagram illustrating the relative spectral output of (a) tungsten, (b) 75 W xenon arc, and (c) 100 W mercury arc lamps. (Reprinted with permission from Taylor and Salmon, 1989).

Fig. 3 A simple schematic of components found in a ratio fluorescence microscopy system using an inverted microscope. In this configuration, a beam splitter in the emission path allows simultaneous photon counting and video image acquisition.

Fig. 4 (A) Emission from a xenon lamp is directed by a turning mirror into a chopper mirror and either reflected or transmitted into monochromators whose output is then directed into a fiber optic bundle which can be coupled to a cuvette system or the epiilluminator of a microscope for photon counting or image acquisition. (B) Components of a single excitation signal showing that 7.5% of the illumination at the beginning and the end of the signal are not in its linear portion and, therefore, are unusable, resulting in a usable period equal to 85% of the total signal.

Fig. 5 Schematic of a dual excitation microspectrofluorometer system equipped for photon counting and low light or phase contrast image acquisition. Excitation illuminator is directed via the fiber optic bundle (FO) to the epiilluminator with UV wavelengths reflected by the 400 nm dichroic mirror (400 DM) through the objective lens (OL) onto the specimen in

the Sykes Moore Chamber (SMC). Fluorescence emission passes through the 400 DM and, in this configuration, is reflected by the 580 nm dichroic mirror (580 DM) into the photomultiplier tube. For simultaneous photon counting and fluorescence image acquisition, the 580 DM is replaced with a beam splitter.

Fig. 6 Structures of Fura 2/AM and Fura 2.

Fig. 7 Spectrofluorometric analyses of $[Ca^{2+}]_i$ responses of Fura 2-loaded suspended rabbit PTE cells to treatment by various agents at 25°C. (A) typical effect of 50 uM $HgCl_2$ in the presence of low and normal $[Ca^{2+}]_e$. (B) effect of 250 uM NEM (upper curve) and 1 mM PCMBS (lower curve). Both cause increases in $[Ca^{2+}]_i$ which were the same in normal or low $[Ca^{2+}]_e$. The NEM treatment shown was in low $[Ca^{2+}]_e$ with 20 uM EGTA added where indicated. Note that NEM caused some quenching and, therefore, the ordinate values are accurate for $[Ca^{2+}]_i$ only after NEM addition. The PCMBS treatment was in the presence of 1.37 mM $[Ca^{2+}]_e$ and always showed a short lag between the time PCMBS was added and the initiation of $[Ca^{2+}]_i$ increase. (C) effect of 5 uM ionomycin in the presence of normal and low $[Ca^{2+}]_e$. With normal $[Ca^{2+}]_e$, the $[Ca^{2+}]_i$ values increase to almost Fura 2 saturation. Cells suspended in low $[Ca^{2+}]_e$ with 20 mM EGTA showed an initial increase of 500-800 nM which rapidly decreased to as low as, or lower than, control values. (D) effect of inhibition of mitochondrial function with 5 mM KCN and 4 uM CCCP and inhibition of glycolysis with 100 uM IAA. The traces shown were made in the presence of normal $[Ca^{2+}]_e$ but are the same as those made in the absence of $[Ca^{2+}]_e$. (E) effect of 500 uM ouabain on suspended cells in the presence of normal $[Ca^{2+}]_e$. (Reprinted with

permission from Phelps et al., 1989).

Fig. 8 Phase micrographs of monolayer cells exposed to 50 uM $HgCl_2$ at 37°C with low $[Ca^{2+}]_e$ for 6 min (A) and 14 min (C), and with normal $[Ca^{2+}]_e$ for 4 min (B) and 14 min (D). In the presence of normal $[Ca^{2+}]_e$, there are at least twice as many blebs as in low $[Ca^{2+}]_e$ at similar times (123X). (Reprinted with permission from Phelps et al., 1989).

Fig. 9 SEM of monolayer cells exposed to 50 uM $HgCl_2$ at 37°C for 7 min with normal $[Ca^{2+}]_e$. The cells display blebs of varying sizes. (16,250X). (Reprinted with permission from Phelps et al., 1989).

Fig. 10 TEM of a monolayer cell exposed to 50 uM $HgCl_2$ for 4 min at 37°C with low $[Ca^{2+}]_e$. Bands of fine filaments resembling actin are shown at the base of a bleb. (25,000X). (Reprinted with permission from Phelps et al., 1989).

Fig. 11 Bar graph illustrating typical x-ray microanalysis ratios ($P\text{-}B_1/B_2$) obtained over a freeze-dried isolated hepatocyte following 30 min treatment with A23187 (A) in the presence of extracellular Ca^{2+}. Measurements were made over the cytoplasm (cyto) and over a bleb. Note the increase in total Ca^{2+} in the bleb, indicating the possible redistribution of this cation in that region. (Reprinted with permission from Trump and Berezesky, 1989).

Fig. 12 Ratioed and analyzed paired images of Fura 2-loaded cells acquired via a Nikon Diaphot inverted fluorescent microscope equipped with a dual wave length excitation illumination system set at 340/380 nm (Tracor Northern Fluoroplex III). The paired images were intensified and transmitted by a video camera (Dage MTI Newvicon) to an image analysis system (Tracor Northern TN-8502) where they were collected and

processed. $[Ca^{2+}]_i$ concentrations were determined from the ratios and grey scales were assigned colors. Low $[Ca^{2+}]_i$ (100 nM) is blue to green with yellow to red (1200 nM) to white representing higher concentrations (note color bar). (Photographs courtesy of M. W. Smith and P. C. Phelps.)

Cultured human kidney proximal tubule cell. (A) Ratioed image at 0-time. (B) Ratioed image at 16 min after treatment with 10 uM ionomycin. $[Ca^{2+}]_i$ has increased significantly in the cytoplasm as well as in the numerous blebs.

Cultured human kidney proximal tubule cell. (C) Ratioed image at 0-time. (D) Ratioed image at 60 min after exposure to 5 mM KCN + 10 mM IAA. Only a slight rise in $[Ca^{2+}]_i$ is seen.

Cultured rabbit kidney proximal tubule cell. (E) Ratioed image at 0-time. (F) Ratioed image at 16 min after addition of 100 uM $HgCl_2$. $[Ca^{2+}]_i$ levels have increased in the cytoplasm as well as in the five obvious bleb formations.

Cultured BEAS-2B cells (cell line of virally transformed normal human bronchial epithelial cells). (G) Ratioed image at 0-time. (H) Ratioed image at 0.75 min after exposure to 8% calcium-free serum. There is a significant spike-like rise in $[Ca^{2+}]_i$ in three cells which returned to 0-time range by 3 min.

Fig. 13 A photon counting experiment showing $[Ca^{2+}]_i$, calibrated in nanomolar, from cultured neonatal rat ventricular myocytes loaded with Fura 2 and treated with 20 mM 2-deoxy-D-glucose (DOG) and 1 mM sodium cyanide (CN) for 60 min before return to control medium for 30 min. Upon exposure to DOG-CN, normal $[Ca^{2+}]_i$ transients cease, and $[Ca^{2+}]_i$ initially

decreases and then increases to peak systolic level. Upon return to control medium, normal $[Ca^{2+}]_i$ transients are restored. (Reprinted with permission from Morris et al., 1989).

Fig. 14 Flow chart of our hypothesis illustrating the relationships between $[Ca^{2+}]_i$ deregulation, toxic cell injury, and carcinogenesis. (Reprinted with permission from Trump and Berezesky, 1987).

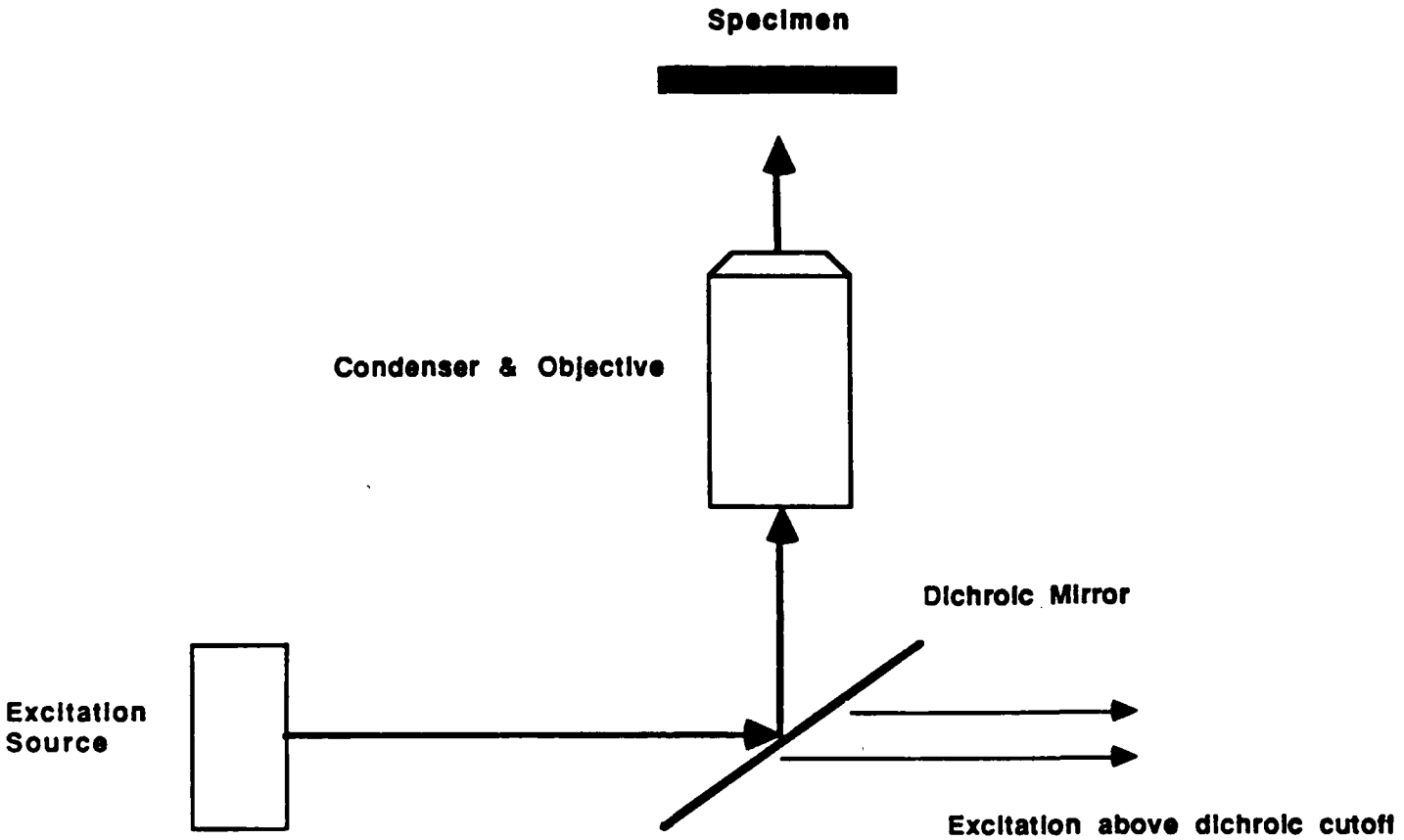

Fig. 1A Trump et al.

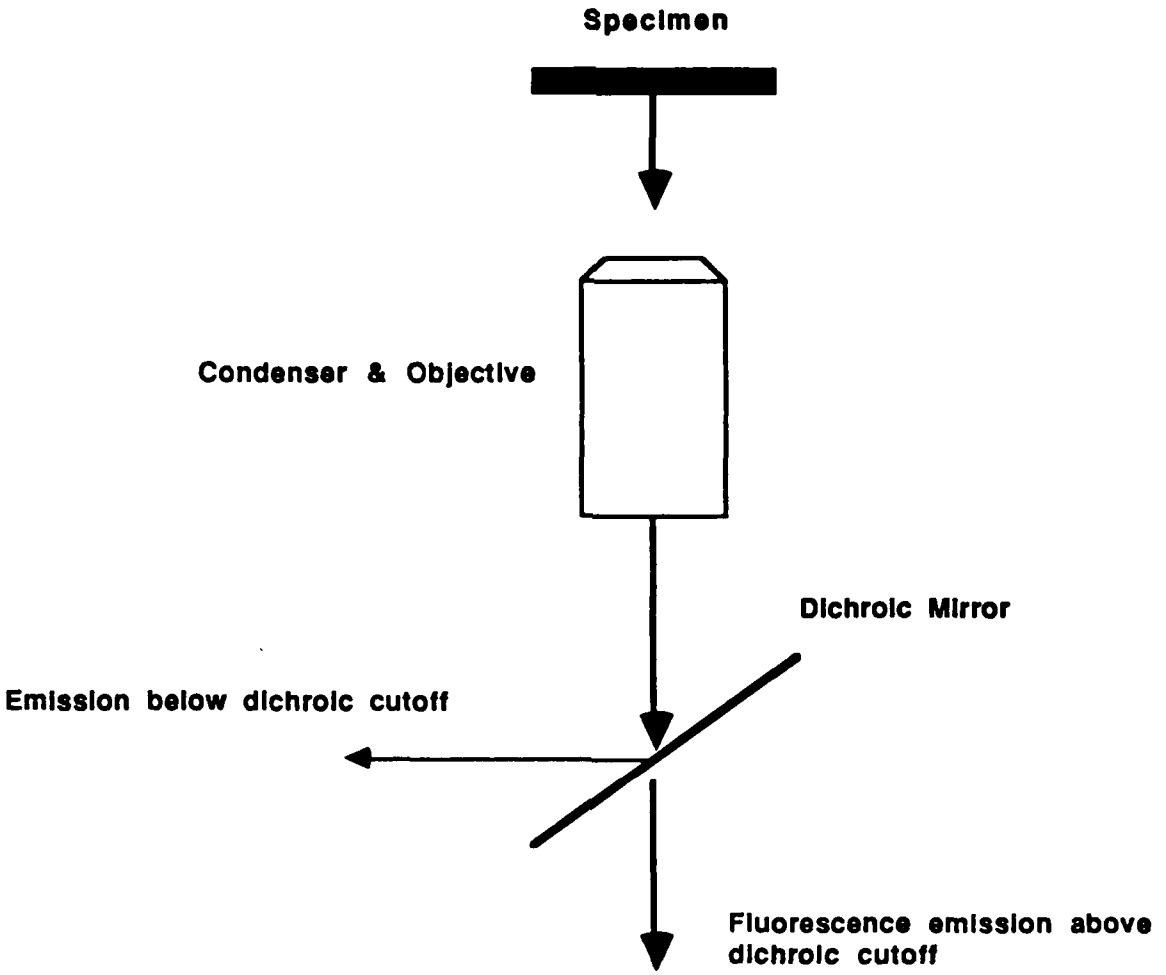

Fig. 1B Trump et al.

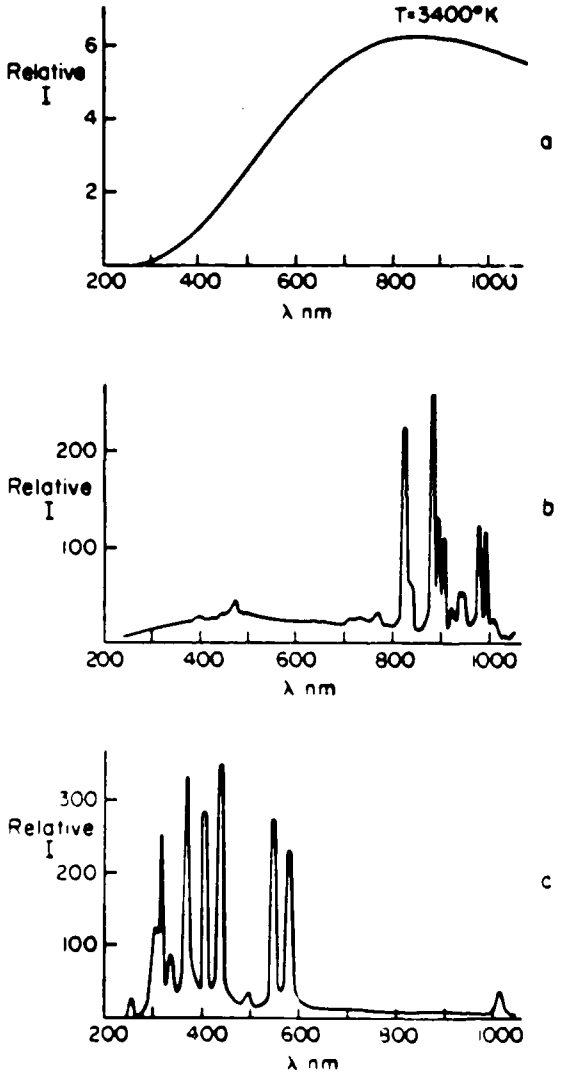

Fig. 2 Trumpler et al.

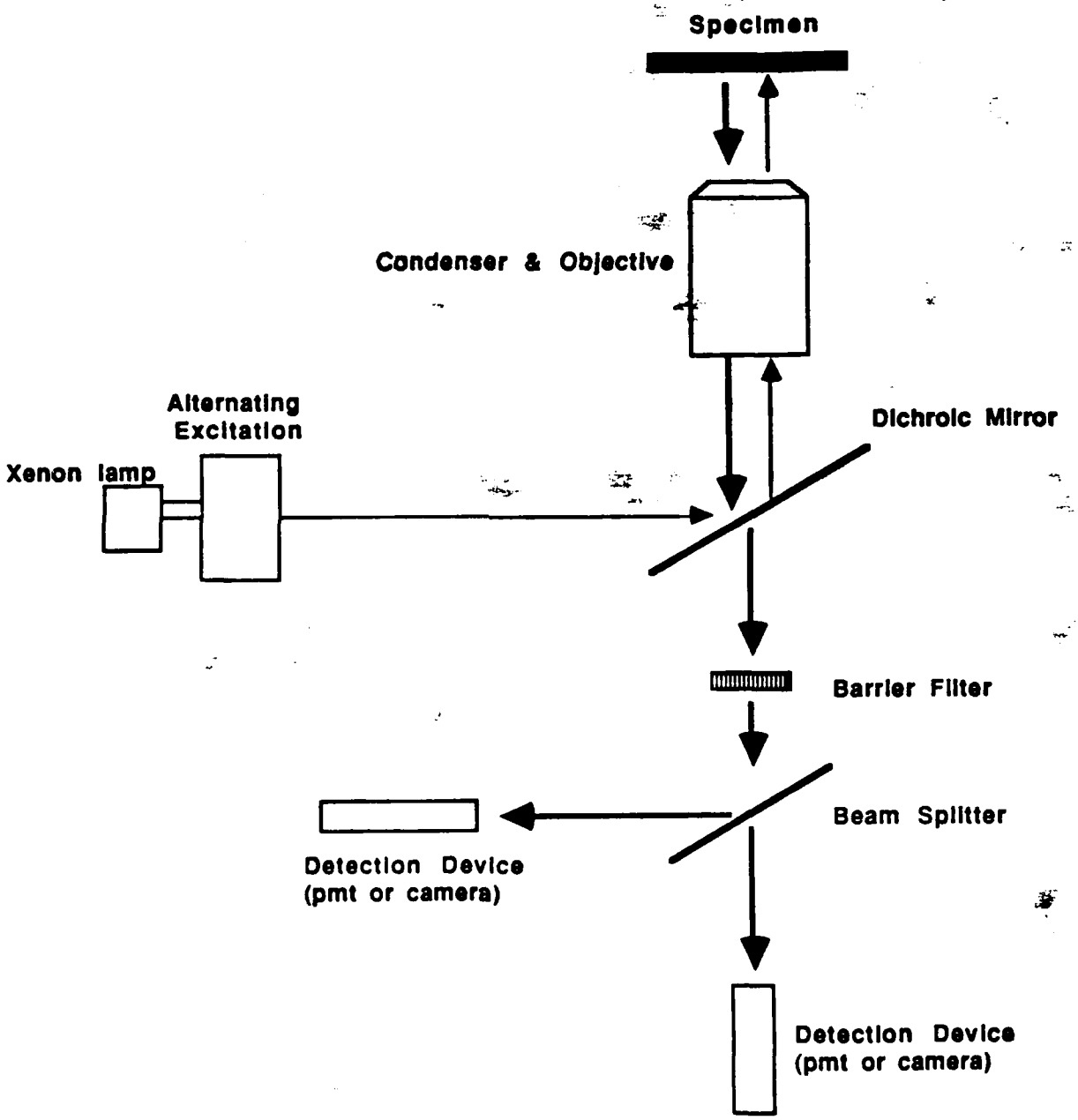

Fig. 3 Tremp et al.

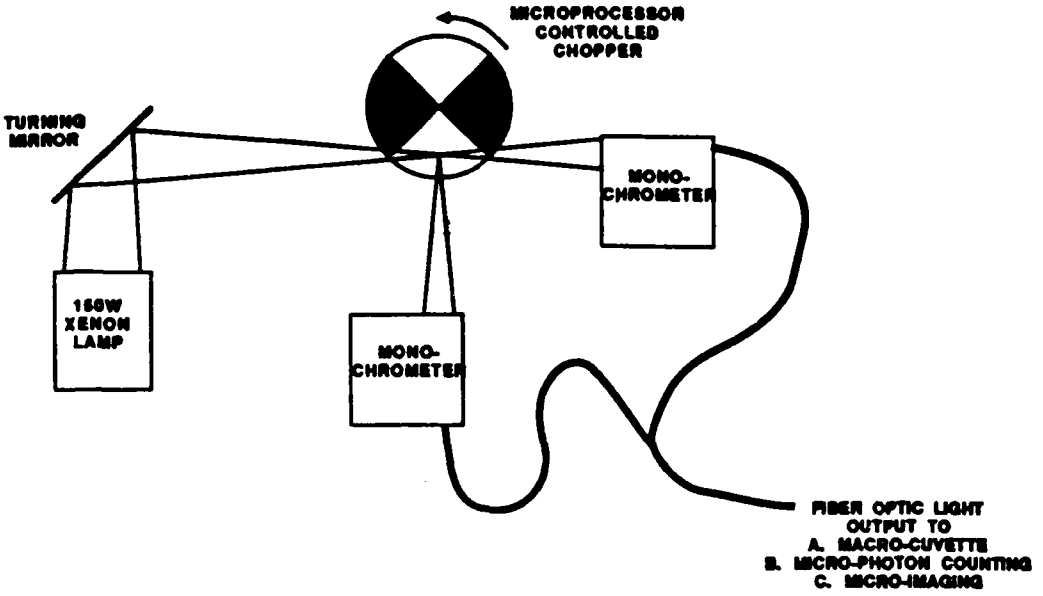

Fig 4A Tsien et al.

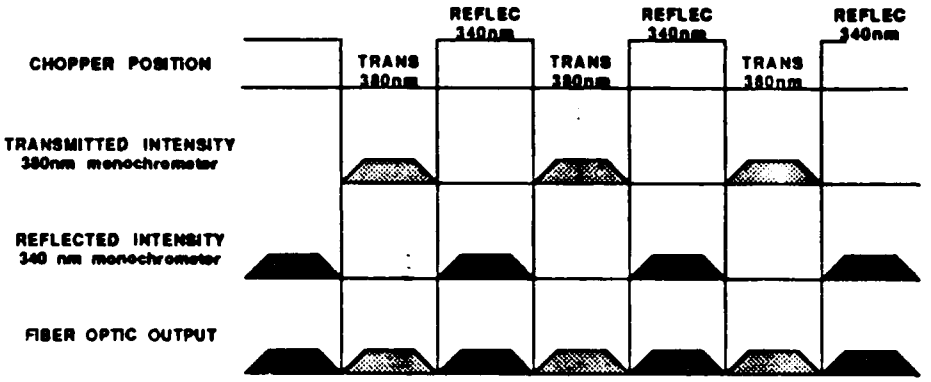

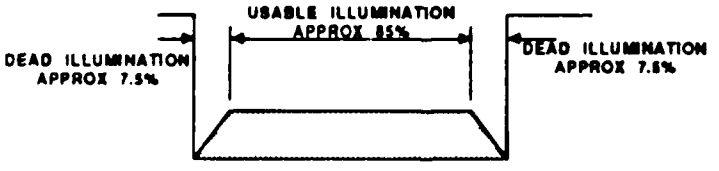

Fig 4B Tsien et al.

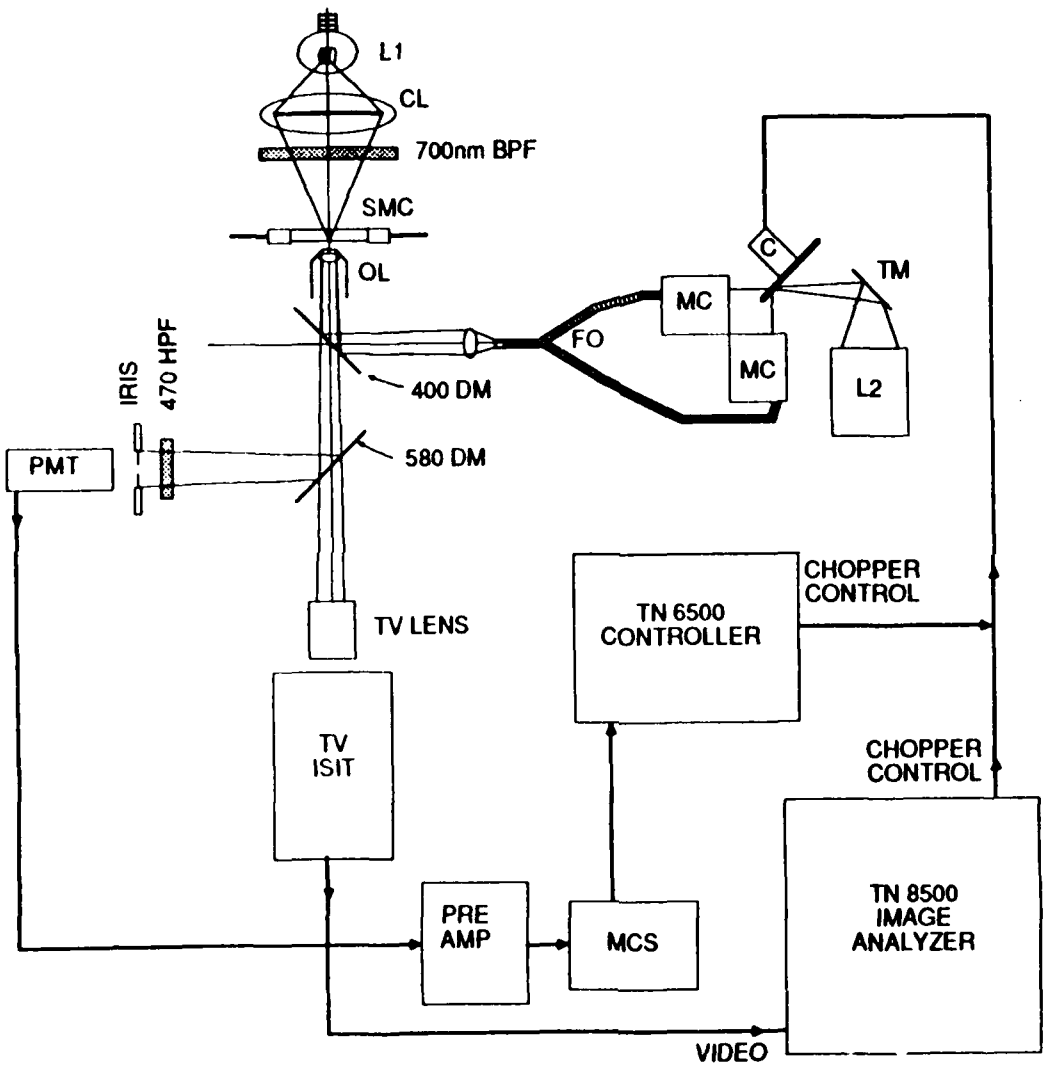

Figure 5

Trump et al.

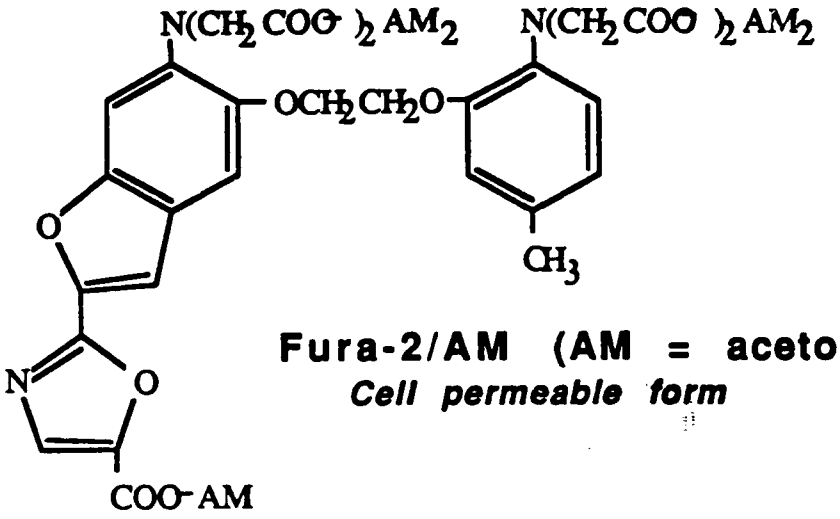

Fura-2/AM (AM = acetoxymethyl ester)

Cell permeable form

Cleavage of AM by intracellular esterases

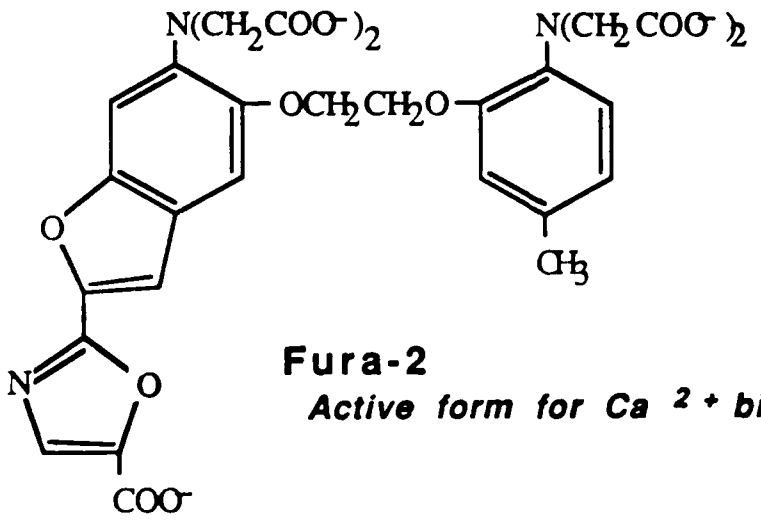

Fura-2

Active form for Ca $^{2+}$ binding

Fig. 6 Trump et al.

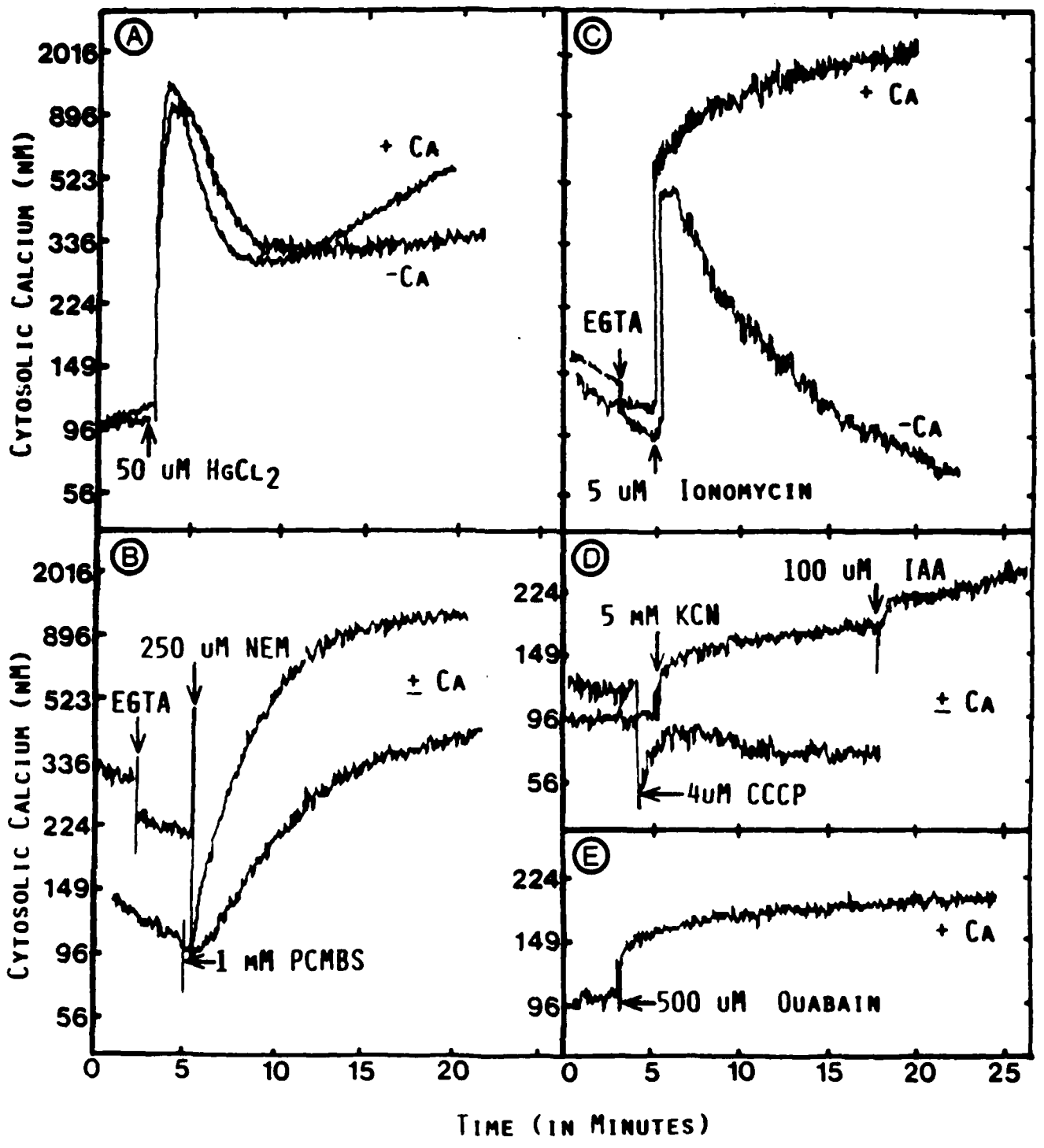
A
2016
896
523
336
224
149
96
56
+ Ca
-Ca
50 uM HgCl2
C
+ Ca
EGTA
-Ca
5 uM Ionomycin
B
250 uM NEM
EGTA
± Ca
1 mM PCMBS
D
100 uM IAA
5 mM KCN
± Ca
4uM CCCP
E
+ Ca
500 uM Ouabain
Cytosolic Calcium (nM)
0
5
10
15
20
25
Time (in Minutes)

Fig. 7

Fig. 8

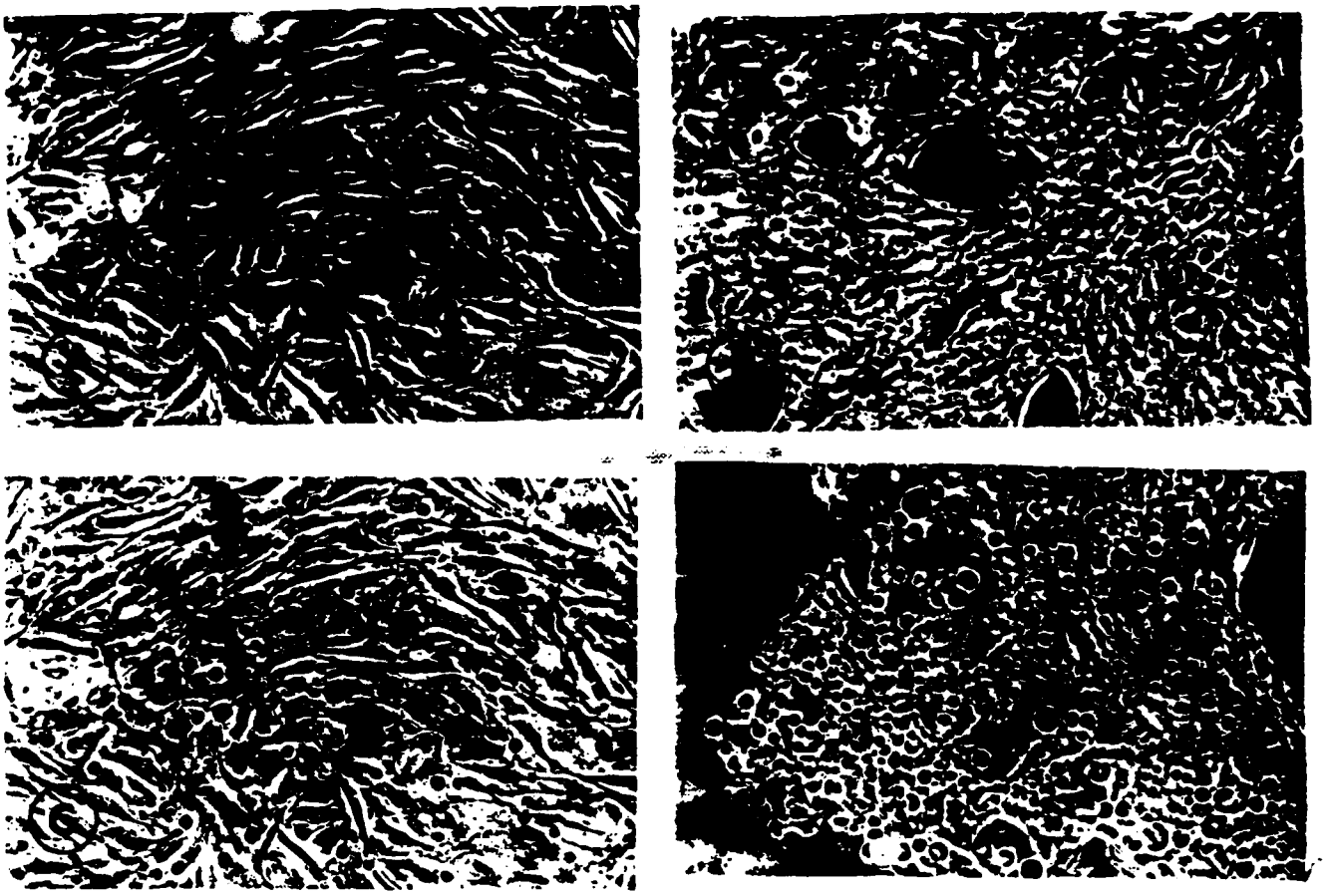

Fig. 9

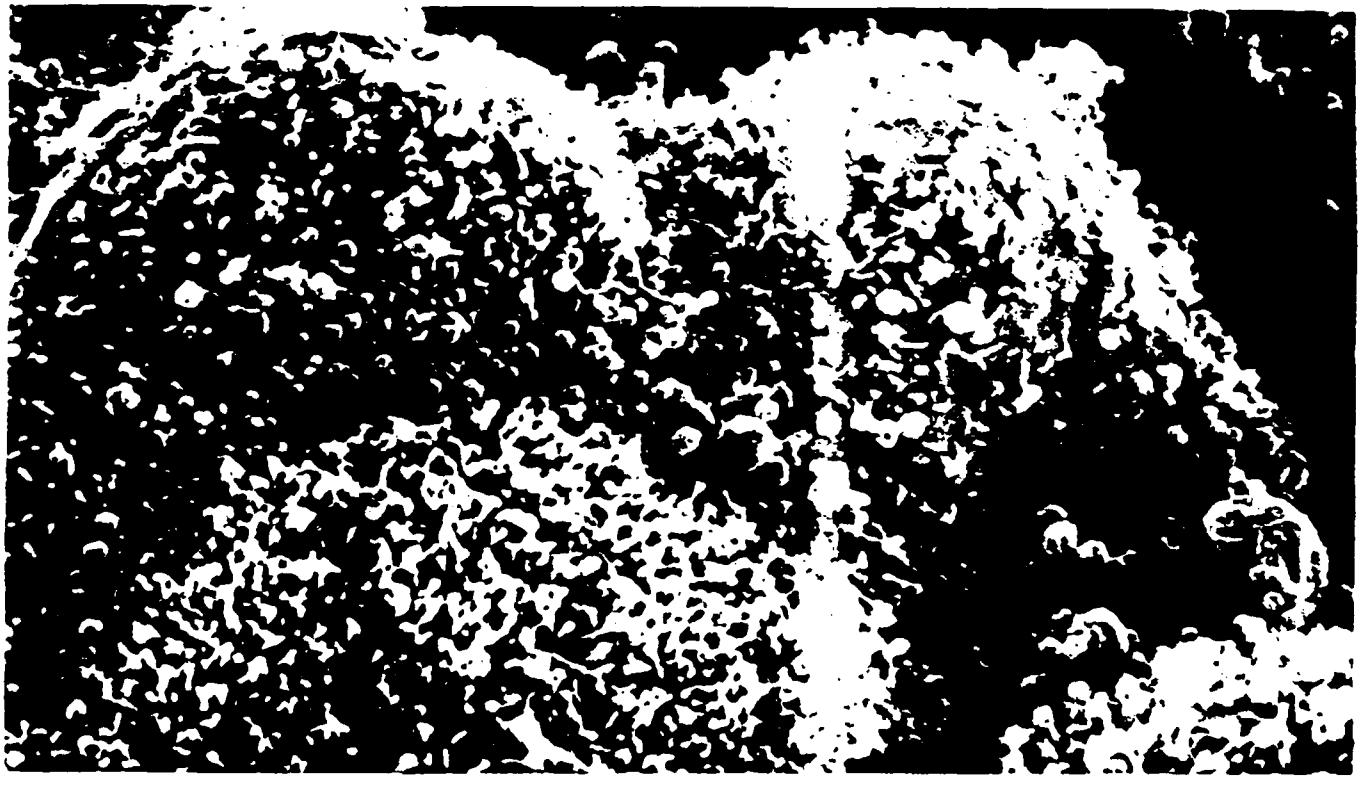

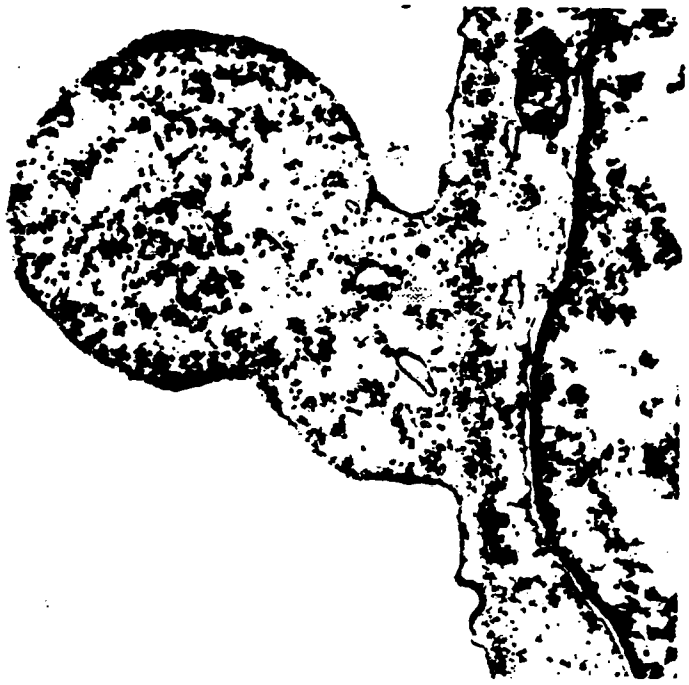

Fig. 10

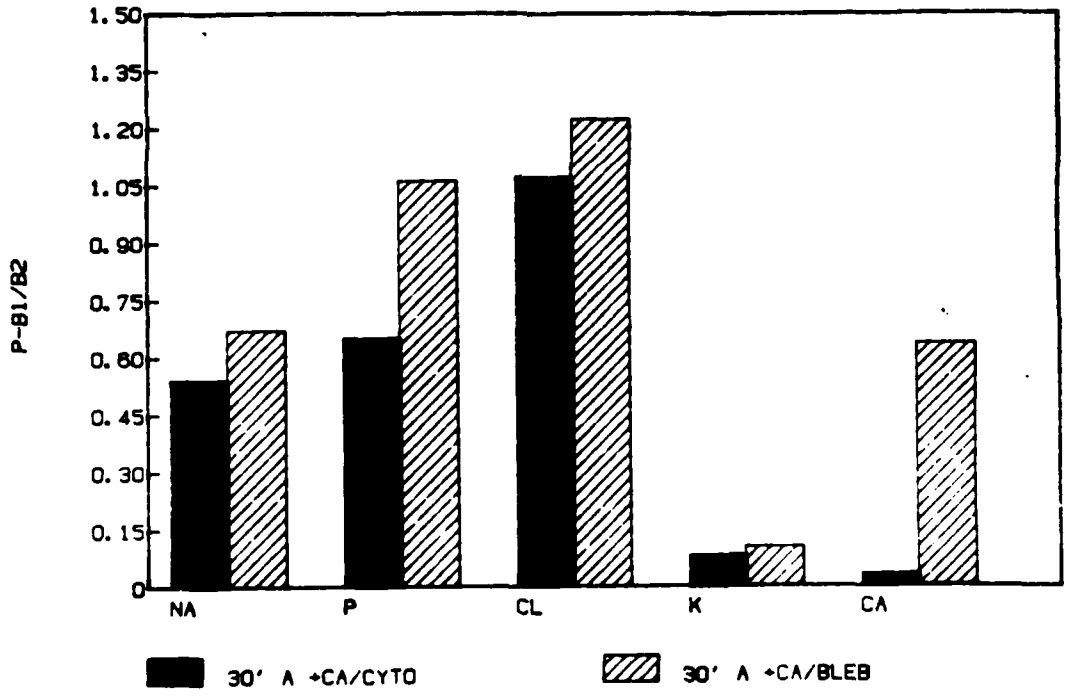
1.50
1.35
1.20
1.05
0.90
0.75
0.60
0.45
0.30
0.15
0
P-B1/B2
NA
P
CL
K
CA
30' A +CA/CYTO
30' A +CA/BLEB

Fig. 11

Fig 12 A-G

Imaging (Slides)

Trump et al.

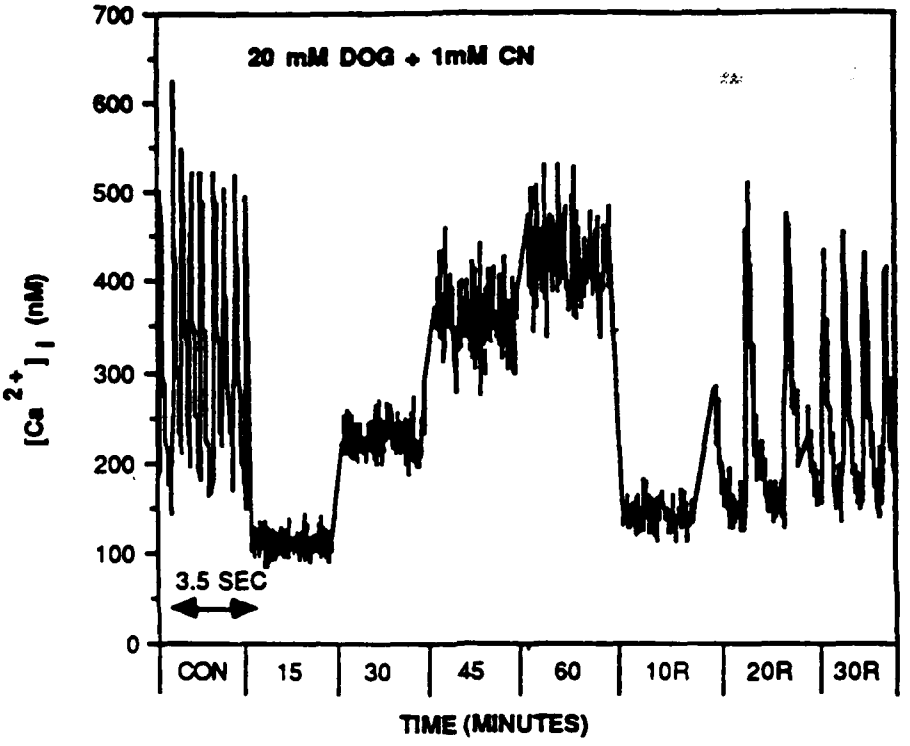

Fig 13 Trump et al.

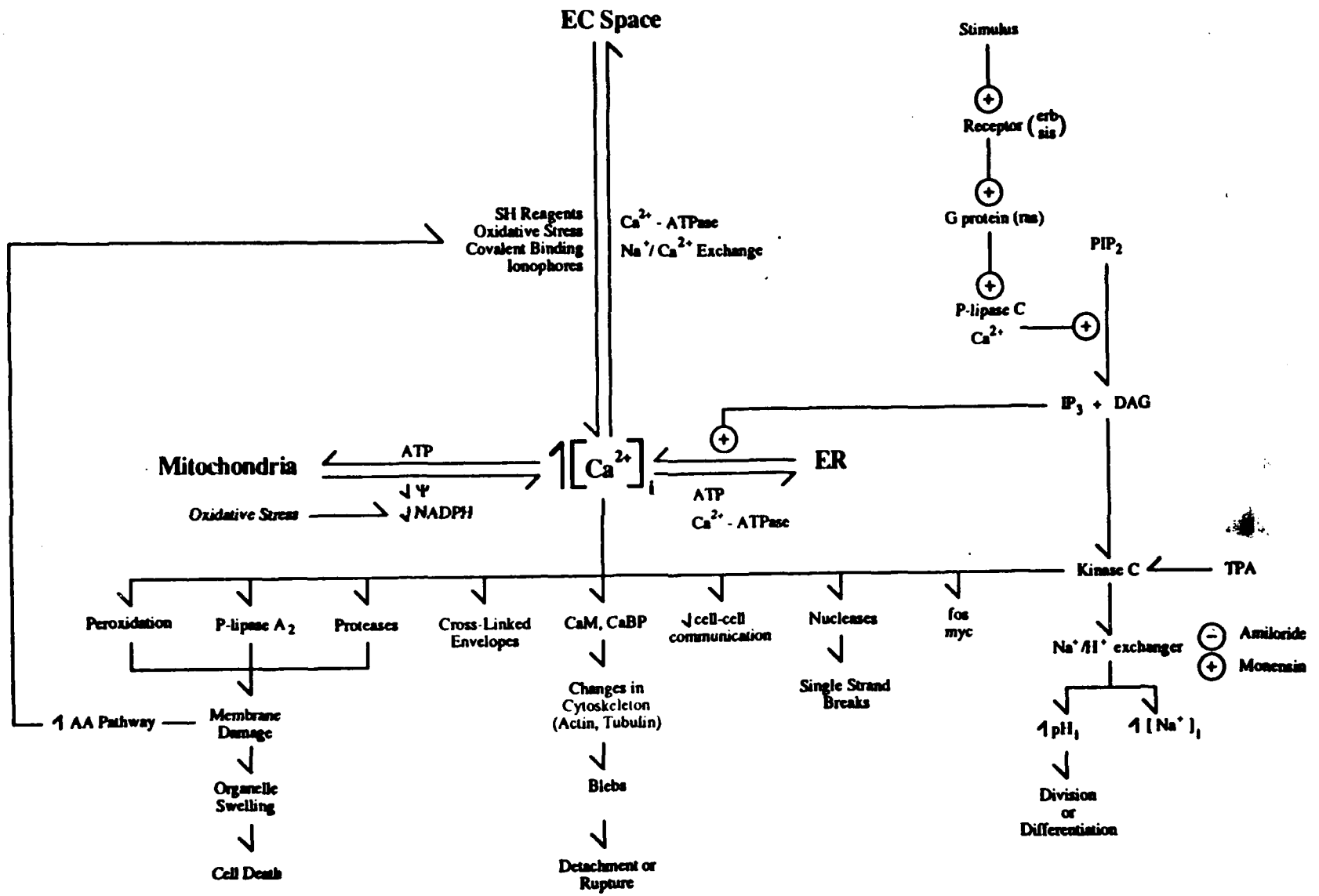

Abbreviations:

PIP_2 = Phosphatidylinositol 4, 5 - diphosphate
Ψ = Mitochondrial membrane potential
CaM = Calmodulin
CaBP = Other calcium-binding proteins
TPA = 12 - O - Tetradecanoylphorbol - 13 - acetate

Fig. 14 Trump et al.

DIGITAL IMAGING FLUORESCENCE MICROSCOPY (DIFM): A NEW APPROACH TO CHARACTERIZE IONIC CHANGES FOLLOWING CELL INJURY.

B.F. Trump, M.D.; I.K. Berezesky, B.A.; M.W. Smith, M.S.; P.C. Phelps, A.B.; K.E. Elliget, M.S.; C.C. Harris, M.D.; T. Tillotson, B.S.; J.R. Resau, Ph.D.; and R.T. Jones, Ph.D. Dept. of Pathology, Univ. of MD Sch. of Med., MD Inst. for Emerg. Med. Svcs. Systs., Balto., MD and the Lab. of Human Carcinogenesis, NIH, Bethesda, MD

The application of DIFM, which involves the adaptation of image intensifiers and computers to the light microscope is revolutionizing the study of living cells. These techniques, when coupled with fluorescent probes (e.g. Fura 2 for calcium determination, BCECF for pH, rhodamine 123 for mitochondrial membrane potential, and propidium iodide for viability), become a powerful tool in the determination of many dynamic changes that accompany cell injury. The cell injuries studied include those which lead to cell death as well as those that may initiate the process of carcinogenesis. Through the use of Fura 2-loaded rat and rabbit proximal tubule epithelium cells (in HBSS + 1.37 $CaCl_2$), 50 µM $HgCl_2$ and 1 µM ionomycin are shown to cause a rapid pulse of $[Ca^{2+}]_i$, whereas 500 µM N-ethylmaleimide and 5 or 10 µM ionomycin cause sustained elevations. After the $[Ca^{2+}]_i$ is significantly elevated, cells also undergo blebbing prior to cell death. Our results indicate a major role for cytosolic calcium and pH in the control of cell injury, cell death and cell proliferation. [Support by NIH AM15440, NO1-CP-51000, and Navy grant #N00014-88-K-0427.]

Lab Invest 90:98A, 1989

UM#2793

Society of Toxicologic Pathologists

VIII International Symposium
Cincinnati, Ohio
May 21-25, 1989

ABSTRACT FORM
For Poster Session
Deadline for Submission: March 15, 1989

TYPE name, address, and telephone number of FIRST AUTHOR to whom all correspondence will be sent.

Name Benjamin F. Trump, M.D., Chairman

Address Department of Pathology, Sch. of Med.
University of Maryland
10 S. Pine St.
Baltimore, MD 21201

Telephone (301) 328-7070

☐ Please consider this abstract for 1989 Junior Investigator Award (separate application required)

Abstracts must be typed on this original form and will be used as camera-ready copy. Proofread abstract carefully. Single space and indent paragraphs. Use authors' last names and initials without degrees. For more forms, call Dr. W. O. Iverson (201) 277-7409

All accepted abstracts will be published in *Toxicologic Pathology*. Senior author will be notified by April 10, 1989, of abstract acceptance. DO NOT FOLD THIS SHEET. Use cardboard backing when mailing.

Mail original typed abstract and two (2) photocopies to:

Nancy M. Streett
Planning Unlimited
P.O. Box 220
New London, PA 19360

THE ROLE OF $[CA^{2+}]_i$ DEREGULATION IN ACUTE TOXIC CELL INJURY OF RENAL PROXIMAL TUBULAR EPITHELIUM (PTE): STUDIES USING DIGITAL IMAGING FLUORESCENCE MICROSCOPY (DIFM). B.F. Trump, M.W. Smith, P.C. Phelps, K.A. Elliget, and I.K. Berezesky, Dept. of Path. Univ. of Md. Sch. of Med. and MIEMSS, Baltimore, MD 21201

Our laboratory has been testing the hypothesis that early changes in $[Ca^{2+}]_i$ play a key role in the events leading to lethal injury. The introduction of DIFM and fluorescent probes for $[Ca^{2+}]_i$ e.g., Fura 2 have made it possible to study changes in $[Ca^{2+}]_i$ in relation to cell injury. We have utilized cultured rat, rabbit, and human PTE and identified three categories of change in $[Ca^{2+}]_i$. These are: (1) increased $[Ca^{2+}]_i$ and cell killing due to influx of $[Ca^{2+}]_e$ with ionomycin; (2) redistribution of Ca^{2+} from intracellular stores after PCMBS, NEM, interference with ATP synthesis, or inhibition of sodium potassium ATPase; and (3) both Ca^{2+} redistribution and influx after $HgCl_2$ which exhibits early release from stores e.g., ER, and followed by $[Ca^{2+}]_e$ influx. It is evident from these studies that early alterations in $[Ca^{2+}]_i$, often regional within the cell, precede and accompany important changes of cell membrane (e.g., blebbing), cytoskeleton, ER, and mitochondria.
(Supported by NIH AM15440 and Navy N00014-88-K-0427.)

Video

UM#2804

THE ROLE OF DIGITAL IMAGING FLUORESCENCE MICROSCOPY (DIFM) IN THE STUDY OF CELL INJURY. B.F. Trump, I.K. Berezesky, M.W. Smith, P.C. Phelps, K.A. Elliget, and T.T. Tillotson, Department of Pathology, University of Maryland School of Medicine and Maryland Institute for Emergency Medical Services System, Baltimore, MD 21201

The introduction of DIFM to the biomedical science community has led to the utilization of this technology for the study of cell injury in single living cultured cells. For some time, our laboratory has been involved in characterizing the events that lead to reversible and irreversible cell injury, cell death, and cell proliferation. We have, therefore, been using the available fluorescent probes and DIFM technology to investigate the relationship between $[Ca^{2+}]_i$, cell injury, and cell death. Our findings reveal that increases in $[Ca^{2+}]_i$ above approximately 400 nM result in the development of blebs at the cell membrane, which can be imaged in phase, Normarski and DIFM. After the initial period following injury, they contain high $[Ca^{2+}]_i$. Parallel studies using analytical electron microscopy (x-ray microanalysis) show high concentrations of total calcium in the blebs. The blebs, however, are only an early indication of cell injury and, as the injury progresses, a variety of systems may be involved, including the endoplasmic reticulum (ER), the cell membrane, and the mitochondria. In our studies using rabbit, rat, and human proximal tubule epithelium (PTE), we have been able to classify a series of model cell injuries into the following categories. These are: (1) agents that cause cell death primarily by influx of Ca^{2+} from the extracellular space and are apparently prevented by lowering $[Ca^{2+}]_e$ (these include ionomycin and A23187); (2) those agents that cause redistribution of Ca^{2+} from intracellular stores, such as the mitochondria and the ER (these include NEM, PCMBS, CN^- + IA, and FCCP), and in which case, reduction of $[Ca^{2+}]_e$ does not result in protection against cell injury; and (3) agents that result in both (1) and (2), including $HgCl_2$, causing an $[Ca^{2+}]_e$-independent release of Ca^{2+} from intracellular stores, e.g., the ER, followed by buffering by cell membrane pumps and an $[Ca^{2+}]_e$-dependent influx of Ca^{2+} to increase $[Ca^{2+}]_i$ in a fashion that is proportional to the rate of cell killing. These studies indicate the importance of DIFM for studies of cell injury and articulate the results of acute cell injury with signalling pathways that affect cell division and cell differentiation. [Supported by NIH AM15440 and Navy N00014-88-K-0427.]

1. Trump et al.: The relationship between cellular ion deregulation and acute and chronic toxicity. Toxicol. Appl. Pharmacol. 97: 6-22, 1989. 2. Trump, B.F., and Berezesky, I.K.: Cell injury and cell death. The role of ion deregulation. Comments Toxicology 3: 47-67, 1989. 3. Phelps et al.: Cytosolic ionized calcium and bleb formation after acute cell injury of cultured rabbit renal tubule cells. Lab Invest 60: 00-00, 1989. 4. Trump et al.: The role of ionized cytosolic calcium ($[Ca^{2+}]_i$) in acute and chronic cell injury. In: Lemasters, J.J., Hackenbrock, C.R., Thurman, R.G., and Westerhoff, H.V., editors. Integration of Mitochondrial Function. New York, Plenum Publishing Corporation, pp. 437-444, 1989. 5. Smith et al.: $HgCl_2$-induced changes in cytosolic Ca^{2+} of cultured rabbit renal tubular cells. Biochem. Biophys. Acta. 931(1): 130-142, 1987.

V INTERNATIONAL CONGRESS OF TOXICOLOGY
ABSTRACT REPRODUCTION FORM

UM#2805

Deadline 31 January 1989

Type Abstract within guidelines

Please read instructions carefully before typing abstract and follow sample below. DO NOT FOLD this form.

I am prepared to chair a Poster Session ☐ ✓

Ref. No.

Principal author's name Dr. Benjamin F. Trump

Address 10 S. Pine Street

City/Town Baltimore, MD 21201 Code ..... Country USA

Telephone (301) 328-7070

CATEGORY NO. 1ST CHOICE: ☐ 2ND CHOICE: ☐

DEREGULATION OF CYTOSOLIC IONIZED CALCIUM $[Ca^{2+}]_i$ IN TOXIC CELL INJURY: STUDIES USING DIGITAL IMAGING FLUORESCENCE MICROSCOPY (DIFM). B.F. Trump, I.K. Berezesky, M.W. Smith, P.C. Phelps, N. Nitta, K.A. Elliget, & T.T. Tillotson. Dept of Pathology, Univ of Maryland Sch of Med & Maryland Institute for Emergency Medical Services System, Baltimore, MD 21201 USA

The recent introduction of DIFM to the fields of pathology and toxicology has enabled us to study a variety of ions such as $[Ca^{2+}]_i$ and $[H^+]_i$ using fluorescent probes in living cells. Although a relation between $[Ca^{2+}]_i$ and cell injury has long been suspected, only recently have such measurements been possible. We have studied the effects of several classes of nephrotoxins on structure and function in relation to $[Ca^{2+}]_i$ in vitro using rat, rabbit, and human proximal tubular epithelium. The classes of compounds studied were: 1) inhibitors of ATP synthesis (KCN + IAA or FCCP); 2) Ca ionophores (ionomycin and A23187); 3) SH reactive compounds ($HgCl_2$, NEM, PCMBS); and 4) oxidative stress (xanthine-xanthine oxidase). All classes resulted in rapid increases of $[Ca^{2+}]_i$ which preceded early cell shape changes, e.g., blebbing and mitochondrial swelling. Classes 1, 3, and 4 resulted in Ca^{2+} mobilization from intracellular stores (ER and mitochondria) though $HgCl_2$ had a later component dependent on Ca^{2+} influx through the plasma membrane. Class 2, in the presence of 1 mM $[Ca^{2+}]_i$, resulted in influx Ca^{2+} influx; cell killing was prevented by $[Ca^{2+}]_i$ reduction. Except for $HgCl_2$, the same rate of cell killing was seen in high or low Ca media.NIH-AM15440&Navy88K0427.

Annual, Final and Technical Reports (one copy each except as noted)

ADMINISTRATORS

Dr. Jeannine A. Majde, Code 1141SB
Office of Naval Research
800 N. Quincy Street
Arlington, VA 22217-5000

Program Manager, Code 1213
Human Factors/Biosciences
Division
Office of Naval Research
800 N. Quincy Street
Arlington, VA 22217-5000

Administrator (2 copies) (Enclose DTIC Form 50)
Defense Technical Information Center
Building 5, Cameron Station
Alexandria, VA 22314

Program Manager, Code 223
Support Technology
Directorate
Office of Naval Technology
800 N. Quincy Street
Arlington, VA 22217-5000

Administrative Contracting Officer
ONR Resident Representative
(address varies - obtain from business office)

Annual and Final Reports Only (one copy each)

DoD ACTIVITIES

Commanding Officer
Naval Medical Center
Washington, DC 20372

Directorate of Life Sciences
Air Force Office of
Scientific Research
Bolling Air Force Base
Washington, DC 20332

Commanding Officer
Naval Medical Research & Development Command
National Naval Medical Center
Bethesda, MD 20814

Library
Armed Forces Radiation
Research Institute
Bethesda, MD 20814-5145

Library
Naval Medical Research Institute
National Naval Medical Center
Bethesda, MD 20814

Commander
Chemical and Biological Sciences Division
Army Research Office, P.O. Box 12211
Research Triangle Park, NC 27709

Commander
U.S. Army Research and Development Command
Attn: SGRD-PLA
Fort Detrick
Frederick, MD 21701

DISTRIBUTION LIST

Cell Biology of Trauma Program

Annual, Final and Technical Reports (one copy each)

INVESTIGATORS

Dr. Michael Artman
Dept. of Pediatrics
Univ. of South Alabama
Medical Center
2451 Fillingim Street
Mobil, AL 36617

Dr. Margaret S. Burns
Dept. of Ophthalmology
Univ. of California, Davis
1603 Alhambra Boulevard
Sacramento, CA 95816

Dr. Robert J. Cohen
Dept. of Biochemistry and
Molecular Biology
College of Medicine
Box J-245, JHMHC
University of Florida
Gainesville, FL 32610

Dr. Dipak K. Das
Department of Surgery
Univ. of Connecticut
Health Center
Farmington, CT 06032

Dr. Thomas M. Devlin
Chairman, Dept. of Biological Chemistry
Hahnemann University
230 Broad Street
Philadelphia, PA 19102

Dr. Marvin A. Karasek
Dept. of Dermatology
Stanford University School of Medicine
Stanford, CA 94305

Dr. John J. Lemasters
Dept. of Cell Biology and Anatomy
School of Medicine
University of North Carolina
Campus Box 7090
Chapel Hill, NC 27599

Dr. Alfred H. Merrill, Jr.
Dept. of Biochemistry
Emory University School
of Medicine
Atlanta, GA 30322

LCDR Douglas H. Robinson
Diving Medicine Dept.
Naval Medical Research Inst.
NMC NCR
Bethesda, MD 20814-5055

Dr. Benjamin F. Trump
Dept. of Pathology
Univ. of Maryland
School of Medicine
Baltimore, MD 21201